THE
PHYSICAL REVIEW
A Journal of Experimental and Theoretical Physics Established by E. L. Nichols in 1893
VOL. 57, NO. 1 JANUARY 1, 1940 SECOND SERIES

Floyd Karker Richtmyer

ON Tuesday, November 7, 1939 death came quietly and unexpectedly to Floyd Karker Richtmyer at the floodtide of an unusually active and fruitful life.

Mr. Richtmyer was born in Cobleskill, New York, on October 12, 1881. As student, teacher, research physicist, and educational administrator he was associated with Cornell University during all but two years of his professional life. He had been Dean of the Graduate School of that institution for the past eight years.

The great breadth of his interests and sympathies, the unflagging zeal and devotion with which he applied himself to them were Richtmyer's outstanding characteristics. Although a gifted research man, he was also profoundly interested in the place of science in the modern world and these interests led him to devote a vast amount of time to organizational and administrative work, particularly in the later years of his life. His competence in these matters and the confidence which his associates placed in his wisdom and judgment is attested by his having held at various times the Presidency of the Optical Society of America, of the American Physical Society, the American Association of Physics Teachers, the National Organization of Sigma Xi, the Vice Presidency of the American Association of University Professors, and the Chairmanship of the Division of Physical Science of the National Research Council. He was connected with the editorial staff of the *Journal of the Optical Society* and the *Review of Scientific Instruments* since the inception of those journals and for many years had been their Editor-in-Chief. At various times he had served as Associate Editor of *The Physical Review* and of the *American Physics Teacher*. He played an important role in the organization of the American Institute of Physics, Inc. and served on the Governing Board of that organization from its beginning.

Without minimizing the importance of these and of many other similar activities, it may fairly be said that the supervision and direction of his program of x-ray research at Cornell University was Richtmyer's most cherished professional activity. This program was initiated in 1919 and followed the interruption in his purely scientific work created by the World War in which he served as radio engineer in the Signal Corps. Prior to this time Richtmyer had contributed significantly to the general fields of photoelectricity and illumination through the publication of a score or more papers on these subjects.

Richtmyer's classic work on absorption of x-rays consisted of a long series of precise measurements which led to the formulation of the famous $\lambda^3 Z^4$ law. Also, of noteworthy significance at the time was his careful study of the controversial "J" radiation in his search for "J" absorption discontinuities with negative results.

While working in the x-ray laboratory in Uppsala, Sweden, Richtmyer became interested in 1927 in the phenomena associated with x-ray satellite lines, and subsequently this interest became a major part of the x-ray program at

Cornell. In 1928 Richtmyer proposed the "double-jump" hypothesis to account for the origin of satellite emission and in 1929–30 as a beautiful conclusion of the last extensive laboratory work he personally carried out, published several papers in support of his proposal. This work shares honors with the absorption work in perpetuating his memory in x-ray annals. In 1929 he was awarded the Levy Medal of the Franklin Institute in recognition of these accomplishments.

Richtmyer was among the first to point out in 1935 that the satellite problem was much more complex than was realized earlier and he immediately integrated the Cornell x-ray program in the study of the broader problem of multiple inner ionization of atoms. This problem includes, as component studies, widths and shapes of x-ray lines and absorption limits, Auger transitions and their probabilities, as well as wave-lengths and relative intensities of satellite lines. The fact that penetrating progress was constantly being made in this complex program during the years that administrative work was consuming almost all of his attention attests to his inspiring scientific leadership.

As a member of the scientific corps on the solar eclipse expedition to Canton Island in 1937 Richtmyer took intensity measurements and polarization photographs of the radiation from the sun's corona. These data were in the process of interpretation at the time of his death.

From one point of view it is unfortunate that Richtmyer, a man of superlative research capabilities, should be drawn out of the laboratory by administrative duties; but from a broader point of view, one that recognizes the far-reaching benefits to research that have come and shall continue to come from his extraordinary administrative talents, it may be said that his many and varied activities have expressed fortunately and adequately his life-devotion to scientific research.

The Council of the American Physical Society at its meeting in Chicago, December 1, 1939, passed the following resolution:

RESOLVED: That in sorrow the Council of the American Physical Society records in its Minutes the great loss to this Society, as to many other scientific bodies, in the death on November 7, 1939 of Floyd Karker Richtmyer, Professor of Physics in Cornell University for many years and Dean of the Graduate School since 1931. The official position that Mr. Richtmyer held in this Society, as a member of its Council, 1934–1936, as one of its Board of Editors, 1929–1931, as its Vice President in 1935 and as its President in 1936 were used by him as opportunities for wise and forward looking service to the Society. But to record only his services in these offices would fall far short of revealing the extent to which his wisdom, his skill in planning and negotiation, his unfailing zeal and devotion to high standards have been availed of by the Society through many years. Officially and unofficially he has been a representative of the American Physical Society on many committees and in many Scientific enterprises among which especial mention may be made of The National Research Council and The American Institute of Physics.

As a member and a fellow of this Society, a contributor of papers at its meetings and in its journals, a physicist of broad outlook and sympathies, interested in research, in the applications of physics to useful ends, and in the teaching of physics, and as a friend of each of us, no less than as a distinguished former president of this Society, the members of this Council honor the life of our colleague which at its prime has been so suddenly ended.

The Instability of the Meson*

MARTIN A. POMERANTZ
The Bartol Research Foundation of the Franklin Institute, Swarthmore, Pennsylvania, and the Randal Morgan Laboratory of Physics, University of Pennsylvania, Philadelphia, Pennsylvania

(Received October 27, 1939)

Values of the proper lifetime of the meson have been deduced from a comparison of the intensity of mesons in an inclined direction under air with that in the vertical under a superposed lead shield equivalent in absorbing power to the difference between the masses of air traversed by the mesons before reaching the apparatus in the two directions. The required mass of lead was calculated from the Bethe and Bloch formula. The reliability of this use of the formula has been verified by an experimental determination of the relative stopping powers of water and lead. We calculate from our experimental data that the average proper lifetime of all mesons having energies exceeding 6.1×10^8 ev upon reaching the apparatus is equal to 3.9 ± 0.3 microseconds, and the average proper lifetime of all mesons with energies exceeding 11.9×10^8 ev upon reaching the apparatus is equal to 3.8 ± 0.4 microseconds. From the same data, the proper lifetime of only those mesons having about 9×10^8 ev energy upon reaching the apparatus is equal to 2.6 ± 0.8 microseconds. With the theory of Euler and Heisenberg, the proper lifetime has also been calculated from measurements of the number of disintegration electrons and their secondaries in equilibrium with the mesons in air. The value obtained by this method is roughly equal to 6 microseconds.

I. INTRODUCTION

THE observations of Ehmert,[1] and of Auger, Ehrenfest, Fréon and Fournier[2] originally indicated that the intensity of the cosmic radiation depends not only upon the quantity of matter traversed by the rays, but also upon the density of the absorbing medium. As an explanation of this effect, Kulenkampf, and Euler and Heisenberg[3] have pointed out that the instability of the meson,[4] predicted theoretically by Yukawa,[5] would result in a lower intensity as the time required for the secondary mesons[6] produced in the upper atmosphere to reach the detecting apparatus is increased. Interpreting Ehmert's results in this manner, Euler and Heisenberg calculated that the proper lifetime, τ_0, of the meson, i.e. the mean life of the meson in its rest system, is of the order of several microseconds. As a further test of the instability hypothesis, Euler[7] assumed that the soft component at sea level consists almost exclusively of electrons arising from the disintegration of mesons, and from the ratio of the intensities of the soft and hard component, he deduced a value of τ_0 of the same order of magnitude. Montgomery and Montgomery determined the proper lifetime from the frequency of occurrence of large bursts produced by the disintegration electrons. Ehrenfest and Fréon[8] compared the intensity of cosmic rays in an inclined direction at a high elevation with that in the vertical at a lower elevation, and calculated τ_0 from this data. Blackett[9] invoked the instability of the meson to account for the temperature coefficient of the cosmic-ray intensity as a change in height of the layer at which mesons are produced. The difference between the coefficient of the barometer effect and the absorption coefficient was given an analogous interpretation by Rathgeber,[10] and by Kolhörster and Matthes.[11] Barnóthy and Forró[12] applied the instability hypothesis in discussing the barometric and temperature effects on the intensity of the soft component. Rossi[13] calculated τ_0 from the differ-

* A preliminary report of the results of these investigations was presented at the University of Chicago Symposium on Cosmic Rays, June 30, 1939.

[1] A. Ehmert, Zeits. f. Physik **106**, 751 (1937).

[2] P. Auger, P. Ehrenfest, A. Fréon and A. Fournier, Comptes rendus **204**, 257 (1937).

[3] H. Euler and W. Heisenberg, Ergeb. d. Ext. Natur. (1938).

[4] For a resumé of the experiments leading to the discovery of the meson see E. E. Witmer and M. A. Pomerantz, J. App. Phys. **9**, 746 (1938).

[5] H. Yukawa, Proc. Phys. Math. Soc. Jap. **17**, 48 (1935).

[6] For arguments favoring the secondary nature of mesons see T. H. Johnson and J. G. Barry. Phys. Rev. **56**, 219 (1939); see also L. W. Nordheim and M. H. Hebb, Phys. Rev. **56**, 494 (1939).

[7] H. Euler, Zeits. f. Physik **110**, 692 (1938).

[8] P. Ehrenfest and A. Fréon, Comptes rendus **207**, 853 (1938); J. de phys. et rad. **12**, 529 (1938).

[9] P. M. S. Blackett, Phys. Rev. **54**, 973 (1938); Nature **142**, 992 (1938).

[10] D. Rathgeber, Naturwiss. **26**, 842 (1938).

[11] W. Kolhörster and I. Matthes, Physik. Zeits. **40**, 142 (1939).

[12] J. Barnóthy and M. Forró, Phys. Rev. **55**, 868 (1939).

[13] B. Rossi, Nature **142**, 992 (1938).

ence in the absorption in equivalent masses of lead and air, and Johnson and Pomerantz[14] independently determined the proper lifetime from the difference in the absorption of mesons in air and water. Although these methods have yielded concordant values of τ_0 of the order of 2×10^{-6} second, the calculations in all cases are based upon more or less arbitrary assumptions and limited experimental data, and the results can be considered only as indicating the correct order of magnitude.

An accurate comparison of the absorption of mesons in lead and air has been undertaken for several reasons. This experiment has the advantage that all measurements are made at a single station, and frequent interchanges of position can be made for the purpose of detecting any possible change of sensitivity in the apparatus itself. Thus, the data are of sufficient accuracy that the uncertainty in the value of τ_0 deduced therefrom resides principally in the assumptions regarding the mass of the meson and the height at which mesons are produced. It was also the purpose of this experiment to ascertain whether the stability of a meson increases in proportion to its energy, as is predicted by the Lorentz dilatation of the time scale. Finally, in order to achieve greater accuracy, it was expedient to discard the mass-absorption law, generally assumed for mesons, in favor of the more accurate theory. It was, however, considered important to check the theoretical absorption law by subsidiary experiments in which the stopping powers of water and lead were compared.

[14] T. H. Johnson and M. A. Pomerantz, Phys. Rev. **55**, 104 (1939).

II. The Relative Meson Stopping Power of Water and Lead

Because of the large mass of the meson, the loss of energy by radiation may be neglected, and, as far as we now know, ionization is the only important process by which mesons dissipate their energy prior to their disintegration. From the theory of Bethe[15] and Bloch,[16] the average energy lost per gram per square centimeter in a substance with N atoms per cm³ by a meson with the velocity $v=\beta c$ and energy E may be expressed in the form:[17]

$$S\equiv -\frac{dE}{\rho dx}=\frac{2\pi NZe^4}{mc^2\beta^2\rho}\left[\log\frac{mc^2\beta^2W}{(1-\beta^2)\bar{I}^2}\right], \quad (1)$$

where m is the rest mass and e the charge of the electron, $\bar{I}$ is the mean ionization energy of the atom equal to $13.5Z$, and W represents the maximum energy which can be transferred in a direct collision from the meson to a free electron. The latter[18] is given by

$$W=(E+2\mu c^2)/[1+mc^2(1+\mu/m)^2/2E], \quad (2)$$

where μ is the rest mass of the meson. S_1/S_2, the relative stopping powers of equal masses of two media, may be calculated from Eq. (1).

An experimental value of S_{H_2O}/S_{Pb} which can be compared with that calculated from Eq. (1) was obtained in the following two experiments. In the first experiment, the quadruple coincidence counting rate of a train of four trays of counters (Fig. 3) was obtained as a function of interposed

[15] H. Bethe, *Handbuch der Physik*, Vol. 24, 1.
[16] F. Bloch, Zeits. f. Physik **81**, 363 (1933).
[17] Several additional terms appear between the brackets in the more exact expression, but these are negligible in the present considerations.
[18] T. H. Johnson, Phys. Rev. **45**, 580 (1934).

TABLE I. *Resumé of data used for comparing the stopping powers of water and lead. The data of experiment 1 is to be compared with that of experiment 2 only insofar as the intensity in arbitrary units is concerned, inasmuch as the sensitivity of the apparatus was adjusted between experiments.*

Exp. No.	Zenith Angle	Superposed Shield, M_1, in g/cm²	Interposed Shield, M_2, in g/cm²	Total Number of Quadruple Coincidences	Total Time in Hours	Coincidences per Hour	Intensity, $\frac{j_0(M_1+M_2)}{j_{60}(M_2)}$	(M_1+M_2) in g/cm²
1	60°	0	403 Pb	2366	46	51.43±1.06		
	0°	1045 Pb	202 Pb	3296	26	126.77±2.22	2.46±0.10	1247
	0°	1045 Pb	403 Pb	4246	37	114.76±1.77	2.23±0.08	1448
	0°	1045 Pb	666 Pb	2023	20	101.15±2.31	1.97±0.09	1711
	0°	1045 Pb	868 Pb	3950	42	94.04±1.54	1.83±0.07	1913
2	0°	890 H_2O	403 Pb	2961	20.17	146.40±3.00	1.76±0.10	
	60°	0	403 Pb	1150	13.82	83.40±3.00		

lead thickness when the counters were beneath a superposed shield of 1045 g/cm² of lead, and in the second experiment, the counting rate of the same arrangement of counters was recorded under 890 g/cm² of superposed water, and with 403 g/cm² of interposed lead. The data are recorded in Table I. Since the experiments were run at different times, the effect of changes of sensitivity have been avoided by expressing all intensities in terms of that measured at the same time by the same arrangement inclined 60° from the vertical (without the superposed shields). Thus, the intensities given in the eighth column of Table I are comparable between the two experiments. The results of the first experiment are plotted in Fig. 1, which shows the cosmic-ray intensity as a function of the sum of the masses of superposed and interposed lead. The abscissa of the point on the lead absorption curve having as ordinate the intensity observed in the second experiment represents the amount of lead which reduces the intensity to the same extent as 890 g/cm² of water and 403 g/cm² of lead. This is found to be 1950 g/cm², and, subtracting the 403 g/cm² of interposed lead, the result indicates that 890 g/cm² of water has the same effect in absorbing mesons[19] as 1547 g/cm² of lead. It follows that these masses have the same stopping power, and hence the ratio of the relative stopping powers per g/cm², S_{H_2O}/S_{Pb}, is equal to 1.72 ± 0.22. The theoretical ratio of the stopping powers per g/cm² is obtained from Eq. (1). The result is not sensitive to the value of the energy E, and with E equal to 10^9 ev, a reasonable average value for the rays as they are passing through the superposed lead and water, and μ equal to $200m$, Eq. (1) gives S_{H_2O}/S_{Pb} equals 1.82, in agreement with the experimental result. Further experimental confirmation of the validity of Eq. (1) has recently been provided by Wilson's[20] cloud-chamber investigations of the specific energy loss in lead of mesons with energies of 2 to 7×10^8 ev. We may conclude, therefore, that Eq. (1) affords a suitable method for determining what thickness of one absorber is equivalent in stopping power to a given thickness of any other, in the experiments to be discussed.

[19] The mesons concerned are those which have sufficient energy after emerging from the superposed shield to just penetrate 403 g/cm² of lead.

[20] J. G. Wilson, Proc. Roy. Soc. **172**, 517 (1939).

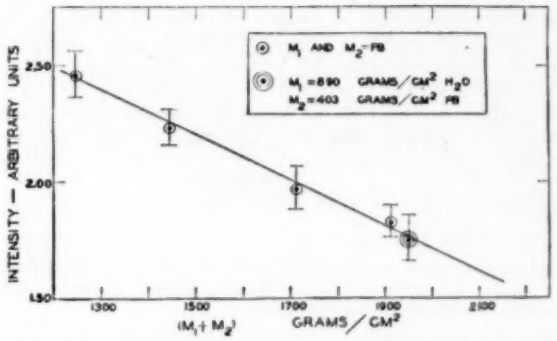

FIG. 1. Lead absorption curve for mesons. The intensity in arbitrary units *vs.* M_1 g/cm² of superposed lead $+M_2$ g/cm² of interposed lead is plotted from the data of Exp. 1, Table I. The abscissa of the point on the lead absorption curve whose ordinate is the intensity found in Exp. 2 is $(M_1+M_2)=1950$ g/cm². As $M_2=403$ g/cm², $M_1=1547$ g/cm² of lead. Actually, M_1 in Exp. 2 was 890 g/cm² of water. Therefore 890 g/cm² of water is equivalent in stopping power to 1547 g/cm² of lead.

III. Theory of the Determination of the Proper Lifetime

By inserting lead above the coincidence counter system in the vertical direction in an amount equivalent in absorbing power to $H(\sec\zeta-1)$ atmospheres, the vertical path through the air and the lead differs from that through the atmosphere at angle ζ only in regard to the time required for the rays to traverse it. When the cosmic rays traverse equivalent thicknesses of absorbing materials, the ratio of the intensity from the inclined direction to that from the vertical, j_ζ/j_0, is a function merely of the probabilities of disintegration of the rays during the times required to traverse the two paths. Since the disintegration probability is a function of the energy, the total intensity in each orientation must be expressed as an integral extending over the energy distribution. On the other hand, the ratio of the differences of the intensities recorded with two thicknesses of interposed lead, $\Delta j_\zeta/\Delta j_0$, is a function of the disintegration probability of rays whose energies are within a certain narrow range determined by the difference in lead thickness. Calculations of the mean lifetime can therefore be carried out by invoking either of these procedures, which shall be designated as the integral and differential method, respectively.

A. The integral method

It is assumed that mesons attaining sea level, incident at a zenith angle ζ, have originated as

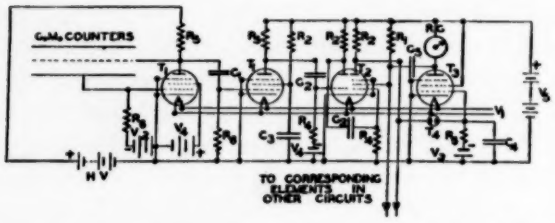

FIG. 2. The three-stage circuit associated with each of the trays of counters in the quadruple coincidence train, and the neon-tube coupled multivibrator delay circuit which recorded quadruple coincidences.

R_1 = 40,000 ohms	C_1 = 6 μμf
R_2 = 0.1 megohm	C_2 = 0.00025 μf
R_3 = .3 megohm	C_3 = .01 μf
R_4 = .5 megohm	C_4 = .005 μf
R_5 = 2.0 megohm	C_5 = .25 μf
R_6 = 10.0 megohm	
V_1 = 6.3 v a.c.	T_1 = RCA. 6C6
V_2 = 4.5 v	T_2 = RCA. 6F7
V_3 = 33.0 v	T_3 = RCA. 89
V_4 = 45.0 v	T_4 = G.E. S-4½
V_5 = 180 v	R.C. = Recording dial

secondaries at an atmospheric depth

$$h = fH \cos \zeta, \tag{3}$$

where H is the depth of the homogeneous atmosphere (8×10^5 cm), and f is the fraction of the homogeneous atmosphere traversed by the primaries prior to the generation of the mesons. The actual height x above sea level corresponding to this depth in an isothermal atmosphere is given by

$$h = He^{-x/H} \tag{4}$$

or

$$x = H \log (\sec \zeta / f). \tag{5}$$

In consequence of the relativistic transformation, the apparent stability should increase with the energy,[21] and for energies large compared with the rest energy, μc^2, the mean life of a meson of energy $\epsilon\mu c^2$ is $\tau = \epsilon\tau_0$, where τ_0 is the proper lifetime, or the mean life of the meson in the coordinate system with respect to which the particle is at rest. If a ray loses energy by ionization at the constant rate $i\mu c^2$ per cm in normal air, the probability $P(\epsilon,\zeta)$ that a ray of initial energy $\epsilon\mu c^2$ will attain sea level without disintegrating can be derived in the following manner. If P is the probability that a ray will survive for a time t, then the probability for disintegration in time t to $t+dt$ is

$$-dP = Pdt/\tau \tag{6}$$

or

$$-dP = P\frac{dx \sec \zeta}{\beta c\tau_0(\epsilon - ih \sec \zeta)}. \tag{7}$$

Making use of Eqs. (4) and (5), and integrating (7) over the path to sea level, we obtain:

$$P(\epsilon,\zeta) = \exp[-(H \sec \zeta/\beta c\tau_0\epsilon) \times \log \{(\epsilon/ifH - 1)/(\epsilon/iH \sec \zeta - 1)\}]. \tag{8}$$

Let $j(\epsilon)d\epsilon$ represent the number of mesons per second per square centimeter per unit solid angle whose initial energies lie in the interval $d\epsilon$ at ϵ, a function which is assumed to be independent of the direction. The total vertical intensity of the penetrating component at sea level may thus be expressed as

$$j_0(t) = \int_{E_0}^{\infty} j(\epsilon)P(\epsilon, 0)d\epsilon, \tag{9}$$

where $E_0 = \alpha(t) + iH(1-f) + \alpha'$, t is the thickness of lead interposed in the counter system for eliminating the soft radiation, $\alpha(t)$ is the energy required to just penetrate the interposed lead, and α' is that lost in penetrating the superposed shield. The intensity which would be measured by an apparatus inclined at a zenith angle ζ with no superposed lead shield filling its solid angle is

$$j_\zeta(t) = \int_{E_\zeta}^{\infty} j(\epsilon)P(\epsilon, \zeta)d\epsilon, \tag{10}$$

where $E_\zeta = \alpha(t) + iH(\sec \zeta - f)$. From counter experiments such as those performed by Wilson[22] and Ehmert,[1] and the cloud-chamber observations of Blackett,[23] the energy distribution at sea level and below is of the form $(\text{Energy})^{-\gamma}$, where $2 < \gamma < 3$. Consequently, in terms of ϵ,

$$j(\epsilon)P(\epsilon,0) = A/[\epsilon - iH(1-f)]^\gamma, \tag{11}$$

and carrying through the integration expressed by Eq. (9),

$$j_0(t) = A/(\gamma - 1)[\alpha(t) + \alpha']^{\gamma-1} = A/K. \tag{12}$$

Combining (10) and (11),

$$j_\zeta(t) = \int_{E_\zeta}^{\infty} \frac{AP(\epsilon, \zeta)d\epsilon}{[\epsilon - iH(1-f)]^\gamma P(\epsilon, 0)}, \tag{13}$$

[21] H. J. Bhabha, Nature **141**, 117 (1938).

[22] V. Wilson, Phys. Rev. **53**, 337 (1938).

[23] P. M. S. Blackett, Proc. Roy. Soc. **159**, 1 (1937).

and finally

$$\frac{j_\zeta(t)}{j_0(t)}=K\int_{E_\zeta}^{\infty}\frac{P(\epsilon,\zeta)d\epsilon}{P(\epsilon,0)[\epsilon-iH(1-f)]^\gamma}. \quad (14)$$

For the determination of τ_0, the ratio of the intensities $j_\zeta(t)/j_0(t)$ is measured and compared with the values obtained from Eq. (14) when various values of τ_0 are introduced. It is, of course, necessary to select specific values of μ, f, and γ. The values thus calculated for $\mu=200m$, $f=0.1$, and $\gamma=2$ and 3 are represented as functions of τ_0 in Fig. 5. The calculated values are least sensitive to γ when $E_\zeta=E_0$, and, in the experimental work, ζ has been selected to fulfil this condition.

B. The differential method

In determining τ_0 by the differential method, we are concerned with the disintegration of only those rays possessing sufficient energy to penetrate an initial thickness t_1 of interposed lead, but without enough energy to pass through a larger thickness t_2 of lead. This calculation has the advantage that it is independent of the energy distribution, and, when $E_\zeta=E_0$, it gives the proper lifetime of rays of initial energy

$$\epsilon_1=iH(\sec\zeta-f)+\bar{\alpha}, \quad (15)$$

where $\bar{\alpha}$ is the average of the minimum energies required for penetrating the two thicknesses of lead. In this instance,

$$\eta\equiv\frac{j_\zeta(t_1)-j_\zeta(t_2)}{j_0(t_1)-j_0(t_2)}=\frac{P(\epsilon,\zeta)}{P(\epsilon,0)} \quad (16)$$

and τ_0 is determined by comparing the observed value of η with those calculated from Eq. (8) with various values of τ_0 (Fig. 6).

IV. Experimental Procedure

A. Apparatus

The intensities of the penetrating component were measured with a quadruple coincidence counter train of large area, but relatively small angular aperture. Each tray consisted of twelve parallel-connected G-M counters with copper cylinders 8″ long and $\frac{3}{4}$″ in diameter. These overlapped in such a manner that the tray presented an unbroken sensitive area of approximately 440 cm². The distance between extreme trays was 132 cm. Provision was made for interposing up to 90 cm of lead between the counter trays. In these experiments, a 6 percent Sb-Pb alloy was used, cast in plates 10″×10″ ×$\frac{3}{8}$″, each weighing about 10 g/cm². The counters were filled with a mixture of hydrogen at a pressure of 5 cm of Hg, and argon at a pressure of 33 cm of Hg. The individual counters had a constant counting rate over a range of 200 volts. The operating potential was approximately 1250 volts.

The three-stage circuit diagrammed in Fig. 2 amplified the pulses, and selected coincidences by means of the usual Rossi parallel-plate connection. Neon-tube coupling to a multivibrator output stage[24] was employed, and an automatic mechanism provided photographic records of the counts obtained during hourly intervals. The counters were quenched by the conventional Neher-Harper[25] arrangement, and the stabilized high voltage was supplied by Gingrich's[26] modification of the Street-Johnson[27] voltage control circuit.

Adjacent to a window in the laboratory a scaffold was erected upon which was placed an inverted truncated pyramid of lead 67.7 cm high filling the solid angle of the counter train. The remaining portion of the absorbing shield was

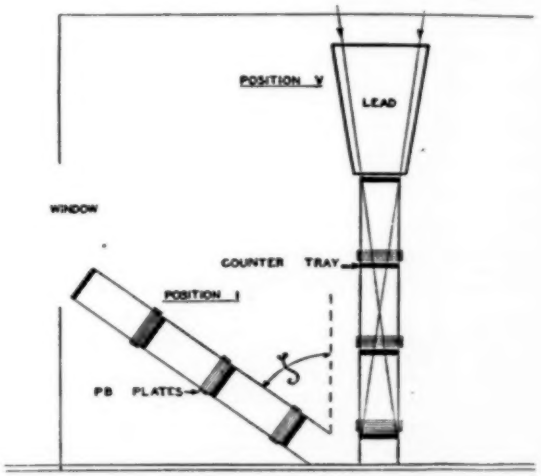

Fig. 3. Scale diagram of the geometry of the experiment.

[24] T. H. Johnson, Rev. Sci. Inst. **9**, 221 (1938).
[25] H. V. Neher and W. W. Harper, Phys. Rev. **49**, 940 (1936).
[26] N. S. Gingrich, Rev. Sci. Inst. **7**, 207 (1936).
[27] J. Street and T. H. Johnson, J. Frank. Inst. **214**, 155 (1932).

provided by the building itself. In position V, the apparatus was placed vertically under the pile, and in position I it was inclined toward the window at an angle ζ from the vertical (Fig. 3).

B. Determination of lead equivalent of building

In order to evaluate α', (Eq. (9)), the amount of lead equivalent in stopping power to the building was determined in the following manner. The counting rate was recorded with the apparatus in a vertical position under the scaffold with the superposed lead removed, but with 42 lead plates interposed. The apparatus was then transferred to a shack on the roof of the building, and the additional quantity of lead required to reduce the counting rate to that recorded in the basement was ascertained. The results are listed in Table II and Fig. 4. The building was found to be equivalent to 32.6 ± 2 lead plates.

In order to determine the angle ζ for which $E_0=E_\zeta$, the mass of air equivalent in stopping power to the superposed shield was calculated by means of Eq. (1). Inasmuch as the Pb plates utilized in these experiments were a 6 percent Sb-Pb alloy, the total shield thickness (building +pile) amounted to 40 g/cm² of Sb and 1060 g/cm² of Pb. Assuming the average energy of the rays during their traversal of the shield to be of the order of a billion ev, Eq. (1) gives the equivalent amounts of air as 28 g/cm² for the antimony, and 670 g/cm² for the lead, yielding a total of 698 g/cm² as the quantity of air equivalent in stopping power to the superposed shield. This assigns the angle of inclination for which $E_0=E_\zeta$ as $\zeta=\sec^{-1}(1.7)\approx54°$.

C. Results

Table III summarizes in chronological order the data used for the determination of τ_0. Runs

TABLE II. *Resumé of vertical runs for determination of stopping power of building. Run No. 131 was made in the basement under scaffold with no superposed Pb. The remainder of the runs were made in the shack on roof.*

Run No.	Pieces of Interposed Lead	Total No. of Counts	Total Time, in Hours	Quadruple Coincidences per Hour
131	42	5252	31	169.42±2.34
132	66	4286	24	178.58±2.63
134	74	3742	22	170.00±2.78
135	80	3608	22	164.00±2.74
136	76	3860	23	167.83±2.70
137	78	4152	25	166.08±2.59

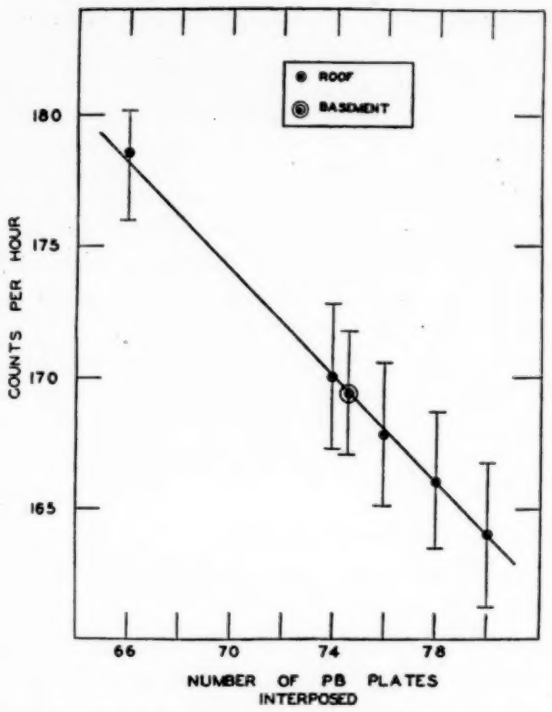

FIG. 4. Plot of the data of Table II used for the determination of the lead equivalent of the building. The points obtained on the roof give the lead absorption curve for mesons. The point obtained in the basement, with no Pb overhead, but with 42 plates of lead interposed in the counter system, is plotted on the curve with ordinate corresponding to the observed intensity. The lead equivalent of the building is the corresponding abscissa less the 42 plates of interposed lead.

with the two thicknesses of interposed lead ($t_1=36$ plates, $t_2=86$ plates) were conducted alternately in the two positions I and V. There was satisfactory evidence that no changes of sensitivity occurred during this experiment. In

TABLE III. *Resumé of data for determination of τ_0. Position V: Apparatus vertical under superposed absorbing shield. Position I: Apparatus inclined toward window, principal axis of counter train 54° from vertical.*

Run No.	Position	Interposed Pb, t	Total No. of Counts	Total Time, Hours	Quadruple Coincidences per hour
210	I	t_1	640	9	71.11±2.82
212	I	t_2	798	12	66.50±2.36
213	I	t_1	520	7	74.29±3.29
214	I	t_2	1346	20	67.30±1.84
215	I	t_1	1688	23	73.43±1.79
216	I	t_2	834	13	64.15±2.23
217	V	t_1	990	8	123.75±3.94
218	V	t_2	1306	13	100.46±2.79
219	V	t_1	1096	9	121.78±3.67
220	V	t_2	2398	24	99.92±2.04
222	I	t_1	1700	24	70.83±1.72
223	V	t_1	708	6	118.00±4.43

all of the data presented herewith, the errors indicated are standard deviations. The statistical fluctuations in hourly values were in satisfactory agreement with the deviations expected from the total number of counts. An average correction for accidentals and showers was determined for each orientation and for each thickness of interposed lead by observing the counting rate with one tray displaced out of line. The values obtained were not sensitive to lead thickness, and the average values for the two thicknesses are given in Table IV.

Figure 5 shows the theoretical ratio $j_\zeta(t)/j_0(t)$ as a function of τ_0 calculated from Eq. (14) for the two values of t used in the experiment. A value of 10^8 ev, corresponding to a rest mass of the meson equal to $200m$ has been selected for μc^2 in these calculations, and the depth fH below the top of the homogeneous atmosphere at which mesons are produced is assumed as one-tenth of an atmosphere: The two curves in each instance represent two choices of the exponent γ in the energy distribution 2 and 3. In making the calculations based upon Eqs. (14) and (16) a value 20 of the energy iH lost in passing through the atmosphere has been used. This is consistent with 78 ion pairs per cm of air, and 32 ev per ion pair, and is the theoretical value given by Eq. (1) assuming an average energy for the mesons during their traversal of the atmosphere of the order of several billion ev. The calculations are not especially sensitive to the choice of the value of iH, and the severe test of changing the value by about 15 percent without compensating with the change of angle which would be entailed modifies τ_0 in the range of the experimental results by about half a microsecond. The energies required to just penetrate the interposed shield have been calculated from the range equation[28] based upon the $1/v^2$ law. The values used are $\alpha(t_1)=6.10$ and $\alpha(t_2)=11.8$. If the value of f is increased to 0.5, the value of τ_0 found from the data is decreased by less than a microsecond. The effect of a change in γ is indicated in Fig. 5. A small change in the angle ζ has a negligible effect upon the calculated values of the ratio $j_\zeta(t)/j_0(t)$ in the region of the experimental results.

TABLE IV. *Cumulative summary of data for determination of* τ_0.

Position	Interposed Pb, t	Total No. of Counts	Total Time, Hours	Quadruple Coincidences per Hour	Correction, Counts per Hour due to Showers and Accidentals	Corrected Data, Counts per Hour
I	t_1	4548	63	72.19±1.07	2.87	$j_\zeta(t_1)=$ 69.32±1.48%
I	t_2	2978	45	66.18±1.22		$j_\zeta(t_2)=$ 63.31±1.84%
V	t_1	2974	23	121.48±2.30	5.35	$j_0(t_1)=$116.13±1.90%
V	t_2	3704	37	100.11±1.65		$j_0(t_2)=$ 94.76±1.64%

$$j_\zeta(t_1)/j_0(t_1)=0.596\pm0.021;\quad j_\zeta(t_2)/j_0(t_2)=0.668\pm0.023;\quad \frac{j_\zeta(t_1)-j_\zeta(t_2)}{j_0(t_1)-j_0(t_2)}=0.281\pm0.093$$

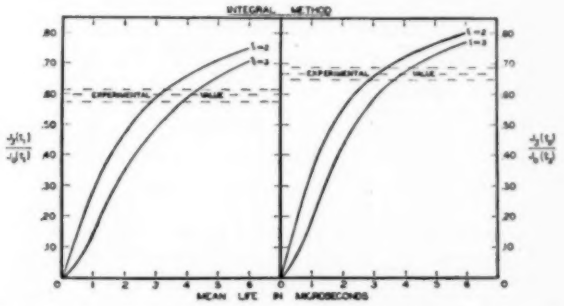

FIG. 5. The integral method for the determination of τ_0. The curves represent $j_\zeta(t)/j_0(t)$ *vs.* τ_0 calculated from Eq. (14) with $f=0.1$, $\mu c^2=10^8$ ev, $t_1=36$ lead plates, $t_2=86$ lead plates, and $\gamma=2$ and 3. The value of τ_0 corresponding to the experimental value of $j_\zeta(t)/j_0(t)$ lies between 3 and 4 microseconds.

Figure 6 is a plot of the expected values of η *versus* τ_0, calculated from Eq. (16). In this case, ϵ_1 is equal to 41 μc^2, or about 4 Bev. This calculation is less sensitive than the integral method to variations in the choice of the parameters iH and α.

V. DETERMINATION OF τ_0 FROM THE RELATIVE INTENSITIES OF THE SOFT AND HARD COMPONENTS[29]

An independent but less accurate value of τ_0 has been calculated from some measurements of the relative intensities of the soft and hard components, using the following formula derived by

[28] See e.g. reference 3, page 39.

[29] A preliminary report of this experiment was presented at the Washington meeting of the American Physical Society, April 27, 1939. A method similar in principle was proposed by J. Clay, K. Jonker, and J. Wiersma, Physica **6**, 174 (1939). In their experiment, they assumed that the ratio of the soft and hard components at a zenith angle of 60° provides a more correct value of κ.

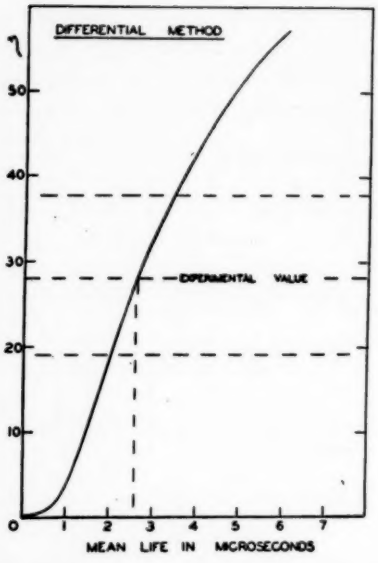

FIG. 6. The differential method for the determination of τ_0. The curve represents η *vs.* τ_0, calculated from Eq. (16), with the values of f, μc^2, and t used in the integral method. From the experimental value of η, $\tau_0=2.6$ microseconds for mesons with an initial energy $\epsilon_1=4$ Bev.

Euler and Heisenberg:[3]

$$\kappa \approx \frac{9X_0\mu c^2}{4\tau_0 c 2E_j}+\frac{\mu c^2}{2aT}, \qquad (17)$$

Here κ is the ratio of the number of disintegration electrons and their secondaries to the number of penetrating particles, X_0 is the unit of length characteristic of a particular absorber in the radiation theory and is equal to 27,500 cm in normal air, E_j is the energy at which an electron loses energy by ionization and by radiation at the same rate, and is equal to 15×10^7 ev in air, a is the rate of loss of energy by ionization of a meson in air, and T is the depth below the top of the atmosphere. The value of κ has been obtained by comparing the amount of soft component under the atmosphere and a meter of lead with that under an equal mass of air alone. The technique of the preceding experiment has been utilized for obtaining the data of Table V.

The decrease in the counting rate caused by the interposition of the first 20 lead plates in the arrangement of coincidence counters is due both to the partial absorption of mesons, and to the complete elimination of the soft radiation. Under the superposed pile of lead, the disintegration electrons are absent and the soft radiation consists of knock-on electrons produced by direct elastic impact of mesons with atomic electrons, and of the secondaries arising from these electrons according to the cascade process. When no dense medium fills the solid angle of the counter system, however, an additional soft radiation, consisting of the electrons together with their secondaries arising from the disintegration of mesons, is present. Data A' and B' of Table V show that, with the apparatus under the superposed lead, the interposition of the first 20 lead plates reduces the counting rate to 84.2 ± 2.7 percent of the original counting rate. Coincidences recorded when 20 lead plates are interposed in the system are due entirely to mesons. The data of Table I show that the subsequent interposition of 20 additional plates absorbs 8 ± 3 percent of the remaining radiation. Extrapolating to zero interposed lead thickness, we find that 91.5 ± 4.2 percent of the original counting rate was due to mesons. Therefore, the soft radiation here accounts for 8.5 ± 4.2 percent of the counting rate without interposed lead, or 9.4 ± 5 percent of the counting rate due to mesons. This agrees, within the experimental limits, with the cloud chamber, and counter observations of Trumpy.[30] However, the value obtained under these conditions is doubtlessly too small, since under the superposed shield, events may occur in which the simultaneous passage of a meson and its secondaries produces a single coincidence. We arbitrarily assume that the intensity of the soft component under lead is of the order of 1.5 times the observed value. Under air, on the other hand, the secondaries originate at a greater distance from the apparatus, and, because of their divergence, the simultaneous passage through the apparatus of the parent meson and one or more of its secondaries is less probable. Thus, the observed intensity of the soft component under air corresponds closely with the actual intensity.

According to Bhabha's[31] theory, which has been experimentally supported by the cloud-chamber observations of Lovell,[32] and by the experiments of Swann and Ramsey,[33] the number

[30] B. Trumpy, Zeits. f. Physik **113**, 582 (1939).
[31] H. J. Bhabha, Proc. Roy. Soc. **164**, 257 (1937).
[32] A. C. B. Lovell, Proc. Roy. Soc. **172**, 568 (1939).
[33] W. F. G. Swann and W. E. Ramsey, Phys. Rev. **56**, 378 (1939).

of knock-on electrons and subsequent secondaries accompanying a meson in air is roughly one-third of the number in lead, or $\frac{1}{3}\times\frac{3}{2}\times 9.4$ percent $= 5\pm 3$ percent.

Data A and B of Table V show that, under air, 77.7 ± 3.6 percent of the original counting rate is observed after the interposition of the first 20 lead plates. The percentage change of the remaining intensity, produced by the interposition of 20 additional plates, as already stated, is equal to 8 ± 3 percent. Again extrapolating to zero lead thickness, the counting rate due to mesons accounts for 84.5 ± 4.8 percent of the total counting rate with no interposed lead. From the above estimate of the number of coincidences per meson-produced coincidence, due to knock-on electrons and associated secondaries, we find that 3.9 ± 2.3 percent of the total counting rate with no interposed lead was attributable to this soft radiation. The contributions of the various components of cosmic radiation to the observed counting rate under air were therefore the following:

Mesons $= 84.5\pm 4.8$ percent
Knock-on electrons and subsequent secondaries $= 3.9\pm 2.3$ percent
Disintegration electrons and subsequent secondaries $= 11.6\pm 5.4$ percent.

From this, the ratio of the intensity of disintegration electrons and their secondaries to the intensity of mesons, κ, is equal to 0.137 ± 0.062. Solving Eq. (17) with this value of κ and with μ equal to $200m$, we find that τ_0 is equal to 6 microseconds. However, this value may be too low, as there may have been more knock-on electrons in air than have been accounted for in the calculation. Furthermore, the experimental uncertainties alone are such that within the range of the probable error, τ_0 may have any value within the range from 4 to 12 microseconds. The value of τ_0 obtained from the intensity of the soft component is slightly higher than that found from the differential and integral methods, but the difference may not be significant in view of the rather large probable error.

TABLE V. *Data for determination of* κ.

Zenith Angle	No. of Pb Plates Interposed	Total No. of Quadruple Coincidences	Total Time in Hours	Quadruple Coincidences per Hour
60°	20	1644	105.8	$A = 15.54\pm 0.50$
60°	0	1062	53.2	$B = 20.00\pm 0.61$
0°	20	1686	48.0	$A' = 35.12\pm 0.86$
0°	0	2566	61.5	$B' = 41.73\pm 0.83$

$A/B = 77.7\pm 3.6\%$; $A'/B' = 84.2\pm 2.7\%$.

VI. Discussion

The data of Fig. 5 reveal that the proper lifetime of the meson, determined by the integral method, lies between 3 and 4 microseconds, depending upon the choice of the constant γ in the energy distribution. The results for the two thicknesses of interposed lead are indeed in striking agreement. This enables one, on the strength of the experimental evidence[1, 22, 23] indicating a value of γ of about 2.8 to assign a most probable value of about 3.8×10^{-6} second to τ_0 as determined by the integral method.

The data of Fig. 6 disclose that the proper lifetime of a meson of about 4 Bev initial energy, as determined by the differential method, is about 2.6×10^{-6} second. It is difficult to conclude that this value disagrees with the value obtained by the integral method, but there is some indication that the latter method yields a longer proper lifetime. Inasmuch as the mesons whose disintegration was considered in the differential experiment are those whose energies are near the lower limit included in the integral calculation, this possible discrepancy would imply that the lower energy particles are less stable relative to the higher energy particles than is accounted for by the relativistic effect alone. In the light of the present state of our knowledge, it is premature to stress the significance of this possible discrepancy.

The uniqueness of the rest mass of the meson has not yet been established, and the existence of a variable mass would obviously play an important role in these considerations. Inasmuch as the experiments are only capable of leading to a determination of the ratio μ/τ_0, the above values of the proper lifetime would be changed by an amount proportional to the change in μ, to the first approximation. More specific information regarding the height at which mesons originate is necessary for further limiting the range of possible values of τ_0. It is possible that

the altitude of the layer at which mesons are produced varies with the energy of the particles, an assumption which has been made by Nordheim[34] in his theory of the production of mesons.

There are several arguments favoring the hypothesis that low energy mesons are less stable. The abrupt termination of meson tracks and the apparent absence of evidence for disintegration electrons in cloud chamber photographs[35] suggest that some process other than ionization and disintegration may be responsible for the removal of slow mesons from the cosmic radiation. This would also explain the failure of Montgomery, Ramsey, Cowie, and Montgomery[36] to detect disintegration electrons with their delayed coincidence counter arrangement. Moreover, despite the inaccuracy in the value of τ_0 determined from the relative intensities of soft and hard components, the fact that the value of the proper lifetime calculated on this basis is larger than those calculated by the other methods may be interpreted as indicating that slow mesons are disappearing by some process not resulting in the formation of an electron.* The high value of τ_0 equal to about 4 microseconds deduced from the analysis of the frequency of occurrence of large bursts by Montgomery and Montgomery[37] is also consistent with this hypothesis.

Finally, the existence of possible nuclear resonance effects, analogous to the selective absorption of slow neutrons, cannot be precluded, and investigations now in progress should elucidate this point. It is noted that if an effect of this nature is to account for the results, the effective cross section would have to be greater in air than in lead, and would have to be of the same order as that for disintegration, i.e., 10^{-5} per cm of air.

Acknowledgments

The author wishes to express his deepest appreciation to Dr. Thomas H. Johnson, under whose guidance this work was performed. His keen advice, earnest and untiring cooperation, and inspiring stimulation were invaluable throughout the course of these investigations. Thanks are due to Mr. Fred G. P. Seidl for his assistance in taking some of the readings, and to Dr. Enos E. Witmer, Dr. W. F. G. Swann, and Dr. C. G. Montgomery for helpful discussions. The Carnegie Institution of Washington contributed toward the support of this work.

[34] L. W. Nordheim, Phys. Rev. **56**, 502 (1939).

[35] S. H. Neddermeyer and C. D. Anderson, Phys. Rev. **54**, 88 (1938); H. Maier Leibnitz, Zeits. f. Physik **112**, 569 (1939).

[36] C. G. Montgomery, W. E. Ramsey, D. B. Cowie, and D. D. Montgomery, Phys. Rev. **56**, 635 (1939).

* *Note added in proof.*—H. Yukawa and T. Okayama have very recently published the results of calculations of the cross section for nuclear capture of mesons. (Scientific Papers of the Institute of Physical and Chemical Research **36**, 385 (1939).) For very slow mesons, their theory assigns a greater probability to this process than to disintegration.

[37] C. G. Montgomery and D. D. Montgomery, Rev. Mod. Phys. **11**, 255 (1939).

Gamma-Rays from Beryllium and Nitrogen Bombarded with Deuterons

H. R. CRANE, J. HALPERN AND N. L. OLESON
University of Michigan, Ann Arbor, Michigan

(Received October 23, 1939)

Measurements have been made on the Compton electrons ejected from a thin lamina of carbon by the gamma-rays from Be+D and N+D. Lines at 3.45 and 1.0 Mev were found in the case of Be+D and lines at 8.2, 6.6, and 5.1 Mev were found in the case of N+D, with a slight indication of two other lines at 4.1 and 2.5 Mev. Possible ways in which these lines may be correlated with the energies of the heavy particles emitted is discussed.

INVESTIGATIONS of the gamma-rays emitted when beryllium[1–4] and nitrogen[5] are bombarded with deuterons have previously been made, and it is already clear that both of these spectra are complex. We have obtained a new set of data on each of these gamma-ray spectra and we believe that sufficient improvement in technique has been accomplished so that more reliable estimates of the energies of the lines can be given that those which were possible in the earlier work. The scale of energy was calibrated directly against the 2.6-Mev line of thorium C″, and was also checked against the calibration obtained by measuring the magnetic field with a flip-coil. Targets of beryllium metal granules (Eimer and Amend) and of ammonium chloride were bombarded with a beam of deuterons of approximately 0.6 Mev energy, from the high voltage accelerating tube.[6] The resulting radiation was allowed to pass into a cloud chamber through a thin aluminum window in the glass wall. Lead blocks were used to prevent the radiation striking any part of the chamber except the window. A lamina of graphite weighing 0.24 g/cm² was placed across the center of the cloud chamber perpendicular to the direction of the radiation, to act as a source of secondary electrons. From the known absorption coefficients in the range of energies studied it was expected that the secondaries would be mainly Compton electrons. A magnetic field was applied by means of a pair of air core coils. Nonstereoscopic photographs were taken by a Sept camera located directly above the chamber. Only those tracks which were due to negative electrons originating in the graphite and having initial directions within 15 degrees of the direction of the gamma-radiation were measured and included in the data. In order to obtain data on thorium C″ a sample of mesothorium and its products of about 1 millicurie strength was placed in the position otherwise occupied by the beryllium or ammonium chloride target, and a block of lead 3 cm thick was interposed to filter out the soft gamma-ray components.

BERYLLIUM

Figure 1 shows the energy distribution of the tracks found. Referring to the 1300-gauss curve (open circles), the very steep front ending at about 3.2 Mev indicates a strong gamma-ray of 3.45±0.2 Mev. A few tracks of higher energy appear, extending up to 6.4 Mev, but it does not seem probable that these arise from Be±D. In the first place, the energy available from the reaction is not great enough to make it possible. They may be the result of some protons[2] in the ion beam, or they may be due to gamma-rays resulting from the capture of neutrons in the material near the chamber. The latter explanation seems the more plausible. No attempt was made to explore the range below 1.5 Mev with the 1300-gauss field, but for this purpose a field of 500 gauss was used. The lower field has the advantage of increasing the resolving power at low energy, but at the same time makes it impossible to measure the lines at the high end of the spectrum. The distribution obtained at

[1] H. R. Crane and C. C. Lauritsen, Phys. Rev. **45**, 226 (1934).
[2] H. R. Crane, L. A. Delsasso, W. A. Fowler and C. C. Lauritsen, Phys. Rev. **47**, 782 (1935).
[3] P. G. Kruger and G. K. Green, Phys. Rev. **52**, 773 (1937).
[4] P. G. Kruger, F. W. Stallmann and W. E. Schoupp, Phys. Rev. **56**, 297 (1939).
[5] H. R. Crane, L. A. Delsasso, W. A. Fowler and C. C. Lauritsen, Phys. Rev. **48**, 100 (1935).
[6] H. R. Crane, Phys. Rev. **52**, 11 (1937).

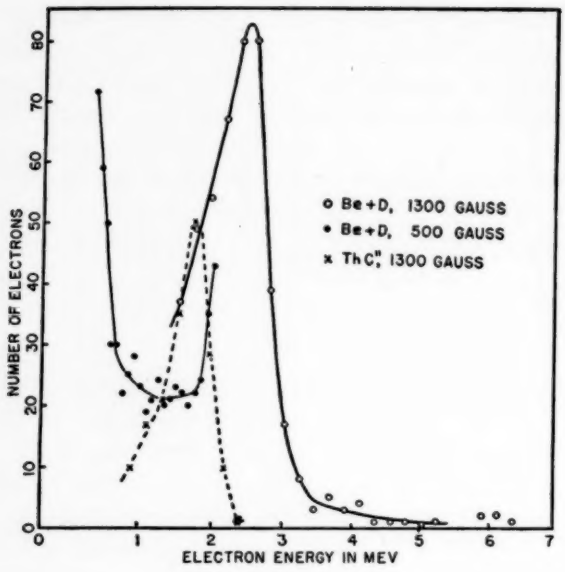

FIG. 1.

500 gauss shows that there is strong radiation of low energy. The steep front ending at 0.8 Mev indicates that there is a line at about 1 Mev, but we cannot say whether or not lines of still lower energy exist. The interpretation of this end of the spectrum is made difficult also by the presence of radiation which comes from inelastic collisions of the neutrons with the nuclei of the material surrounding the chamber, such as the copper coils.

Bonner and Brubaker[7] have found neutron groups having Q values (energies corrected for the bombarding energy and the recoil of the nucleus) of 4.25, 3.7, 2.1 and 0.8 Mev. Staub and Stephens[8] have published a neutron spectrum which is in agreement with that of Bonner and Brubaker. The simplest level scheme based upon these neutron energies would predict gamma-ray lines at 3.45, 2.15 and 0.55 Mev. Our gamma-ray spectrum gives a line in good agreement with the 3.45-Mev line which is predicted, and the strong radiation which we found at low energy could easily include the predicted 0.55-Mev line. The neutron data indicate that the product nucleus (B^{10}) is formed also on level 2.15 Mev above ground. The absence of a 2.15-Mev gamma-ray in our data indicates that this level does not combine with the ground state, and the presence of the radiation of about 1 Mev in our data would be consistent with the view that the transition occurs in two nearly equal jumps. It is premature, however, to attempt to construct an actual level diagram.

Kruger, Stallmann and Schoupp[4] have recently reported 31 gamma-ray lines from beryllium bombarded with 0.96-Mev deuterons. Although we cannot claim great enough resolving power to detect lines so close together, we find little similarity between our curves and theirs, even as to the general distribution of intensity.

NITROGEN

The energy distribution of electrons found when nitrogen was bombarded with deuterons is shown in Fig. 2. We can be quite certain of the existence of three gamma-ray lines, of 8.2 ± 0.5, 6.6 ± 0.3 and 5.1 ± 0.3 Mev. There is a slight indication of a line at about 4.1 Mev, and a somewhat better indication of a line at about 2.5 Mev. It is not possible to say anything regarding the possibility of lines below 2.5 Mev, except to say that there is none of very large intensity. Holloway and Moore[9] have recently measured the ranges of the particles emitted in the reactions $N^{14}(d\alpha)C^{12}$ and $N^{14}(dp)N^{15}$. Their results indicate that the C^{12} nucleus is formed on an excited level of 4.35 Mev and that the N^{15} nucleus is formed on two levels, 5.31 and 1.53 Mev. Previous work by others[10, 11] is in fair agreement with this. Our

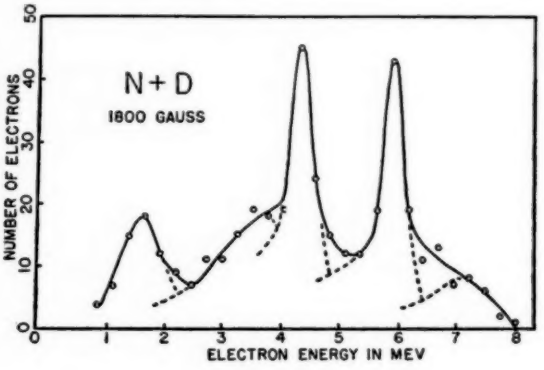

FIG. 2.

[7] T. W. Bonner and W. M. Brubaker, Phys. Rev. **50**, 308 (1936).
[8] H. Staub and W. E. Stephens, Phys. Rev. **55**, 131 (1939).
[9] M. G. Holloway and B. L. Moore, Phys. Rev. **56**, 706 (1939).
[10] J. D. Cockcroft and W. B. Lewis, Proc. Roy. Soc. **A154**, 261 (1936).
[11] E. O. Lawrence, E. McMillan and M. C. Henderson, Phys. Rev. **47**, 273 (1935).

4.1- and 5.1-Mev gamma-ray lines can probably be identified with the above 4.35- and 5.31-Mev nuclear levels. We cannot attempt to correlate the intensities of the gamma-ray lines with the intensities of the particle groups until the complete energy level scheme is known, because there may be alternative or competing ways in which an excited nucleus may make the transition to the ground state. As to our 6.6-Mev gamma-ray line, the particle ranges show that neither C^{12} nor N^{15} is formed on a level of that energy; therefore the line must arise as part of a complex transition from a higher level. The particle ranges also show that C^{12} is not formed on a level of 8 Mev, corresponding to our 8-Mev gamma-ray line, but do not preclude the possibility that the N^{15} is formed on that level. The protons in the latter case would have only 0.5 Mev, and would escape detection. One prediction can be made on the basis of the above argument: If the 8-Mev gamma-ray (and possibly others also) arises from an 8-Mev level in N^{15}, the intensities of these lines should be sensitive to the energy of the deuteron beam. This is because of the low energy of the ejected proton.

This research was made possible by a grant from the Horace H. Rackham Fund.

JANUARY 1, 1940 PHYSICAL REVIEW VOLUME 57

Zeeman Effects in Complex Spectra at Fields up to 100,000 Gauss

GEORGE R. HARRISON AND FRANCIS BITTER
Massachusetts Institute of Technology, Cambridge, Massachusetts

(Received November 4, 1939)

A newly constructed electromagnet of the Bitter type has been arranged to give fields up to 100,000 gauss, uniform to 1 percent over a volume of 25 cc. A special type of horizontal arc, with electrodes of salts compressed in silver powder, is operated at 4 amp. and furnishes light transversely to the field to three grating spectrographs, which can be used to cover the range 2000 to 8000A in a single exposure. Plane-polarized components of the light are separated with a 2-inch quartz Rochon prism, and exposures of 5 to 30 minutes give dense spectrograms at resolutions of 100,000 and greater. Plates in the ultraviolet region have been obtained for cerium, columbium, erbium, europium, gadolinium, iron, neodymium, praseodymium, rhodium, ruthenium, thorium, tungsten, and ytterbium. On most of the plates lines of the second and third spectra are more in evidence than those of the first, and air lines are prominent. Typical portions of a rhodium plate at 90,500 and 70,000 gauss are shown, and data are given for a number of cerium, rhodium, and ruthenium lines.

THOUGH the study of Zeeman effects affords one of the most powerful aids to the classification of spectra, it has been limited in great degree by the relatively weak magnetic fields which could be maintained over appreciable periods, by the small volume and lack of uniformity of these fields, and by the low intensities of light sources operated in magnetic fields. Kapitza[1] and his co-workers have produced fields up to 320,000 gauss in electromagnets, but these fields remained constant for only about 0.01 second, and were used to photograph Zeeman effects of very strong lines in simple spectra only. Jacquinot[2] and various colleagues have used the large Bellevue electromagnet for Zeeman effect studies, but the strongest fields used were apparently not over 65,800 gauss, 50,000 gauss being the usual value. Most of the Zeeman effect studies reported in the literature have involved fields of 43,000 gauss or less, obtainable with commercial iron-core magnets of the Weiss type.

The new type of electromagnet which one of us has designed[3] has been used successfully to resolve Zeeman patterns of complex spectra at fields up to 99,830 gauss, accommodating a bright electric arc with which 5- to 30-minute exposures suffice to give dense spectrograms with gratings of resolving power 100,000 and over. We have thus been able to resolve very complex

[1] Kapitza, Strelkov and Laurman, Proc. Roy. Soc. **A167**, 1 (1938).
[2] Jacquinot and Belling, Comptes rendus **201**, 778 (1935).
[3] F. Bitter, Rev. Sci. Inst. **10**, 373 (1939).

patterns, patterns arising from transitions between terms having nearly equal g values, and patterns lying at short wave-lengths. This last is of particular importance, for the wave-length splitting of a line at 2000A is only one-ninth that of a similar line at 6000A.

The Magnet

The magnet, which is shown in Fig. 1 in position before the spectrographs, has been described in detail in another paper,[3] where it may be identified as magnet No. 3. It consists of a coil composed of 200 turns of copper strip through which currents up to 10,000 amp. can be sent continuously, enclosed in a bronze jacket. Heat is removed by water which flows past the coil at the rate of 800 gallons per minute. A 1700-kilowatt motor-generator set furnishes d.c. power at voltages up to 170. Various safety devices are provided to insure that the magnet will be properly cooled during operation, and an operator who controls the current through the magnet can keep the field-strength constant to within ± 0.1 percent for hours on end.

When first assembled the magnet gave 100,000 gauss on full power, but this field fell gradually to 90,000 gauss during 20 hours of operation. On disassembling the coil it was found that electrolytic deposition between successive turns had partially short-circuited them. Improved internal insulation has been installed to offset or at least delay this deterioration.

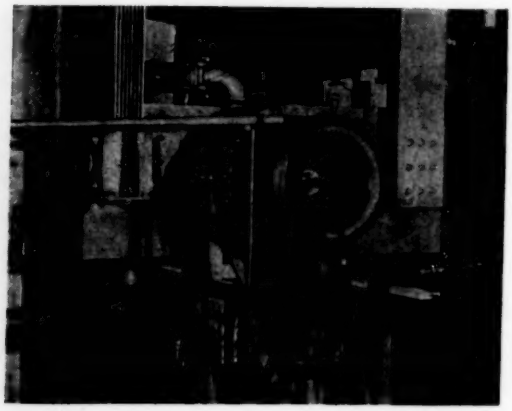

FIG. 1. The electromagnet mounted in position before two spectrographs. Currents up to 10,000 amperes are brought to the solenoid through the bus bars at left and right, while water for cooling passes through the 4-inch pipes which enter the case from above and below. One arc, with its rubber tubes carrying air and water for cooling, is in position; a spare arc, ready to be substituted quickly for the one in the coil, rests on the shelf at the right.

The Light Source

The central tube of the solenoid has an internal diameter of 3 cm and the field is constant to 1 percent over a length of 4 cm of the tube. This much greater volume of uniform flux than has been available hitherto made possible the design of a new form of arc holder, in which the arc stream could be sent parallel to the lines of force. This holder was mounted in an inner tube which would slide into the solenoid tube from one end. A central water-cooled insulated tube carries the current to one electrode; the arc is struck between this and another electrode colinear with the first, which is mounted in a holder fastened to the grounded outside of the inner tube. To conserve space both electrodes are offset from the axis of the tube, and a small crystal-quartz right-angle prism is mounted so as to throw light from the arc axially out the end of the tube toward the spectrographs. This prism is mounted on a second draw-tube which enters the solenoid tube from the end through which the light is sent, so that it can be withdrawn for rapid cleaning without disturbing the arc. A jet of air blown between the arc and the prism keeps this cool and clean for several minutes of operation, and a spare tube-and-prism unit is kept available for quick replacement.

Since it was desired to study rare earths and other elements which are most conveniently obtained as powdered salts, a new technique was necessary to obtain electrodes which could be burned in the horizontal arc. Professor John Wulff compressed mixtures of 20 percent of the desired salt and 80 percent silver powder, and produced electrodes which can be machined and held in ordinary holders. Electrodes of $\frac{1}{8}$-inch diameter are used, with currents of 4 amperes.

Even with its air or nitrogen blast in operation the arc is so stable that its holder can be moved rapidly through the air without affecting the steadiness of the arc. The arc can be inserted into the solenoid without going out only if the field is off; once in the uniform field, it can be struck at will by turning a knurled rim on the

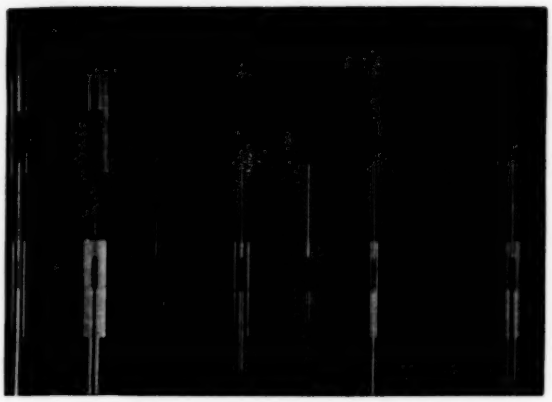

FIG. 2. Portions of the spectrum of rhodium in the region 3500 to 3460A. The spectra in order from the top represent: p component, 90,500 gauss; s component, same field; no field; s component, 70,000 gauss; p component, same field.

arc tube to advance and retract the live electrode. It then burns quietly and continuously when the arc column is established exactly parallel to the lines of force; if the arc stream starts flowing at an angle to the field a frittering noise is produced, probably due to whipping of the arc back and forth, and the brightness of the arc is diminished. Under these conditions most of the spectrum lines correspond to the spectra of singly- and doubly-ionized atoms, the lines from neutral atoms being very weak. When the arc burns quietly it is more brilliant than when the field is off.

OPTICAL ARRANGEMENTS

On account of the large power consumption of the magnet it was desired to shorten runs as much as possible, and arrangements were made to send light from the one arc simultaneously into three 35-foot concave diffraction-grating spectrographs. The right-angle prism inside the solenoid was cut with its crystalline axis parallel to its hypotenuse. The light which is sent through this, after leaving the tube, passes through a 2-inch Rochon prism of crystal quartz, transparent to 2000A, and through a quartz-fluorite achromat of 4-cm diameter and 50-cm focal length, which focuses the two polarized components of the light as twin images of the source magnified threefold and separated by about 1.5 cm. One of these is sent directly through the slit of one grating, while that part of the image which does not pass through the slit is reflected from an aluminized plane mirror to a large glass achromat which focuses it on the slit of another grating spectrograph. The second image is reflected from an aluminized plane mirror to an aluminized concave mirror, which focuses it on the slit of a third spectrograph. By rotating the Rochon prism about a horizontal axis the two polarized components of the light can be interchanged.

One component is photographed in the first order of a fairly rapid 35-foot grating, set with its normal at 3500A, and covering the range 2000 to 4300A with a dispersion of 0.8A/mm. At the same time the visible portion of this component can be photographed with a stigmatically mounted 35-foot grating, covering the range 4300 to 8000A with a dispersion of 3.3A/mm. The second component is simultaneously photographed with a third concave grating having its normal at 6000A, giving the range 2500 to 8000A at 0.8A/mm and 2000 to 4000A at 0.4A/mm. The relative speeds of these gratings are approximately as 4 : 30 : 1. In the second exposure the two components are interchanged. Since photographic plates are much slower at wavelengths above 4300A than between 2500 and

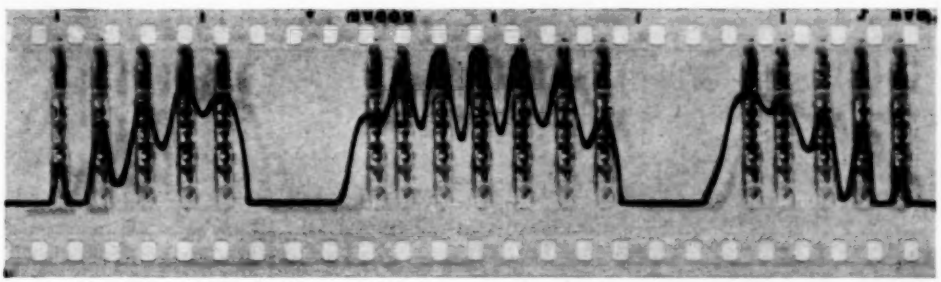

FIG. 3. Section of a record from the automatic comparator, giving density trace and wavelengths for the Zeeman pattern at 89,000 gauss of the europium line 4205.046A.

TABLE I. *Zeeman patterns for cerium II.*

WAVE-LENGTH	INTENSITY	PATTERN	$J1$ $J2$	$g1$ $g2$	COMBINATION BETWEEN TERMS
4202.944	40	(0.084) (0.249) (0.432) 0.637 0.842 1.002 1.171 1.279	$2\frac{1}{2}$ $3\frac{1}{2}$	0.732 0.904	18 115
4135.443	20*l*	(0.040) (0.137) (0.241) 0.599 0.689 0.786 0.887 0.983	$2\frac{1}{2}$ $2\frac{1}{2}$	0.740 0.836	18 230
4101.772	35 (—)	(—) (0.178) (0.290) (0.526) (0.643) (0.761) 0.472 0.594 0.700 0.813 0.927 1.054 1.173 1.285 1.407 1.519 1.623 1.740 1.855	$6\frac{1}{2}$ $6\frac{1}{2}$	1.225 1.108	$^4H_{6\frac{1}{2}}$ $^2I_{6\frac{1}{2}}$
3923.109	15	(—) (0.167) (0.286) 0.541 0.661 0.778	$2\frac{1}{2}$ $2\frac{1}{2}$	0.723 0.837	18 152
3896.804	35	(0.154) (0.474) (0.774) 0.887 1.193 1.503 1.807	$2\frac{1}{2}$ $3\frac{1}{2}$	0.728 1.036	18 127
3442.380	25	(0.096) (0.276) (0.457) 0.457 0.638 0.823 1.045	$2\frac{1}{2}$ $2\frac{1}{2}$	0.731 0.915	18 142
3341.868	40	(0.399) (0.659) 0.336 0.595 0.878	$2\frac{1}{2}$ $2\frac{1}{2}$	0.730 1.145	18 147
3314.721	25	(0) 0.947	— —	— —	14 141
3314.721	25	(—) (0.433) (0.682) (0.960) 0.204 0.461 0.729 — 1.271 1.551 1.814	$3\frac{1}{2}$ $3\frac{1}{2}$	0.868 1.138	15 147
3286.029	18	(0.224) (0.597) (0.990) 0.528 0.933 1.325 1.699	$2\frac{1}{2}$ $3\frac{1}{2}$	0.730 1.128	18 149

TABLE II. *Zeeman patterns for rhodium I.*

WAVE-LENGTH	INTENSITY	PATTERN	$J1$ $J2$	$g1$ $g2$	COMBINATION BETWEEN TERMS
3984.40	25	(—) (0.185) 1.392 1.513 1.636	$1\frac{1}{2}$ $1\frac{1}{2}$	1.571 1.453	$^4P_{1\frac{1}{2}}$ $^4P_{1\frac{1}{2}}$
3942.716	60	(0.241) 1.332 1.815	$1\frac{1}{2}$ $\frac{1}{2}$	1.573 2.657	$^4P_{1\frac{1}{2}}$ $^4P_{\frac{1}{2}}$
3748.217	200	(0.210) (0.624) 0.517 0.934 1.358 1.782	$1\frac{1}{2}$ $2\frac{1}{2}$	1.568 1.147	$^4P_{1\frac{1}{2}}$ $^4D_{2\frac{1}{2}}$
3674.765	10	(0.722) 0.485 1.929	$\frac{1}{2}$ $1\frac{1}{2}$	2.652 1.208	$^4P_{\frac{1}{2}}$ 4
3605.863	25	(0.240) (0.671) 0.914 1.353 1.795	$1\frac{1}{2}$ $1\frac{1}{2}$	1.578 1.130	$^4P_{1\frac{1}{2}}$ $^4D_{1\frac{1}{2}}$
3583.528	10	(0.177) (0.551) 1.024 1.393 1.763	$1\frac{1}{2}$ $1\frac{1}{2}$	1.578 1.262	$^4P_{1\frac{1}{2}}$ 9
3541.912	50	(0.695) 0.567 1.957	$\frac{1}{2}$ $1\frac{1}{2}$	2.652 1.262	$^4P_{\frac{1}{2}}$ 9
3525.658	50	(0.145) (0.423) 1.146 1.436 1.716	$1\frac{1}{2}$ $1\frac{1}{2}$	1.574 1.291	$^4P_{1\frac{1}{2}}$ 5
3505.409	30	(0.583) 0.917 2.072	$1\frac{1}{2}$ $\frac{1}{2}$	1.495 2.650	11 $^4P_{\frac{1}{2}}$
3469.624	100	(0.127) (0.379) 0.940 1.193 1.447 1.692	$2\frac{1}{2}$ $1\frac{1}{2}$	1.318 1.570	8 $^4P_{1\frac{1}{2}}$
3457.071	100	(0.156) (0.468) 1.106 1.417 1.732	$1\frac{1}{2}$ $1\frac{1}{2}$	1.575 1.209	$^4P_{1\frac{1}{2}}$ 4
3344.198	100	(0.710) 0.520 1.950	$1\frac{1}{2}$ $\frac{1}{2}$	1.235 2.659	19 $^4P_{\frac{1}{2}}$

TABLE III. *Zeeman patterns for ruthenium I.*

WAVE-LENGTH	INTENSITY	PATTERN							J1 J2	g1 g2	COMBINATION BETWEEN TERMS
4032.205	20		(0)	(0.429)	(0.844)				2	0.987	$^5F_2$
		—	0.972	1.419	1.859	2.275			3	1.417	$^5D_3$
3882.006	12		(0.328)	(0.655)					2	1.000	$^5F_2$
		0.682	1.013	1.323	1.637				2	1.328	$^5D_2$
3819.033	50		(0)	(0.297)	(0.591)				2	0.999	$^5F_2$
		0.682	1.001	1.299	1.589	1.890			3	1.295	$^5F_3$
3742.280	70		(0.169)	(0.309)					2	0.994	$^5F_2$
		0.847	0.994	1.142	1.306				2	1.150	$^5F_2$
3579.768	3		(0)	(0.248)	(0.497)				3	1.247	$^5F_3$
		0.755	1.001	1.243	1.496				2	1.494	17
3539.369	60		(0.624)	(1.247)					2	1.001	$^5F_2$
		0.378	1.004	1.623					2	0.378	$^5G_2$
3528.683	60		(0)	(0.202)	(0.398)				2	1.013	$^5F_2$
		0.823	1.010	1.213	1.407	1.607			3	1.211	16
3514.488	70		(0)	(0.313)	(0.622)	(0.921)			3	1.248	$^5F_3$
		0.327	0.634	0.937	1.248	1.554	1.861		3	0.940	$^5G_3$
3430.772	70		(0)	(0.123)	(0.265)				2	1.004	$^5F_2$
		0.619	0.743	0.875	1.004	—			3	0.875	$^5G_2$
3417.353	1		(0)	(0.136)	(0.259)	(0.391)			3	1.230	$^5F_3$
		0.724	0.848	0.970	1.106	1.239	1.347	1.482	4	1.101	15
3223.274	60		(0)	(0.477)					2	0.976	$^5F_2$
		—	—	1.448	1.948				2	1.457	14
3189.976	50		(0.233)	(0.457)	(0.739)				3	1.266	$^5F_3$
			1.048	1.247	1.529	1.739	1.947		3	1.501	13
3186.044	80		(0)	(0.520)					2	0.994	$^5F_2$
		0.482	0.998	1.503					1	1.508	12
3020.882	60		(0)	(0.268)	(0.540)				2	1.007	$^5F_2$
		0.741	1.002	1.289	1.560	1.821			3	1.280	11
2905.650	50		(0)	(0.480)	(0.939)				2	0.986	$^5F_2$
		0.532	1.003	1.449	1.932	2.344			2	1.452	10

4300A, and since less resolution and dispersion are needed for the patterns of longer wave-length, resolution may well be sacrificed for speed in the visible region.

SPECTRA STUDIED

From 12 to 21 plates each 20 inches long are exposed simultaneously to the spectrum from 2000 to 8000A. Exposures have ranged from five minutes to half an hour, and five exposures are usually taken on each set of plates. The two strongest silver lines usually produce over-exposed Zeeman patterns in 1 minute. Runs have been made on cerium, columbium, erbium, europium, gadolinium, iron, neodymium, praseodymium, rhodium, ruthenium, thorium, thulium, tungsten, and ytterbium. On most of the plates the second and third spectra are more in evidence than the first, and air lines are prominent.

Typical portions of a rhodium plate are shown in Fig. 2. In Fig. 3 is shown a pattern of a europium line as traced and measured on the automatic density comparator.[4] This instrument is particularly useful with Zeeman patterns, for wave-lengths or wave numbers of hundreds of patterns on one plate, some split into as many as 27 components, can be recorded to seven-figure

[4] G. R. Harrison, J. Opt. Soc. Am. **25**, 169 (1935).

precision in two minutes, with results for resolved lines which are more precise than those obtained by ordinary methods.

Results Obtained

The data for the various elements are being used in the classification of their respective spectra, and will be published in full separately. Typical results for cerium, rhodium, and ruthenium are recorded in Tables I, II, and III, in which column 1 gives the wave-length as given by the M.I.T. Tables,[5] column 2 the arc intensity from the same source, column 3 the Zeeman pattern in terms of the normal separation, column 4 the J values of the combining terms, column 5 the g values of the combining terms, and column 6 the term combination.

Data have been included in the tables whereby the g values of certain levels are determined from six or more lines. Average g values are found to be consistent within 0.003 unit, and can probably be determined at wave-lengths longer than 3000A to within 0.1 percent. The principal uncertainties in the g values arise from uncertainties in the determination of field intensities, which have thus far been obtained only from lines showing the normal Zeeman effect.

Of particular interest in the cerium data are the confirmations of unusual classifications of lines given by Albertson and Harrison[6] in Ce II. The line Ce 3314.732A was classified as two independent transitions; under the influence of the field it broke up into two patterns which correspond to the proper pairs of J values. The line Ce 4101.772 was classified as $6\frac{1}{2}-6\frac{1}{2}$, and is shown by its pattern to be ${}^4H_{6\frac{1}{2}}-{}^2I_{6\frac{1}{2}}$. Hundreds of other line classifications have been confirmed and extended.

Acknowledgments

We are grateful to Dr. A. R. Kaufmann for assisting in the operation of the magnet during the first exposures, when its behavior was uncertain, and to Julius Molnar and Henry Rich for aiding in the operation of the spectrographs. The work has been greatly assisted by grants from the Penrose Fund of the American Philosophical Society for the operation of the magnet, from the Rumford Fund of the American Academy of Arts and Sciences for the provision of the chemicals whose spectra were studied, and from the Hale Spectroscopic Fund for apparatus.

[5] *M. I. T. Wavelength Tables* (John Wiley & Sons, New York, 1939).

[6] W. Albertson and G. R. Harrison, Phys. Rev. **52**, 1209 (1937).

Internuclear Distances in Se_2, Te_2, and HgCl by Electron Diffraction

LOUIS R. MAXWELL AND V. M. MOSLEY
Bureau of Agricultural Chemistry and Engineering, U. S. Department of Agriculture, Washington, D. C.

(Received October 23, 1939)

Electron diffraction photographs have been obtained from the gas molecules Se_2, Te_2, and HgCl. The internuclear distances found for Se_2 and Te_2 were 2.19±0.03A and 2.59±0.02A, respectively, while for HgCl a separation of 2.23±0.03A was obtained. Additional photographs were taken of $HgCl_2$ indicating an Hg-Cl distance of 2.27±0.03A near to the above value for HgCl. Comparison is made with band spectrum data on the internuclear distances for Se_2 and Te_2.

INTRODUCTION

MEASUREMENTS of the internuclear separations in diatomic selenium and tellurium have been undertaken by the electron diffraction method since band spectrum values for these distances are somewhat uncertain. In general, the rotational structure for the sulphur group molecules S_2, Se_2, and Te_2 has been difficult to analyze. In the case of S_2 the internuclear separation was obtained by the electron diffraction method[1] after several widely variant band spectrum values for this distance had been reported. Olsson[2] has given values for the rotational constants of Se_2 which involve a measurement of small combination frequency differences. Przeborski[3] has reported several possible distances for the ground state of Te_2 from band spectrum data. No information is available on the nuclear separation in HgCl although an indication of the distance to be expected can be obtained from previous electron diffraction work[4] on $HgCl_2$.

PROCEDURE AND EXPERIMENTAL ARRANGEMENT

Electron diffraction photographs were obtained by the transmission method through concentrated beams of the gas molecules. The method of analysis used, which has been previously described,[5] involved only visual measurements of the electron diffraction patterns. For the study of selenium it was necessary to raise the temperature of the vapor to at least 750°C at about 100 mm of Hg pressure in order to dissociate the higher molecular forms of selenium to Se_2.[6] Fig. 1 illustrates the quartz boiler used for this purpose. A nozzle 15 mm long having a bore 0.4 mm in diameter was heated to about 900°C to ensure the presence of a sufficient number of Se_2 molecules for diffraction. The lower part of the boiler containing the supply of material was kept at approximately 615°C for vaporizing the selenium. Three platinum radiation shields not illustrated were placed around the boiler for reduction of heat losses. The jet temperatures were measured by means of an optical pyrometer. For the case of tellurium and mercurous chloride a metal boiler as described previously[5] was used. The plate

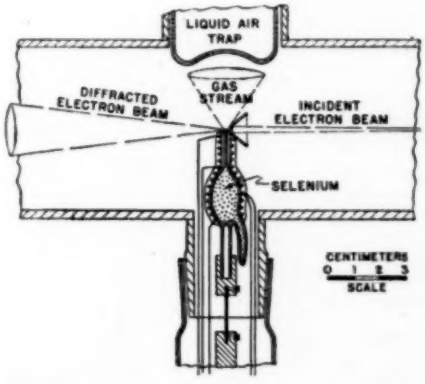

FIG. 1. Diagram of quartz boiler used in obtaining electron diffraction photographs from selenium.

[1] L. R. Maxwell, V. M. Mosley and S. B. Hendricks, Phys. Rev. **50**, 41 (1936).
[2] E. Olsson, Zeits. f. Physik **90**, 138 (1934); also Doctor's Thesis, Stockholm Högskola, October, 1938.
[3] A. Przeborski, Zeits. f. Physik **63**, 280 (1930); Acta phys. polon. **3**, 527 (1934), abstracted in Chemisches Zentralblatt **107**, 3640 (1936).
[4] H. Braune and S. Knoke, Zeits. f. physik. Chemie **B23**, 163 (1933); A. H. Gregg, G. C. Hampson, G. I. Jenkins, P. L. F. Jones, and L. E. Sutton, Trans. Faraday Soc. **33**, 852 (1937).
[5] L. R. Maxwell, S. B. Hendricks and V. M. Mosley, J. Chem. Phys. **3**, 699 (1935).
[6] G. Preuner and I. Brockmöller, Zeits. f. physik. Chemie **81**, 129 (1912–13).

TABLE I. *Summary of electron diffraction results obtained from* Se_2, Te_2, *and* HgCl. *Numbers in parenthesis give the number of plates measured. Variations given are the average deviations from the mean without regard for sign.*

Maximum	x	Se_2 $(1/\lambda)\sin\frac{1}{2}\theta$	l	Te_2 $(1/\lambda)\sin\frac{1}{2}\theta$	l	HgCl $(1/\lambda)\sin\frac{1}{2}\theta$	l
1	—	present	—	present	—	present	—
2	13.70	0.498 (6)	2.19±0.03	0.4218 (8)	2.58±0.03	0.493 (11)	2.21±0.03
3	20.20	0.730 (6)	2.20±0.03	0.6185 (8)	2.60±0.02	0.719 (10)	2.23±0.02
4	26.50	0.963 (3)	2.19±0.01	0.8146 (8)	2.59±0.02	0.933 (4)	2.26±0.02
5	32.95	1.192 (2)	2.20±0.01	1.0176 (3)	2.58±0.01		
Average Values		2.19±0.03A		2.59±0.02A		2.23±0.03A	

distance was 10 cm and the de Broglie wavelengths ranged between 0.064 to 0.074A.

RESULTS AND DISCUSSION

Selenium[7]

Table I contains a summary of the electron diffraction results obtained from the molecules studied. Five interference maxima were obtained for Se_2 agreeing closely in intensity and position with the values required by a diatomic molecule.

The average value of the nuclear separation obtained from the various maxima is 2.19±0.03A. This distance can be compared with Olsson's[2] band spectrum value of 2.15A for a $^1\Sigma$ ground state which is slightly lower than the electron diffraction value but almost within the range of the average deviations obtained by the electron diffraction method. A somewhat similar situation arose for the case of S_2 where Olsson's band spectrum value for a $^3\Sigma$ ground state gave 1.88A while the electron diffraction value was 1.92±0.03A. He has suggested that this small difference might be due to the S_2 molecule having a $^1\Sigma$ state with nearly the same energy as the $^3\Sigma$ ground state but with somewhat greater nuclear separation, thus making the average electron diffraction value slightly higher than the band spectrum separation.

Magnetic measurements on selenium vapor by Bhatnagar, Lessheim, and Khanna[8] show that as the temperature is raised towards 1000°C the gas becomes paramagnetic due to the presence of Se_2 molecules. They concluded therefore that the ground level of Se_2 is a $^3\Sigma$ state. In view of these magnetic measurements Olsson has postulated that Se_2 also may have two low energy states, a $^1\Sigma$ and $^3\Sigma$ with a small energy difference between them. Assuming this situation for the Se_2 molecule the electron diffraction value may represent an average of these two levels and thus possibly give a greater internuclear distance than reported by Olsson. However, Rosen[9] has questioned the existence of a $^1\Sigma$ ground state on the basis of his absorption spectrum determinations which seem to indicate that the main system can be represented by $^3\Sigma\rightarrow{}^3\Sigma$ instead of $^1\Sigma\rightarrow{}^1\Sigma$ transition.

Photographs were also taken from the selenium vapor directly without providing any special means for dissociation. This low temperature form contained higher polymers which gave a different type of pattern both as regards intensity and position of the interference rings. Howe and Lark-Horovitz[10] have previously obtained such electron diffraction photographs and the positions of the maxima found in the present work are in essential agreement with their results. Actually, maxima were found at $(1/\lambda)\sin\frac{1}{2}\theta = 0.16$, 0.29, 0.46, 0.709, and 0.897 as compared with the values 0.157, 0.290, 0.454, and 0.698, respectively, determined by Howe and Lark-Horovitz.

Tellurium[11]

Little information is available concerning the vapor density of tellurium, so the material was heated in a simple type boiler until sufficient vapor was emitted to give electron diffraction photographs. The type of pattern formed showed clearly that the molecule was diatomic, as de-

[7] Preliminary report, L. R. Maxwell and V. M. Mosley, Phys. Rev. **55**, 238 (1939).
[8] S. S. Bhatnagar, H. Lessheim, and M. L. Khanna, Nature **140**, 152 (1937); Proc. Ind. Acad. **A6**, 155 (1937).
[9] B. Rosen, Physica **6**, 205 (1939).
[10] J. D. Howe and K. Lark-Horovitz, Phys. Rev. **51**, 380 (1937).
[11] Preliminary report, L. R. Maxwell and V. M. Mosley, Phys. Rev. **51**, 684 (1937).

termined by the intensities and positions of the interference maxima. In Table I a summary of the results obtained gives 2.59±0.02A as the average nuclear separation for Te_2. Table II lists the internuclear distances of the sulphur-group molecules which have been measured by the electron diffraction method. Various possible band spectrum values for Te_2 obtained by Przeborski[3] are 2.87A, 2.77A, and 2.44A; none of these, however, is in agreement with the electron diffraction value.

Huggins[12] has calculated by a semi-empirical method the nuclear separation of Te_2 from the vibrational constants ω_e, $\omega_e x_e$, and a basic radius obtained from I_2. This led to $r_e = 2.61$A, which is in good agreement with the electron diffraction value. A separation of 2.55A for r_e was given by Huggins for Te_2, using an empirical formula developed by Badger; this is also near to the electron diffraction distance.

Mercurous chloride (HgCl)[7]

Considerable uncertainty has existed concerning the nature of mercurous chloride vapor. Vapor density measurements generally agree on the composition of the vapor as either HgCl or $Hg+HgCl_2$, these alternatives being indistinguishable by this method. Gucker and Munch[13] found that dry mercurous chloride vapor, when sublimed in a vacuum at 200°C on a liquid-air trap, shows no decomposition as determined by the absence of a mercury deposit. This indicates that if mercurous chloride were heated in the electron diffraction boiler it might give a vapor which has a high concentration of the single HgCl molecules. The interference pattern obtained was characteristic of a diatomic molecule and led to a nuclear separation of 2.23±0.03A as summarized in Table I. The photographs were rather poor; this is to be expected on account of the large scattering power of the mercury atom as compared to chloride. Chemical analysis[14] made of the material deposited on the liquid-air trap after the exposures had been made showed that at least 95 percent remained as the mercurous compound. Additional identification of HgCl in this deposit was made by x-ray powder photographs.[15] It is safe to conclude therefore that the material studied was the HgCl molecule. Electron diffraction results from $HgCl_2$ by Braune and Knoke[4] gave a Hg-Cl separation of 2.28A, which agrees fairly well with the present value for HgCl. However, Gregg, Hampson, Jenkins, and Jones[4] have reported a somewhat larger distance of 2.34±0.01A for the HgCl distance in $HgCl_2$. In view of the small error which these workers have reported for their distance, it appears that their Hg-Cl separation is definitely greater than the value obtained here for the mercurous compound.

In order to provide additional information on the possible constancy of the Hg-Cl distance, photographs were also taken of $HgCl_2$ with the same boiler and experimental set-up as used for HgCl. The $(1/\lambda)\sin\frac{1}{2}\theta$ values obtained for the 2nd, 3rd, and 4th maxima were 0.484, 0.709, and 0.922, respectively, with an average variation of about 1 percent. These data agree closely with the results of Braune and Knoke who gave the values 0.484 and 0.696 for the positions of the 2nd and 3rd maxima, but they are slightly higher than 0.474, 0.691, and 0.907, which are the respective positions given by Gregg *et al.* Since the Hg-Cl scattering term for this molecule is large compared to the Cl-Cl term, the x values for the different maxima are close to those obtained for a diatomic molecule. Thus if we take the x values used above for the diatomic molecules, i.e., 13.7, 20.2, and 26.5, we obtain Hg-Cl distances of 2.25, 2.27, and 2.29A, respectively, which give an average of 2.27±0.03A. This distance is only slightly greater than the above value for Hg-Cl in the mercurous chloride molecule.

TABLE II. *Internuclear distances of the sulphur-group molecules determined by the electron diffraction method. Variations given are the average deviations from the mean without regard to sign.*

Molecule	Separation (A)
S_2	1.92±0.03
Se_2	2.19 0.03
Te_2	2.59 0.02

[12] M. L. Huggins, J. Chem. Phys. **4**, 308 (1936); J. Chem. Phys. **5**, 201 (1937).

[13] F. T. Gucker, Jr. and R. H. Munch, J. Am. Chem. Soc. **59**, 1275 (1937).

[14] The authors are indebted to Mrs. E. K. Rist of this laboratory for carrying out this analysis.

[15] The authors are indebted to Dr. Sterling B. Hendricks for taking the x-ray powder photographs of the mercurous chloride deposits.

Multiple Scattering of Electrons

See pg 552, 573

S. GOUDSMIT AND J. L. SAUNDERSON*
University of Michigan, Ann Arbor, Michigan

(Received November 8, 1939)

A theoretical treatment of multiple Rutherford scattering is given which is exact if one considers electrons with the same total path length in the scatterer. The approximations necessary for the actual solution of the problem for a thin scatterer can be shown to have little effect on the results for small angle scattering. The distribution of scattering is expressed as a series in Legendre polynomials which has been evaluated numerically; the final result for thin scattering is approximately a Gaussian curve. It is shown that this distribution depends in a sensitive way upon the deviation from the Rutherford law for small angle scattering due to screening by electrons. This may perhaps explain the discrepancies between experiments and theory.

1. INTRODUCTION

EXPERIMENTS on the scattering of electrons have, to some extent, lacked importance because of the uncertainties concerning their interpretation. It is very difficult to investigate any theory of single scattering since observation must be made at large angles where the intensity of scattered electrons is very small. Moreover, for somewhat smaller angles, it is difficult to determine exactly how multiple scattering influences the observed scattering. The Wentzel criterion, which is at best only a qualitative statement and can even be shown to be too lenient, is of very little help. A general theory of scattering would therefore be an immense help, inasmuch as it could be compared with observations made on small angle scattering. In principle, this paper uses a method which should yield the complete distribution of scattering. So far, however, calculations have been made which give information concerning only the multiple scattering regions; to extend the theory in order to find the distribution at larger angles requires, as will be seen, additional refinements and calculations.

The most recent theoretical treatment of this problem has been given by E. J. Williams.[1] Comparison of Williams' results with the experimental data[2] indicates a rather serious and consistent discrepancy. Though somewhat more involved mathematically, the present paper uses a different method of approach and one which is to a certain extent exact. To facilitate the calculations, certain approximations are made, but the theory shows clearly at which points the use of approximations may influence the results.

2. THE USE OF LEGENDRE POLYNOMIALS

In the following, we think of a particle being scattered a certain number of times, n, after which it has a certain direction, θ. It is a property of the Legendre polynomials that the average value of any polynomial after n impacts is equal to the nth power of the average value of the polynomials after one impact, provided that the law of scattering is cylindrically symmetrical.[3] To show this, let θ_1 be the angle of deflection after the first collision, and θ_2 that caused by the second. If the two azimuthal angles are ϕ_1 and ϕ_2, respectively, and the total deviation from the original direction, θ, the addition theorem for spherical harmonics gives the relation

$$P_l(\cos\theta)=P_l(\cos\theta_1)P_l(\cos\theta_2)+\sum_m P_l^m(\cos\theta_1)P_l^m(\cos\theta_2)\sin m(\phi_2-\phi_1). \quad (1)$$

If the elementary law of scattering has cylindrical symmetry, the average over $\sin m(\phi_2-\phi_1)$ gives zero, and only the first term remains. A repetition of this averaging process for n collisions yields

* Now at the Dow Chemical Company.

[1] E. J. Williams, Proc. Roy. Soc. **169**, 531 (1939).

[2] W. A. Fowler, Phys. Rev. **54**, 773 (1938); N. L. Oleson, K. T. Chao, J. Halpern, H. R. Crane, Phys. Rev. **56**, 482 (1939); C. W. Sheppard and W. A. Fowler, Phys. Rev. **56**, 849 (1939).

[3] Compare L. S. Ornstein, Proc. Amsterdam Acad. **40**, 464 (1939).

the result stated above, that[4]

$$\langle P_l(\cos\theta)\rangle_n = \langle P_l(\cos\theta_1)\rangle_{\text{Av}}{}^n. \tag{2}$$

The final total average of any Legendre polynomial will be the average considering all possible values of n, the number of collisions suffered by the electron. Denoting the average by G_l, and by $W(n)$, the probability that an electron makes n collisions, we have

$$G_l = \sum_0^\infty W(n)\langle P_l(\cos\theta_1)\rangle_{\text{Av}}{}^n. \tag{3}$$

These averages completely determine the angular distribution of the emerging electrons. The intensity of scattering per unit solid angle in the direction θ is given by

$$f(\theta) = \frac{1}{4\pi}\sum(2l+1)G_l P_l(\cos\theta). \tag{4}$$

This function can be evaluated numerically, if necessary, for various values of θ, when the averages G_l are known. It is well to notice that this formula is normalized such that

$$2\pi\int_0^\pi f(\theta)\sin\theta d\theta = 1 \tag{5}$$

and that all averages are meant to be taken over the spherical distribution. For example, G_l would be given by the relation

$$G_l = 2\pi\int_0^\pi P_l(\cos\theta)f(\theta)\sin\theta d\theta. \tag{6}$$

With the G_l known, various other averages can easily be obtained from the explicit expressions for the polynomials, such as,

$$\langle\cos\theta\rangle_{\text{Av}} = G_1, \tag{7}$$

$$\langle\cos^2\theta\rangle_{\text{Av}} = \tfrac{1}{3}(1+G_2), \tag{8}$$

$$\langle\sin^2\theta/2\rangle_{\text{Av}} = \tfrac{1}{2}(1-G_1), \tag{9}$$

$$\langle\sin^4\theta/2\rangle_{\text{Av}} = \tfrac{1}{8}(2-3G_1+G_2), \text{ etc.} \tag{10}$$

The main problem is thus reduced to the evaluation of the average values of the Legendre polynomials. In order to do this, we must know the probability distribution of the number of impacts suffered by an electron traversing a scattering material and, also, the average values of the Legendre polynomials for a single collision according to the chosen law of scattering.

3. The Number of Collisions

We shall denote the total collision cross section of an atom by $\pi\rho^2$, the number of atoms per cc by N and the thickness of the scatterer by t. The average number of collisions ν which one electron makes in traversing the scatterer is

$$\nu = \pi\rho^2 Nt. \tag{11}$$

The probability that an electron has n collisions is expressed by a Poisson distribution

$$W(n) = e^{-\nu}\nu^n/n! \tag{12}$$

This formula would be strictly valid if t were the true path length of the electron in passing through the foil, and if this path length were the same for all electrons. It will be pointed out below that this uncertainty in actual length of path in the foil can have very little effect upon the accuracy of the results when foils of such thickness are used such that the distribution of the emerging electrons does not approach complete diffusion.

Using the Poisson formula (12) in (3), we obtain

$$G_l = \sum e^{-\nu}\nu^n\langle P_l(\cos\theta_1)\rangle_{\text{Av}}{}^n/n! = e^{-\nu Q_l}, \tag{13}$$

where

$$Q_l = 1-\langle P_l(\cos\theta_1)\rangle_{\text{Av}}. \tag{14}$$

In most cases we shall find that $Q_l \ll 1$ for a large range of values of l. Therefore, any probability distribution $W(n)$ which has a rather sharp maximum at $n=\nu$ will yield the result given in

---

[4] If we restrict ourselves to small angles, we can use the approximation

$$P_l(\cos\theta) \sim J_0(l\theta).$$

The average value after n trials is again the nth power of the average after one trial

$$\langle J_0(l\theta)\rangle_{\text{Av}} = \langle J_0(l\theta_1)\rangle_{\text{Av}}{}^n.$$

This can be proved strictly for a centrally symmetrical probability distribution of a variable θ in a plane using the addition theorem of Bessel functions. The coefficient l can then have arbitrary values, but should be chosen equal to the roots of J_0 for use in expansions in series. For a symmetrical probability distribution of the variable θ on a line it is easy to show that $\cos l\theta$ is the function which possesses this multiplicative property of the averages.

Eq. (13). This can, for instance, be verified easily when $W(n)$ is assumed to be Gaussian. Unless the distribution $W(n)$ is very wide and has a half-width of the same order as the average value, the result will still be almost identical with Eq. (13). It is understood that $\nu \gg 1$, if we are to have multiple scattering.

It is fortunate that the result given in Eq. (13) does not require an exact knowledge of $W(n)$ for thin scatterers. When the average path length is taken as the actual thickness t of the foil, the value obtained for ν will be slightly too small. This can be corrected to a first approximation by taking for the path length $t/\langle\cos\theta\rangle_{Av} = t/G_1$. Important modifications may be necessary only when the scatterer is very thick, in which case $W(n)$ becomes very wide, and also, perhaps, when the atoms of the scatterer are distributed in some regular way as in single crystals.

4. The Scattering Law

The following formulas can be expressed conveniently in terms of

$$y = \sin\theta/2. \tag{15}$$

The distribution of scattering for a single collision, normalized for one incident electron per cm², can be written

$$2\pi I(\theta)\sin\theta d\theta = 2\pi\kappa^2 g(y)dy/y^3, \tag{16}$$

where

$$\kappa = (Ze^2/mc^2)(1-\beta^2)^{\frac{1}{2}}/\beta^2, \tag{17}$$

in which the symbols have their usual meaning. The factor $g(y)$ is applied to the Rutherford formula in order to correct for the screening of the nucleus by the orbital electrons. For a bare nucleus $g(y)=1$. For neutral atoms $g(y)$ approaches unity rapidly for larger angles of scattering, that is, as y approaches unity. For values of y near zero, $g(y)$ is very small and keeps the various integrals over y from diverging. The total cross section per atom is

$$\pi\rho^2 = 2\pi\kappa^2\int_0^1 g(y)dy/y^3. \tag{18}$$

We consider three cases for $g(y)$:

A. *Rutherford scattering with a sharp cut-off of the Coulomb field at the radius a.* From classical calculations we obtain

$$\begin{aligned} g(y) &= 1 \quad \text{for} \quad y > y_0 \\ g(y) &= 0 \quad \text{for} \quad y < y_0, \end{aligned} \tag{19}$$

where

$$y_0 = (1+a^2/\kappa^2)^{-\frac{1}{2}} \sim \kappa/a. \tag{20}$$

B. *The Born approximation for a field of the form*

$$V(r) = (Ze^2/r)e^{-r/a}. \tag{21}$$

This gives[5]

$$g(y) = y^4/(y^2+y_0'^2)^2, \tag{22}$$

with

$$y_0' = \lambda\!\!\!^{-}/2a, \tag{23}$$

in which $2\pi\lambda\!\!\!^{-}$ is the wave-length of the incident electron. The exponential factor is supposed to represent approximately the screening effect. In both cases A and B, it is usual to take

$$a = a_0/Z^{\frac{1}{3}} = \hbar^2/me^2Z^{\frac{1}{3}}, \tag{24}$$

where a_0 is the Bohr radius of hydrogen. Hence,

$$y_0' = \tfrac{1}{2}(e^2/\hbar c)Z^{\frac{1}{3}}/(w^2-1)^{\frac{1}{2}}, \tag{25}$$

in which w is the total energy of the particle in units mc^2.

C. *The field as given by the Thomas-Fermi atom.* The function $g(y)$ can be obtained easily from the tables of Bullard and Massey.[6]

5. The Average Values of the Legendre Polynomials After One Collision

We use Murphy's expansion expressing the Legendre polynomials in powers of $\sin\theta/2$,

$$P_l(\cos\theta) = \sum_0^l (-1)^k \frac{(l+k)!}{(l-k)!k!^2} y^{2k}. \tag{26}$$

The average value after one collision is

$$\langle P_l(\cos\theta_1)\rangle_{Av} = 2\pi\kappa^2 \sum_0^l (-1)^k \frac{(l+k)!}{(l-k)!k!^2} \times \int_0^1 g(y)y^{2k-3}dy/\pi\rho^2. \tag{27}$$

Substituting for $\pi\rho^2$ as given in Eq. (18), and separating from the summation the first two

[5] G. Wentzel, Zeits. f. Physik **40**, 590 (1927).

[6] E. C. Bullard and H. S. W. Massey, Proc. Camb. Phil. Soc. **26**, 556 (1930) or N. F. Mott and H. S. W. Massey, *Atomic Collisions* (Oxford, 1933), p. 126.

terms, we obtain

$$\langle P_l(\cos\theta_1)\rangle_{Av}=1-Q_l=1-2(\kappa^2/\rho^2)$$
$$\times\left[l(l+1)\int_0^1 g(y)dy/y\right.$$
$$\left.-\sum_2^l(-1)^k\frac{(l+k)!}{(l-k)!k!^2}\int_0^1 g(y)y^{2k-3}dy\right]. \quad (28)$$

6. The Average Values After Multiple Scattering

The average number of collisions in a path length t is

$$\nu=\pi\rho^2Nt.$$

If the conditions mentioned in Section 3 are valid, we find for the final averages of the Legendre polynomials

$$G_l=e^{-\nu Q_l}$$

with

$$\nu Q_l=2\pi\kappa^2Nt\left[l(l+1)\int_0^1 g(y)dy/y\right.$$
$$\left.-\sum_2^l(-1)^k\frac{(l+k)!}{(l-k)!k!^2}\int_0^1 g(y)y^{2k-3}dy\right]. \quad (29)$$

It is important to note that the factor in front is always the same, independent of $g(y)$.

7. Evaluation of the Integrals

We shall denote the sum in the bracket expression of Eq. (29) by S_l and consider it first. For the higher powers of y, the main contribution to the integrals comes from the region near $y=1$ where $g(y)=1$ and thus we can approximate the result by omitting the screening factor. This gives

$$S_l=\sum_2^l(-1)^k\frac{(l+k)!}{(l-k)!k!^2}\frac{1}{(2k-2)}$$
$$=l(l+1)(\tfrac{1}{2}+\tfrac{1}{3}+\tfrac{1}{4}\cdots+1/l). \quad (30)$$

The proof we have for this last identity is somewhat too lengthy to be included in this paper.[7]

[7] The sum is also equal to

$$2(l+1)\sum_2^l(-1)^k c(l,k)/(2k-2),$$

where $c(l,k)$ denotes binomial coefficients.

The omission of $g(y)$ is not permissible for very large values of l. This can be shown most easily by taking the example of case A, which gives for the sum

$$S_l=\sum_2^l(-1)^k\frac{(l+k)!}{(l-k)!k!^2}\frac{1-y_0^{2k-2}}{(2k-2)} \quad (31)$$

as long as

$$ly_0\ll 1. \quad (32)$$

The approximation (30) is sufficient, but for larger l values the terms containing y_0 do not decrease at first and may, therefore, give appreciable contributions. The relation $ly=1$ gives the approximate value of y where the Legendre polynomial has its first root.

Writing for the first integral in Eq. (29)

$$\int_0^1 g(y)dy/y=\log\xi, \quad (33)$$

and using Eqs. (19) and (20), we find by direct integration for case A,

$$\log\xi_A=\log(a/\kappa). \quad (34)$$

In a similar manner for case B, with the use of Eqs. (22) and (23), integration gives

$$\log\xi_B=\log(2a/\lambda\!\!\!^{-})-\tfrac{1}{2}=\log(1.21a/\lambda\!\!\!^{-}). \quad (35)$$

Finally, from an approximate numerical integration of Bullard and Massey's data for the Thomas-Fermi field,[8] the result is

$$\log\xi_C=\log(1.10a/\lambda\!\!\!^{-}). \quad (36)$$

Assuming in all cases that $a=a_0/Z^{\frac{1}{3}}$, we see that cases B and C give practically the same result. Case A, however, usually differs very much from the other two, since

$$\xi_B/\xi_A\sim\kappa/\lambda\!\!\!^{-}=(Z/137)w^{\frac{1}{2}}/(w^2-1)^{\frac{1}{2}}.$$

For the radius of the total scattering cross section in each case, we find

$$\rho_A=a$$
$$\rho_B=2\kappa a/\lambda\!\!\!^{-}$$
$$\rho_C=2.9\kappa a/\lambda\!\!\!^{-}.$$

It is possible, of course, to choose a different value for a in each case so as to yield equal

[8] In the formula following formula (13) on page 125 in Mott and Massey, reference 6, the exponent 17/3 should read 7/3.

values for ρ or ξ. It is clear that the results are quite sensitive to the behavior of $g(y)$ near $y=0$.

In view of Eqs. (30) and (33), we may now write for the average value of the Legendre polynomials after multiple scattering

$$G_l=e^{-2\pi s^2 Ntl(l+1)\,[\log \xi-(\frac{1}{2}+\frac{1}{3}+\cdots+1/l)]}, \quad (37)$$

for not too large values of l. The restriction on l is that the exponent must remain negative (compare Eq. (32)).

8. The Probability Distribution for Multiple Scattering

As was mentioned above, it is possible to write the scattering probability as a series in Legendre polynomials. This was given by Eq. (4)

$$f(\theta)=\frac{1}{4\pi}\sum(2l+1)G_lP_l(\cos\theta).$$

The summation does not need to be extended to too large values of l, the restriction being given in this case by Eq. (32).

An approximate Gaussian behavior of $f(\theta)$ for small angles would have the form

$$4\pi f(\theta)=e^{-y^2/\alpha^2}/\alpha^2\sim e^{-\theta^2/4\alpha^2}/\alpha^2. \quad (38)$$

Note that this Gaussian curve is again normalized to unity on the sphere, that is,

$$2\pi\int_0^\pi f(\theta)\sin\theta d\theta\sim\int_0^\infty e^{-y^2/\alpha^2}2ydy/\alpha^2=1, \quad (39)$$

provided we may extend the integration over y to infinity.

It is possible to transform the sum for $f(\theta)$ into a power series in y by again using Murphy's expansion for Legendre polynomials. The coefficients of the various powers are then sums themselves, which may be approximated by replacing with integrals. It is, however, not difficult to use numerical values directly in the expansion (4). In this way the numerical examples given in Table I were obtained, by using from 10 to 20 terms in the series.[9] The numerical results closely follow a Gaussian curve in y over a range extending from $y=0$ to well beyond the half-value, with

$$1/\alpha^2\sim\sum(2l+1)G_l. \quad (40)$$

The calculations are made for case B of Section 4.

Table I. *Numerical calculations.*

	t	w	πs^2Nt	$\log\xi$	ν	θ_{max}* calc.	θ_{max}* obs.
Al	0.0025 cm	2.8	0.00103	5.22	96	6°	6°
	0.010	2.8	0.00411	5.22	380	14°	11°
	0.025	2.8	0.0103	5.22	960	23°	19°
Pb	0.0038	2.8	0.035	4.60	940	43°	22°
	0.013	20	0.0018	6.63	2800	11°	6°
	0.0063	9	0.0045	5.82	1400	16°	11°
C	0.3	9	0.0045	6.70	6900	15°	11°

* θ_{max} actually means the angle corresponding to the most probable value of $\sin\theta/2$ and is simply a measure for the width of the Gaussian curve, $\sin(\theta_{max}/2)=\alpha/\sqrt{2}$.

The experimental results on the first four foils of the table were obtained by using electrons of approximately uniform energy,[10] while a range of energies was used in the experiments on the last three.[2] For the first lead foil the calculated angle is so large that it is unlikely that the conditions mentioned in Section 3 are valid. The discrepancy with the last three examples is unexplained.

9. Comparison with Williams' Theory

The theoretical treatment of the problem by Williams is based on the assumption that small angle multiple scattering will yield a Gaussian distribution. The width of the Gaussian curve is calculated by multiplying the mean square deflection for a single collision by the average number of collisions. In this calculation large deflections, occurring on the average less than once for each electron, are at first omitted and afterwards added as a small correction, giving the so-called "single scattering tail." We shall not go into a detailed analysis of Williams' method, but his result can be obtained with the present method by proceeding as follows. We integrate Eq. (29) up to a value $y=y_1$ instead of $y=1$ and omit the partial harmonic series. This gives for

[9] Tables up to P_{32} by Hj. Tallqvist, Soc. Scient. Fennica or Finska Vet. Soc., Comm. Phys.-Math. Vol. 6, No. 3 and No. 6 (1932).

[10] M. M. Slawsky and H. R. Crane, Phys. Rev., to be published.

the exponent of G_l

$$\nu Q_l = 2\pi\kappa^2 Nt l(l+1) \log(\xi y_1), \quad (41)$$

which, substituted in Eq. (4), yields approximately a Gaussian curve with

$$\alpha^2 = 2\pi\kappa^2 Nt \log(\xi y_1). \quad (42)$$

The upper limit y_1 is defined by[11]

$$2\pi\kappa^2 Nt \int_{y_1}^{1} dy/y^3 = 2 \sim \pi\kappa^2 Nt/y_1^2, \quad (43)$$

which means that the two largest deflections have been omitted. In our examples, however, these deflections are almost as large as the average angle due to multiple scattering. The omission of the partial harmonic series has a more subtle meaning and is connected with the way in which the distribution approaches a Gaussian curve. Neither for a very small nor for a very large number of impacts do we expect a Gaussian distribution. It will be a good approximation only in some intermediate cases.

10. Discussion and Conclusions

The approximations frequently encountered in the several solutions of the scattering problem may be classified as follows:

I. Assumption of a Gaussian distribution

In this case it is assumed that the single scattering intensity decreases rapidly enough with increasing angle to insure the validity of a Gaussian distribution for multiple scattering. In the more general case, this assumption leads to the treatment of the problem by means of a diffusion equation.[12]

IIa. Assumption of equal path lengths

Here it is assumed that all angles involved are very small so that the path length of the electrons can be taken equal to the thickness of the scatterer.[13] The situation may be somewhat improved by a simple first-order correction (compare Section 3).

IIb. Disregard of back scattering

It is frequently assumed that all electrons are scattered only in the forward direction, and that all electrons which enter the scatterer on one side leave it at the other.

III. Disregard of inelastic scattering

The effect of energy loss by the electrons upon the distributions of scattering is very difficult to determine, hence the assumption is made that all scattering is elastic.

Inasmuch as no one has satisfactorily treated the relation between energy loss and scattering, all theories contain assumption III. The theory of Williams makes the other assumptions listed above as well. The present paper makes all except the first approximation, and is valid for thin scatterers only. It is an exact solution (except for III) for the ideal case of electrons with equal total path lengths. The theory of Bethe, Rose and Smith does not involve assumptions IIa and IIb, but their solution is, according to them, valid only for thick scatterers. It is not easy to see what effect assumption I has upon their results.

In regard to this paper, several more remarks may be made concerning the reliability of the results. An approximation of a different nature arises from the circumstance that we have no exact knowledge of the single scattering law. We believe that more precise information about $g(y)$ is likely to improve considerably the agreement between theory and experiment, which is at present quite bad even for thin foils. The sensitivity of the results to $g(y)$ is clearly seen from Eq. (33).

For high velocities and small Z the relativity corrections add a factor $(1-y^2)$ to $g(y)$ for large angles. It is also possible that higher terms in the series of Eq. (4) give more important contributions than expected, but preliminary investigations make this appear unlikely.

We wish to express our appreciation for discussions about the scattering problem with Professors Crane, Fermi and Williams during the Summer Symposium at the University of Michigan, and more recently with Professor Uhlenbeck. This investigation was undertaken in connection with work supported by the Horace H. Rackham Fund.

[11] Setting this equation equal to 2 instead of 1 is not very essential and is done because Williams considers the projection on a plane of the scattered beam as observed in a cloud chamber.

[12] W. W. Bothe, Zeits. f. Physik **54**, 161 (1929); H. A. Bethe, M. E. Rose and L. P. Smith, Proc. Am. Phil. Soc. **78**, 573 (1938).

[13] This would mean neglecting the factor $\cos\theta$ in Eq. (11) of the paper of Bethe *et al.*

The Concentration of Carbon 13 by Thermal Diffusion

ALFRED O. NIER
Department of Physics, University of Minnesota, Minneapolis, Minnesota
(Received October 30, 1939)

A thermal diffusion column employing methane gas has been constructed for the purpose of concentrating C^{13}. A determination of the separation factor of the column for various pressures indicated a quantitative agreement between experiment and the theory of Furry, Jones and Onsager. When a reservoir was attached to the top of the column it was possible to produce methane containing over four times the normal amount of $C^{13}H_4$.

THE recent experiments of Clusius and Dickel[1] and other investigators[2–7] indicate that by confining a gas in the annular space between two long vertical concentric cylinders at different temperatures, the combination of the convection currents and the thermal diffusion effect gives rise to an appreciable isotopic separation in the gas. Waldmann,[8] Furry, Jones and Onsager[9] have published papers dealing with the theoretical aspects of the problem.

To the writer's knowledge, there is at present no published account of any quantitative correlation between theory and experiment. It was the purpose of the present research to construct a column employing methane gas for the purpose of separating C^{13}. In addition it was hoped that by studying the performance of the column under various conditions it would be possible to obtain a check of the theory.

Description of Apparatus

A cross-sectional view of the thermal diffusion column used in the present experiments is shown in Fig. 1. Along the axis of the column is a No. 8 Nichrome V heating wire. This is surrounded by porcelain insulators to separate it from the steel tube 0.75″ O. D., wall thickness 0.035″. Next there is a steel tube 1.375″ O. D., wall thickness 0.035″. This tube constitutes the inner wall of the annular space confining the gas. For the outer wall of this space is used 2″ O. D. brass tubing, wall thickness 0.032″. The outermost tube is a water-cooling jacket made of brass tubing 2.50″ O. D. with a wall thickness of 0.032″. The dimensions are given in inches as these are stock sizes of tubing. The column was 24′ long; in order to obtain tubing of this length two standard 12′ lengths were butted together and surrounded by a short sleeve at the point of the butt. The sleeve connecting the two lengths of 1.375″ steel tubing was inside rather than outside the tubes. Thus there was no obstruction in the annular gas space at this point to interfere with the streamline flow of the gas. At the upper end the 1.375″ steel tube was brazed to a cover which in turn was soft soldered to the 2″ brass tube. The 0.750″ steel tube extended up through the cover and was free to move in a vertical direction relative to the cover to allow for differential expansion of the two steel tubes. The only purpose of the 0.75″ steel tube was to insure centering of the heating element.

At the lower end, the 0.75″ and 1.375″ steel tubes were brazed concentrically to a circular steel plate 1.375″ in diameter. A 0.375″ rod was also brazed to this plate and served as a guide to center the steel tubing assembly. The Nichrome wire extended through this rod and was silver-soldered to it. The position of the end of the Nichrome wire thus measured directly the expansion of the 1.375″ steel tube and could therefore be used as a temperature indicator.

Although the tubes were centered at the ends, it was felt necessary to introduce spacers to insure that the tubes were also concentric all

[1] K. Clusius and G. Dickel, Naturwiss. **26**, 546 (1938); **27**, 148 (1939).
[2] A. K. Brewer and A. Bramley, Phys. Rev. **55**, 590 (1939).
[3] A. K. Brewer and A. Bramley, J. Chem. Phys. **7**, 553 (1939).
[4] W. Groth, Naturwiss. **27**, 260 (1939).
[5] H. S. Taylor, Nature **144**, 8 (1939).
[6] T. I. Taylor and G. Glockler, J. Chem. Phys. **7**, 851 (1939).
[7] W. W. Watson, Phys. Rev. **56**, 703 (1939).
[8] L. Waldmann, Naturwiss. **27**, 230 (1939).
[9] W. Furry, R. Jones and L. Onsager, Phys. Rev. **55**, 1083 (1939).

along the length. Tightly fitting lavite spacer rings placed at intervals of 3 ft. separated the two steel tubes. In the annular gas space, spacers were placed at 6-ft. intervals along the length. In this case the spacer at the end of one of these 6-ft. sections consisted of three small lavite cylinders about $\frac{1}{4}''$ in diameter, of height equal to the space between the tubes and placed at 120° intervals around the tube. To hold the spacers in place a hole was drilled along their axes and they were slipped over steel pins brazed to the 1.375″ steel tube. These pins were shorter than the heights of the cylinders so that there was no metallic connection between the two walls of the annular space. This prevented any appreciable loss of heat at these points.

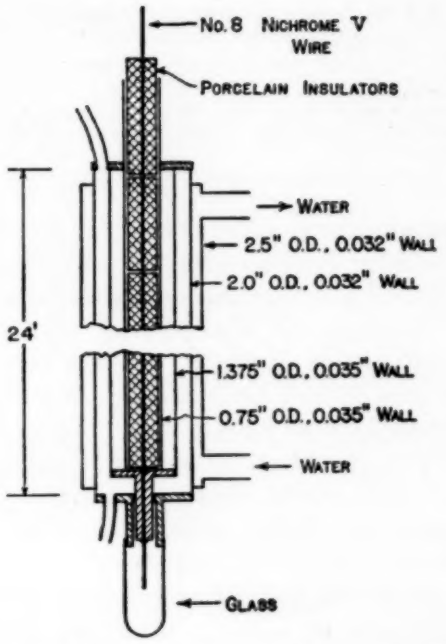

Fig. 1. Cross-sectional view of column. The column itself is used as a return lead for the current flowing through the Nichrome wire.

Procedure and Results

Prior to admitting the methane gas, the column was outgassed by heating the inner wall of the annular gas space (the 1.375″ tube) to a temperature of approximately 375°C for several days while the column was attached to a Hyvac pump. The pressure at the end of this time as measured with a Pirani gauge was less than 10^{-3} mm. It was found that 1.22 kilowatts were necessary for heating the column under these conditions. Radiation was responsible for practically all of the heat transferred across the annular space in this case.

The methane used in the experiments was purified by distillation at liquid-air temperature by using a standard Podbielniak low temperature fractionating column.

In order to study the performance of the column itself runs were made at several pressures. No reservoirs were used at the ends of the column. Samples were removed periodically from the top and from the bottom so that the rate at which the column approached equilibrium could be determined. The average temperature of the inner wall of the annular gas space was approximately 300°C in each case. This was determined from the ratio of pressures in the column when hot and when cold as well as from the linear expansion of the steel tubing. Unfortunately a direct measurement of temperature was not possible as a result of an accident which destroyed thermocouple wires leading away from the hot wall. However, as the performance of the column should not depend in any critical way upon the temperature[9] this factor is not very important. The average temperature of the outer wall was approximately 27°C. Water was passed through the cooling jacket at such a rate that the rise in temperature from bottom to top was approximately 5°C. The power consumption under these circumstances was 2.75 kilowatts.

In Table I are recorded data obtained when the CH_4 pressure in the column was 65.6 cm Hg. The samples removed from the column were analyzed with a mass spectrometer similar to one already described.[10] It differed mainly in that the slits S_1, S_2 and S_3 which appeared in Fig. 1 of reference 10 were 0.25, 0.23, and 0.90 mm wide. This type mass spectrometer uses a 180° magnetic analyzer. Positive ions are formed by electron impact of the gas at low pressure. The analyzed ion currents are measured with an electrometer tube amplifier. As the dissociation product $(O^{16}H)^+$ of water vapor, a residual impurity in a mass spectrometer, has the same mass as $C^{13}H_4^+$ one might expect some difficulty in accurately measuring the $(C^{13}H_4^+)/C^{12}H_4^+$ ratio. However, by employing

[10] A. O. Nier, Phys. Rev. **52**, 933 (1937).

TABLE I. $C^{13}H_4/C^{12}H_4$ *ratio at top and at bottom of column as a function of time. Pressure = 65.6 cm.*

Time (hours)	0	9	23.5	46	73
$C^{13}H_4/C^{12}H_4$ (bottom)	0.0112	0.0198	0.0215	0.0214	0.0213
$C^{13}H_4/C^{12}H_4$ (top)	0.0112	0.00611	0.0054	0.00505	0.00525
Ratio bottom/top	1.000	3.23	3.99	4.23	4.06

electrons having an energy of only about 15 volts for producing ions, no $(OH)^+$ ions were formed, whereas $(CH_4)^+$ ions were produced in sufficiently large numbers for the purpose of analysis. Although the ion $(C^{12}H_3D)^+$ contributes slightly to the mass 17 peak in the mass spectrometer, we will imply in what follows that this peak is due entirely to $(C^{13}H_4)^+$. That this is permissible follows immediately when we recall that we are interested principally in changes in the abundance ratio for mass 17/mass 16.

In Tables II and III are recorded the data obtained for pressures of 40.0 and 21.7 cm, respectively.

In addition to studying the variation of the $C^{13}H_4/C^{12}H_4$ ratio it seemed worth while to investigate what effect the separating effect of the column had on the impurities present in the methane. The principal impurities which appeared to be present had masses 28 and 44. The 28 ion was probably due to CO whereas the 44 ion was definitely shown to be associated with CO_2. In Table IV are recorded the CO/CH_4 and CO_2/CH_4 ratios as found for the 40.0-cm run. In computing these values allowance was made for the difference in ionization efficiency of CH_4, CO and CO_2 by calibration of the mass spectrometer with mixtures of gases of known proportions.

As the mass spectrometer itself contained traces of CO and CO_2 as residual impurities, some difficulty was encountered in measuring accurately the CO and CO_2 content for the samples removed from the top of the column. Although the data in Table IV can thus only be regarded as rough, they do show that the column is very effective in separating heavier molecules from CH_4. The concentration of these heavy impurities is so low in all but the very lowest part of the column that one should expect the presence of the impurities would have little effect upon the performance of the column.

COMPARISON OF THEORY AND EXPERIMENT

According to Furry, Jones and Onsager[9] the equilibrium separation factor for a column of the sort employed here may be written in the form

$$(C_1^L/C_1^U)(1-C_1^U)/(1-C_1^L)=\epsilon^{2A_dL}, \qquad (1)$$

where C_1^L and C_1^U represent the equilibrium concentrations of $C^{13}H_4$ in the lower and upper ends of the column, respectively. The length of the column is L and

$$A_d=A/(1+K_d/K), \qquad (2)$$

where

$$A=H/2K=252(\alpha\eta D/\rho g d^4)f(\Delta T/T) \qquad (3)$$

and

$$K_d/K=1890(T_1^2+T_1T_2+T_2^2)\times(8D\eta/d^3\rho g\Delta T)^2 \qquad (4)$$

η = coefficient of viscosity; D = coefficient of diffusion; ρ = density of gas; g = acceleration of gravity; d = thickness of annular gas space; T_1, T_2 = absolute temperature outer, inner tube, $\Delta T = T_2 - T_1$; α is given by the equation $D_T/D=\alpha C_1C_2$ where D_T = coefficient of thermal diffusion and C_1, C_2 represent concentrations of heavy, light components of gas mixture.

As $D \propto 1/\rho$ and $p \propto \rho$ we see from an inspection of Eqs. (2), (3), and (4), that we may write

$$2A_dL=(a/p^2)/(1+(b/p^4))=x, \qquad (5)$$

where a and b are constants independent of pressure and p = pressure measured in atmospheres. Also, as the concentration of $C^{13}H_4$ is always small, we can drop the $(1-C_1^U)$ and $(1-C_1^L)$ terms. Thus, we have

$$C_1^L/C_1^U=\epsilon^{(a/p^2)/[1+(b/p^4)]}=\epsilon^x. \qquad (6)$$

TABLE II. $C^{13}H_4/C^{12}H_4$ *ratio at top and at bottom of column as a function of time. Pressure = 40.0 cm.*

Time (hours)	0	12	23	47	71
$C^{13}H_4/C^{12}H_4$ (bottom)	0.0111	0.0202	0.0233	0.0248	0.0255
$C^{13}H_4/C^{12}H_4$ (top)	0.0111	0.00615	0.00486	0.00404	0.00414
Ratio bottom/top	1.000	3.29	4.78	6.14	6.16

TABLE III. $C^{13}H_4/C^{12}H_4$ *ratio at top and at bottom of column as a function of time. Pressure = 21.7 cm.*

Time (Hours)	0	12	24	48	72	9*	23*
$C^{13}H_4/C^{12}H_4$ (bottom)	0.0109	0.0143	0.0158	0.0161	0.0161	0.0141	0.0155
$C^{13}H_4/C^{12}H_4$ (top)	0.0109		0.0076	0.0075	0.0074	0.0089	.0079
Ratio, bottom/top	1.000		2.09	2.15	2.17	1.59	1.95

* Obtained in a second run. Pressure = 21.3 cm.

From our data in Tables I, II and III we can determine the numerical values of a and b. To do so we will assume that for $p=21.7$ cm $=0.285$ atmos., $C_1^L/C_1^U=2.25$; for $p=40$ cm $=0.527$ atmos., $C_1^L/C_1^U=6.25$; and for $p=65.6$ cm $=0.863$ atmos., $C_1^L/C_1^U=4.25$. As there are only two unknowns, a and b, in Eq. (6), two of these three sets of data are sufficient to determine them. The third set of data may thus be regarded as a check upon the theory. In Fig. 2 is shown a plot of $x=(a/p^2)/[1+(b/p^4)]$ *versus* p for $a=1.34$ and $b=0.126$. The fact that all three experimental points fall on the curve indicates an excellent check of the theory, at least as far as variation of separation factor with pressure is concerned.

The next question that arises is whether or not these experimentally determined values of a and b are in numerical agreement with the theoretical predictions given in Eqs. (2), (3) and (4). As the column used in the present experiments operated over the same temperature range as the one proposed by Furry, Jones and Onsager, we may use some of the same numerical data as were employed by these authors, namely: $\eta=1.60\times10^{-4}$ poise; $\rho=0.433\times10^{-3}$ g/cm^3 at atmospheric pressure; $D=1.4\eta/\rho=0.52$ cm^2/sec.; $\lambda=1.20\times10^{-4}$ cal./cm sec. deg.; and $f(\Delta T/T)=1.016$. However, we will use the experimentally determined value[11] of $\alpha(=0.0077)$ rather than the value 0.0106 assumed by Furry, Jones and Onsager. That α is somewhat smaller than was assumed by these authors accounts for the fact that the separation factor found in the present experiments is materially lower than for the hypothetical column designed by them.

The dimensions given earlier in this paper, when converted to metric units, give L (the length of the column) $=730$ cm and d (the thickness of the annular space) $=0.712$ cm. If now we

TABLE IV. CO/CH_4 *and* CO_2/CH_4 *ratios at top and at bottom of column as a function of time for the same run as the data in Table II were obtained.*

Time (hours)	0	12	23	47	71
CO/CH_4 (bottom)	0.012	0.183	0.176	0.192	0.203
CO/CH_4 (top)	0.012	0.00099	0.00118	0.003	0.0021
Ratio, bottom/top	1.000	185	150	64	97
CO_2/CH_4 (bottom)	0.00010	0.090	0.092	0.114	0.12
CO_2/CH_4 (top)	0.00010	0.00006	0.0001	.00006	.00006
Ratio, bottom/top	1.000	1500	920	1900	2000

[11] A. O. Nier, Phys. Rev. **56**, 1009 (1939).

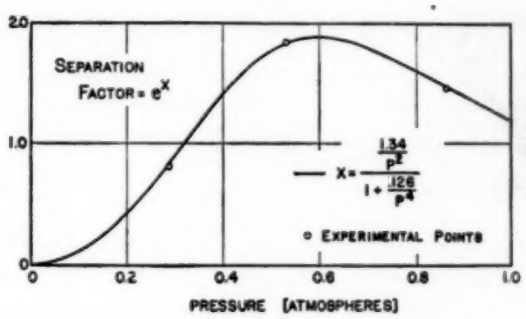

FIG. 2. Graph showing how the separation factor of the column depends upon pressure of methane. Note that separation factor is e^x, where x is the ordinate.

substitute in (2), (3) and (4), remembering that $D\propto 1/p$ and $p\propto\rho$, we find that

$$2A_dL=2AL/(1+K_d/K)$$
$$=(2.19/p^2)/(1+0.25/p^4), \quad (7)$$

where p is in atmospheres pressure.

The experimentally determined expression for this quantity is:

$$2A_dL=(1.34/p^2)/(1+0.126/p^4). \quad (8)$$

To bring the numerators of (7) and (8) into numerical agreement we can multiply numerator and denominator of (8) by 2.19/1.34. Eq. (8) then becomes

$$2A_dL=(2.19/p^2/(1.63+0.208/p^4)). \quad (8a)$$

One sees immediately that except for the factor 1.63 in (8a) rather than 1.0 as in (7) the experimental and theoretical values for $2A_dL$ are in remarkable agreement. The slight difference in the coefficients of the $1/p^4$ term is not serious when one considers that the values of this term depend upon d^6 and p^4.

The difference between 1 and 1.63 can readily be attributed to imperfections in the column. Furry, Jones and Onsager showed if there was an azimuthal variation of temperature around the column the denominator of Eq. (7) would contain an extra term which for an azimuthal temperature variation of as little as 5°C had a numerical value of one. Whether or not one should associate the extra 0.63 with such an effect cannot be told from the present data. However, it seems quite reasonable to attribute it to some sort of a remixing effect due to asymmetry or some other imperfections in the column. As alternating current heated the Nichrome wire, there was

TABLE V. $C^{13}H_4/C^{12}H_4$ *ratio at bottom of column as a function of time when a 20-liter reservoir is attached to the top. Pressure = 46 cm.*

Time (hours)	0	16	23.5	41	63	87	111	157.5	183	208
$C^{13}H_4/C^{12}H_4$	0.0113	0.0227	0.0245	0.0278	0.0314	0.0342	0.0376	0.0428	0.044	0.0457
Rel. Concentration	1.000	2.01	2.17	2.46	2.78	3.03	3.33	3.78	3.90	4.05

some vibration present which may possibly have introduced some remixing.

The power expended because of the conduction of the gas was shown by Furry, Jones, and Onsager to be

$$P_c = 4.18\lambda LB\Delta T/d \text{ watts}, \qquad (9)$$

where λ = thermal conductivity of methane $= 1.20\times10^{-4}$ cal./cm-sec.-deg. and B the average circumference of the annular space. If we substitute numerical quantities in (9) we find $P_c = 2030$ watts. Experimentally it is found that the column consumes 2750 watts, of which approximately 750 watts (determined from vacuum conditions) may be attributed to radiation. The difference, 2000 watts, is seen to be in agreement with theory and may be taken as evidence that there is no appreciable turbulence of the gas.[12]

OPERATION OF COLUMN WITH A RESERVOIR ATTACHED TO TOP

If one plans to use the column to produce methane containing a maximum concentration of $C^{13}H_4$ one should maintain a normal concentration at the top; this may be achieved by attaching a large reservoir.

To test the column under these conditions a run was made for a pressure of 46 cm (=0.6 atmos.), the pressure for which one should expect the largest separation factor (see Fig. 2). Under these circumstances one should expect by Eq. (1) to obtain a concentration factor of approximately 6.2 provided that the reservoir at the top was infinite. Actually, however, the reservoir used had a volume of 20 liters, whereas the column has a volume of approximately 7 liters. The depletion of $C^{13}H_4$ in the reservoir thus prevents one from attaining the full concentration at the bottom. If one assumes an exponential variation of concentration with length in the column and a total conservation of methane, one can readily show that the maximum attainable concentration of $C^{13}H_4$ would be 4.84 times.

In Table V are tabulated values for the concentration at the bottom of the column for various times after admitting the gas. From this it appears that, had the column been in operation for a long enough time, the full predicted concentration would have been reached.

Although no attempt has as yet been made to use the column for producing heavy methane on a practical scale, preliminary calculations based upon Eqs. (30) and (45) of the Furry, Jones and Onsager paper indicate that the column, if operated at a pressure of 46 cm, could produce every 24 hours, 148 mg of methane containing 4.5 percent of $C^{13}H_4$. If operated at a pressure of 61 cm the column could produce 376 mg of methane containing 3.4 percent of $C^{13}H_4$ every 24 hours.

In the paper that follows, additional correlations between experiment and theory will be presented.

The writer wishes to express his appreciation to Professor John Bardeen for many valuable discussions of the problem. The purified methane used in these experiments was very kindly supplied by Dr. T. I. Taylor and Professor George Glockler of the Chemistry Department. This research was aided by a grant from the Graduate School.

[12] L. Onsager and W. W. Watson, Phys. Rev. **56**, 474 (1939).

Concentration of Isotopes by Thermal Diffusion: Rate of Approach to Equilibrium

J. BARDEEN
Department of Physics, University of Minnesota, Minneapolis, Minnesota
(Received October 30, 1939)

The time-dependent partial differential equation involved in the theory of the operation of a Clusius thermal diffusion column is discussed. Solutions presented give the concentration of a given isotope at any point in the column as a function of time. Some are compared with experimental results of Nier, and good agreement is obtained.

I. INTRODUCTION

THE thermal diffusion column, invented by Clusius and Dickel[1] promises to be of some importance for the concentration of isotopes. The theory of the method has been given independently by Waldmann[2] and by Furry, Jones, and Onsager.[3] These authors consider only the equilibrium condition of the column. It is important to know how rapidly equilibrium is approached, and it is the purpose of the present paper to solve the time-dependent partial differential equation involved, with various boundary conditions at the ends of the column. Solutions obtained for several cases are compared with experimental results of Nier,[4] who studied the operation of a column containing methane gas. The column was to be used for the separation of the carbon isotopes.

We use in large part the notation and many of the results obtained by Furry, Jones and Onsager. The discussion will be confined to the case where there are but two species of molecules present, whose concentrations we denote by c_1 and c_2, so that $c_1+c_2=1$. Let $\mathbf{v}_1$ be the convection velocity of species 1 and let $\mathbf{v}$ be that of the gas as a whole. Then if both ordinary and thermal diffusion are present

$$c_1\mathbf{v}_1=c_1\mathbf{v}-D\ \text{grad}\ c_1+(D_T/T)\ \text{grad}\ T. \quad (1)$$

Here D is the coefficient of ordinary diffusion and D_T that of thermal diffusion. In the case of similar molecules (isotopes), these are related, according to the theoretical treatments of Enskog[5] and Chapman[6] by the equation:

$$D_T/D=k_T=\alpha c_1c_2. \quad (2)$$

The parameter α is independent of the concentration, and, for the case of elastic spheres, also of the temperature.

The equation of continuity for species 1 is:[7]

$$\begin{aligned}\partial\rho c_1/\partial t&=-\text{div}\ (\rho c_1\mathbf{v}_1)\\&=-\text{div}\ [\rho c_1\mathbf{v}-\rho D\ \text{grad}\ c_1\\&\qquad+(\rho D_T/T)\ \text{grad}\ T],\end{aligned} \quad (3)$$

in which ρ is the density of the gas. This equation is to be solved subject to the appropriate boundary conditions.

In the actual operation of the column, the gas is confined in the annular space between two vertical concentric cylinders, the inner one heated and the outer one cooled. Following Furry, Jones and Onsager, we may, for the purpose of analysis, suppose that the gas is enclosed in a thin flat slab of thickness d, equal to the difference in radii, of breadth B, equal to the mean circumference, and of length L, equal to the length of the column.[8] Let T_1 and T_2 be the absolute temperatures of the outer and inner walls and let $\Delta T=T_2-T_1$. Let the coordinate $x(0<x<d)$ run across the width of the slab, and $z(0<z<L)$ along its length. We suppose that the thermal convection of the gas as a whole takes place only in the vertical direction. (This will be true except near the ends of the

[1] K. Clusius and G. Dickel, Naturwiss. **26**, 546 (1938); **27**, 148 (1939); **27**, 487 (1939). For further references to the experimental data, see the paper by A. O. Nier in the present issue.
[2] L. Waldmann, Naturwiss. **27**, 230 (1939).
[3] W. H. Furry, R. C. Jones and L. Onsager, Phys. Rev. **55**, 1083 (1939). *Added in proof.*—Two theoretical papers have appeared recently. P. Debye, Ann. d. Physik **56**, 284 (1939); L. Waldmann, Zeits. f. Physik **114**, 53 (1939). The first of these overlaps to some extent the results of the present investigation.
[4] A. O. Nier, in the present issue.
[5] D. Enskog, Physik. Zeits. **12**, 56 and 533 (1911); Thesis, Upsala (1917).
[6] S. Chapman, Phil. Trans. **A217**, 115 (1917).
[7] Cf. H. Korsching and K. Wirtz, Naturwiss. **27**, 367 (1939).
[8] Our d, L are related to w, l of Furry, Jones and Onsager by the equations: $d=2w$, $L=2l$.

column.) Then $v_x=v_y=0$ and $v_z=v(x)$ is independent of z. Furthermore, T, and consequently ρ and D, are independent of z. The differential Eq. (3) then becomes:

$$\frac{\partial \rho c_1}{\partial t}=-\rho v\frac{\partial c_1}{\partial z}+\rho D\frac{\partial^2 c_1}{\partial z^2}+\frac{\partial}{\partial x}\left[\rho D\frac{\partial c_1}{\partial x}+\frac{\rho D_T Q}{T\lambda}\right], \quad (4)$$

in which we have replaced $\partial T/\partial x$ by its value Q/λ, where Q is the heat flow per sq. cm and λ is coefficient of thermal conductivity. The boundary conditions at the walls of the slab require that

$$c_1 v_{1x}=-D(\partial c_1/\partial x)+D_T Q/T\lambda=0 \quad \text{at} \quad x=0 \quad \text{and} \quad x=d. \quad (5)$$

The condition that there be no net flow of gas along the tube is:

$$\int_0^d \rho v(x)dx=0. \quad (6)$$

A solution of (4) may be obtained by using conditions (5) and (6) and by making use of the fact that the actual variation of c_1 across the width is very small and that the width is small compared with the length. It will be simpler, however, to start with the expression derived by Furry, Jones and Onsager for the total net flow, τ_1, in grams per second, of molecules of species 1 along the column:[9]

$$\tau_1=H[c_1c_2-(2A)^{-1}(\partial c_1/\partial z)], \quad (7)$$

in which the constants H and $H/2A$ are, for the case of Maxwellian molecules, as follows:

$$H=(d^3\rho^2\alpha gB/720\eta)(\Delta T/T)^2 f(\Delta T/T), \quad (8)$$

and

$$H/2A=d^7\rho^3 g^2 B(\Delta T/T)^2/362880\eta^2 D + BdD(T_1^2+T_1T_2+T_2^2)/3T^2. \quad (9)$$

The coefficient of viscosity, η, and the acceleration of gravity, g, have been introduced from the solution of the thermal convection problem. All the gas constants (ρ, D, η) are to be taken at the mean temperature $T=(T_1+T_2)/2$. The function $f(\Delta T/T)$ arises from the variation of the gas constants with temperature, and is always very close to unity. The first term on the right-hand side of (9) arises from remixing by transverse diffusion which results from the combination of convection currents and a vertical concentration gradient, and the second term represents simply the ordinary diffusion along the column.

The conservation of species (1) requires that

$$\rho\mathfrak{A}\partial c_1/\partial t=-\partial\tau_1/\partial z =-H[(\partial c_1c_2/\partial z) -(2A)^{-1}(\partial^2 c_1/\partial z^2)], \quad (10)$$

in which $\mathfrak{A}=Bd$ is the cross-sectional area of the column. In what follows we make the assumption that the concentration of species 1 is always small, so that we may replace $c_2=1-c_1$ by unity without appreciable error. The resulting equation is then linear in c_1 and can be solved by standard methods. We further assume that Eq. (10) applies throughout the entire length of the column. The equation is, of course, incorrect near the ends where the convection currents are not vertical, but the length of these regions is but a small part of the total.

Four special cases are treated, in all of which it is assumed that the lower end of the column is closed. For the condition at the upper end we take: (1) The upper end is closed. (2) The upper end is directly connected to a reservoir of infinite capacity, so that the concentration, c_1, is independent of time at this point. (3) The upper end is directly connected to a reservoir of finite capacity. (4) The reservoir is connected to the top of the column by a tube along which a concentration gradient can exist, so that the concentration in the reservoir is not the same as that in the top of the column.

Cases (1), (2) and (3) can be solved by the usual method of expansion in a series of characteristic functions of the partial differential equation which satisfy the proper boundary conditions at the ends. These functions form an orthogonal set, so that the expansion coefficients can be easily determined. In case (4) the characteristic functions are not orthogonal, but the solution can be obtained without difficulty by the operational method (Laplace transform). As (2) and (3) are really special cases of (4), we give the analysis only for case (1) which we treat by standard methods and case (4) for which we use the operational method.

II. Both Ends of Column Closed

We suppose that a heavy isotope is being concentrated at the lower end of the column, and

[9] Our A is equivalent to the A_d of FJO, (reference 3).

let $z=0$ represent the upper end and $z=L$ the lower end. The boundary conditions require that there be no flow ($\tau_1=0$) at these points. It will be simplest to first find τ_1 as a function of z and t, and then derive c_1 from τ_1. The equation for τ_1 is the same as that for c_1

$$\rho\mathfrak{A}\partial\tau_1/\partial t=-H[(\partial\tau_1/\partial z)-(2A)^{-1}(\partial^2\tau_1/\partial z^2)], \quad (11)$$

and the boundary conditions are:

$$\tau_1=0 \text{ at } z=0 \text{ and } z=L \text{ for all } t, \quad (12)$$

and

$$\tau_1=Hc_1^0 \text{ at } t=0 \text{ for all } z. \quad (12')$$

In the last equation, c_1^0 is the (constant) initial concentration.

The particular solution of (11) which satisfies the boundary condition (12) is

$$\tau_1^{(n)}=\sin(n\pi z/L)\times\exp[Az-(AH/2\rho\mathfrak{A})(1+n^2\pi^2/A^2L^2)t], \quad (13)$$

where n is a positive integer. We take

$$\tau_1=\sum a_n\tau_1^{(n)}. \quad (14)$$

Setting $t=0$, we find (using (12')):

$$Hc_1^0e^{-Az}=\sum a_n\sin(n\pi z/L). \quad (15)$$

Thus, evaluating the Fourier coefficients,

$$a_n=(2Hc_1^0/L)\int_0^L e^{-Az}\sin(n\pi z/L)dz$$
$$=(2n\pi Hc_1^0/A^2L^2)(1-(-1)^ne^{-AL})/(1+n^2\pi^2/A^2L^2). \quad (16)$$

The expression for c_1 can be divided in two parts, a steady-state term giving the equilibrium concentration and a transient term. The equilibrium term is of the form

$$c_1^{(e)}=Ke^{2Az}, \quad (17)$$

where K is a constant which may be determined from the fact that the total mass is conserved. Thus

$$Lc_1^0=K\int_0^L e^{2Az}dz$$

or

$$K=2ALc_1^0/(e^{2AL}-1). \quad (18)$$

The transient term may be found from the expression (14) for τ_1 and the equation $\rho\mathfrak{A}\partial c_1/\partial t=-\partial\tau_1/\partial z$. We must take the negative of the derivative of τ_1 with respect to z, integrate with respect to t, and divide by $\rho\mathfrak{A}$. We thus finally obtain

$$c_1=Ke^{2Az}+\sum b_n\{\cos(n\pi z/L)+(AL/n\pi)\sin(n\pi z/L)\}\exp[Az-t/t_n], \quad (19)$$

in which K is given by (18),

$$b_n=2a_nn\pi/LAH(1+n^2\pi^2/A^2L^2)$$
$$=4c_1^0(n^2\pi^2/A^3L^3)(1-(-1)^ne^{-AL})/(1+n^2\pi^2/A^2L^2)^2, \quad (20)$$

and

$$t_n=2(\rho\mathfrak{A}/AH)(1+n^2\pi^2/A^2L^2)^{-1}. \quad (21)$$

The series in (19) converges extremely rapidly. For all except small values of t, only the first term is required.

Numerical calculations based on Eq. (19) have been made for the purpose of comparing the theory with the experimental results of Nier.[4] Methane gas was used in Nier's work, and $C^{13}H_4$ was concentrated at the bottom of the column.[10] For convenience, the dimensions of the column are listed below.

$$\begin{array}{ll} L=730 \text{ cm} & \mathfrak{A}=dB=9.4 \text{ cm}^2 \\ d=0.712 \text{ cm} & \text{Volume}=\mathfrak{A}L=6880 \text{ cm}^3 \\ B=12.5 \text{ cm} & T_1=300^\circ\text{K},\ T_2=600^\circ\text{K}. \end{array} \quad (22)$$

The gas constants, extrapolated to the mean temperature, are, for one atmosphere of pressure,

$$\begin{array}{l} \rho=0.433\times10^{-3} \text{ g/cm}^3, \\ \eta=1.60\times10^{-4} \text{ poise}, \\ D=1.4n/\rho=0.52 \text{ cm}^2/\text{sec}., \\ \alpha=0.0077. \end{array} \quad (23)$$

The value of α is that found in a direct measurement by Nier.[11] Using these values we find that at one atmosphere

$$H=2.5\times10^{-5} \text{ gram/sec}.$$

Values for other pressures may easily be found from the fact that H is proportional to the square of the pressure.

Empirical values of AL, determined from the equilibrium separation, are used in the calcula-

[10] Since the normal concentration of C^{13} is about one percent, the condition that c_1 be small is well satisfied.

[11] A. O. Nier, Phys. Rev. **56**, 1009 (1939).

tion. The extent of the agreement between the theoretical and experimental values of A is discussed in Nier's paper. Runs were made at three different pressures; 21.7, 40, and 65.6 cm of Hg. The ratio of the concentration at the bottom of the column to that at the top of the column is equal to exp $[2AL]$ when equilibrium is attained. The values obtained by Nier are given in Table I.

Formulae for the ratio of the concentration of $C^{13}H_4$ at each end of the tube to the initial concentration, in which only the first term of the series in (19) is used, are listed below. In each case the time is in hours.

$P=21.7$ cm

$$2AL=0.81.$$

$$2\rho\mathfrak{A}/AH=19\times10^5 \text{ sec.}=530 \text{ hours.}$$

Top: $c_1/c_1^0=0.65+0.26\exp(-t/8.6)$.

Bottom: $c_1/c_1^0=1.46-0.40\exp(-t/8.6)$.

$P=40$ cm

$$2AL=1.83.$$

$$2\rho\mathfrak{A}/AH=4.9\times10^5 \text{ sec.}=136 \text{ hours.}$$

Top: $c_1/c_1^0=0.35+0.44\exp(-t/10.6)$.

Bottom: $c_1/c_1^0=2.18-1.10\exp(-t/10.6)$.

$P=65.6$ cm

$$2AL=1.45.$$

$$2\rho\mathfrak{A}/AH=3.8\times10^5 \text{ sec.}=105 \text{ hours.}$$

Top: $c_1/c_1^0=0.45+0.40\exp(-t/5.3)$.

Bottom: $c_1/c_1^0=1.90-0.81\exp(-t/5.3)$.

These formulae are valid for values of t greater than three or four hours.

Figure 1 gives a plot of the relative concentrations of $C^{13}H_4$ at the top and bottom of a column operating at a pressure of 40 cm as a function of time. Also shown are the experimental points. The agreement on the whole is good.

In Fig. 2 we show the ratio of the concentration at the bottom of the column to that at the top of the column as a function of time for the three different pressures. Again the agreement between experiment and theory is satisfactory. The measurements indicated by the solid triangles were taken at a pressure of 21.3 cm, while the curve (and the measurements indicated by the open triangles) refers to a pressure of 21.7 cm. This difference is sufficient to account for the discrepancy shown.

TABLE I. *Equilibrium separation factor, exp (2AL), for $C^{13}H_4$, according to measurements of Nier.*

Pressure (cm)	21.7	40	65.6
exp (2AL)	2.25	6.25	4.25
2AL	0.81	1.83	1.45

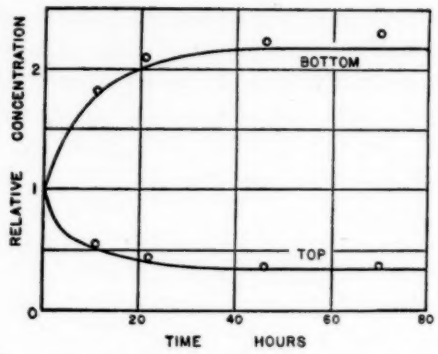

FIG. 1. Comparison of the theoretical and experimental values of the relative concentration of $C^{13}H_4$ at the top and bottom of a thermal diffusion column. Both ends of the column are closed. In plotting the experimental values of Nier, an allowance of one hour was made for the column to heat up. Methane pressure = 40 cm.

III. Operation with a Reservoir at the Top

We now discuss case (4) referred to above. The top of the column is connected to a reservoir containing gas of mass M by means of a tube along which a concentration gradient can exist. It is supposed that the net flow of the molecules of species 1 through the tube is proportional to the concentration gradient. The bottom of the column is closed.

Again we let $z=0$ represent the top of the column and $z=L$ the bottom. The concentration c_1 at any point in the column as a function of time is given by the solution of the equation

$$\rho\mathfrak{A}\partial c_1/\partial t=-H[(\partial c_1/\partial z)-(2A)^{-1}(\partial^2 c_1/\partial z^2)], \quad (24)$$

subject to the boundary conditions:

$$\tau_1=H[c_1-(2A)^{-1}(\partial c_1/\partial z)]=0 \quad \text{at} \quad z=L, \quad (25)$$

$$\text{and} \qquad c_1^{(\text{res})}-c_1=R\tau_1/H \quad \text{at} \quad z=0. \quad (26)$$

In Eq. (26) $c_1^{(\text{res})}$ represents the concentration in the reservoir and c_1 that in the top of the column. The constant R depends on the dimensions of the tube connecting the top of the column with the reservoir. If the tube has length l and area a,

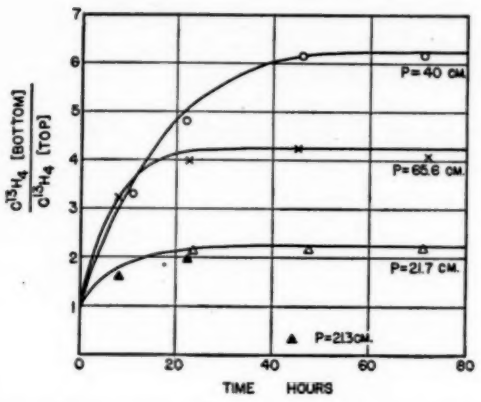

FIG. 2. Comparison of the theoretical and experimental values of the ratio of the concentration of $C^{13}H_4$ at the bottom of the column to that at the top of the column. Both ends of the column are closed. In plotting the experimental values of Nier, an allowance of one hour was made for the column to heat up.

and if the flow is by ordinary diffusion;

$$R=lH/a\rho D, \tag{27}$$

in which ρ is the density and D the coefficient of diffusion of the gas in the connecting tube.

The total mass of molecules of species 1 in the reservoir at any time is equal to the initial mass minus the mass which has flowed out. This gives

$$Mc_1^{(res)}=Mc_1^0-\int_0^t \tau_1(0,t')dt'. \tag{28}$$

Thus condition (26) may be written:

$$c_1^0-c_1-M^{-1}\int_0^t \tau_1(0,t')dt'=R\tau_1/H. \tag{26'}$$

The operational method of solution will be used. The Laplace transform of $c_1(z,t)$ is

$$h(z,p)=\int_0^\infty e^{-pt}c_1(z,t)dt. \tag{27}$$

We will also need

$$\int_0^\infty e^{-pt}(\partial c_1/\partial t)dt=-c_1^0+ph, \tag{28}$$

which result follows by partial integration, and the fact that at $t=0$, $c_1=c_1^0$, the initial concentration.

Multiplying (24) by $\exp[-pt]$ and integrating with respect to t between the limits zero and infinity, we find the following differential equation for h:

$$\rho\mathfrak{A}(c_1^0-ph)=H[(dh/dt)-(2A)^{-1}(d^2h/dt^2)]. \tag{29}$$

The general solution of this equation is:

$$h=p^{-1}c_1^0+e^{Az}\{K_1\sinh\gamma A(z-L)+K_2\cosh\gamma A(z-L)\}, \tag{30}$$

where K_1 and K_2 are constants, and

$$\gamma=\{1+(2\rho\mathfrak{A}p/AH)\}^{\frac{1}{2}}. \tag{31}$$

The constants K_1 and K_2 are to be determined from the boundary conditions (25) and (26'), which, by the same transformation become:

$$h=(2A)^{-1}(dh/dz) \quad \text{at} \quad z=L, \tag{32}$$

and

$$p^{-1}c_1^0-h=\{R+(H/Mp)\}\{h-(2A)^{-1}(dh/dz)\} \quad \text{at} \quad z=0. \tag{33}$$

Substituting the expression for h given by Eq. (30) into Eq. (32) we find

$$p^{-1}c_1^0+(e^{AL}/2)(K_2-\gamma K_1)=0 \quad \text{or} \quad K_2=\gamma K_1-(2c_1^0/p)e^{-AL}. \tag{34}$$

Similarly Eq. (33) becomes:

$$K_1\sinh\gamma AL-K_2\cosh\gamma AL=\{R+(H/Mp)\}\{p^{-1}c_1^0-\tfrac{1}{2}(K_1-\gamma K_2)\sinh\gamma AL+\tfrac{1}{2}(K_2-\gamma K_1)\cosh\gamma AL\}. \tag{35}$$

Substituting the value for K_2 given by Eq. (34) into Eq. (35) and solving for K_1, we find

$$\gamma K_1=c_1^0G(p)/pF(p), \tag{36}$$

in which
$$G(p)=\{R+(H/Mp)\}\{1-e^{-AL}(\gamma\sinh\gamma AL+\cosh\gamma AL)\}-2e^{-AL}\cosh\gamma AL, \tag{37}$$

and
$$F(p)=\gamma^{-1}\sinh\gamma AL-\cosh\gamma AL+(2\gamma)^{-1}(1-\gamma^2)(R+(H/Mp))\sinh\gamma AL. \tag{38}$$

Finally, substituting the values of K_1 and K_2 given by Eqs. (34) and (36) into Eq. (30), we find

$$ph/c_1^0=1-2e^{A(z-L)}\cosh\gamma(z-L)+e^{Az}\{G(p)/F(p)\}\{\gamma^{-1}\sinh\gamma A(z-L)+\cosh\gamma A(z-L)\}. \quad (39)$$

To transform back to find c_1 as a function of time, we make use of the following rules:[12] If $ph(p)=1$, then

$$c_1(t)=1. \quad (40)$$

If $ph(p)=p^n$ (n a positive integer) then

$$c_1(t)=0. \quad (41)$$

If $$ph(p)=f(p)/F(p)$$

then $$c_1(t)=f(0)/F(0)+\sum_k\{f(p_k)/p_kF'(p_k)\}e^{p_kt}, \quad (42)$$

where $f(p)$ and $F(p)$ are series of positive powers of p, and p_k is a root of

$$F(p_k)=0. \quad (43)$$

The roots are assumed to be distinct, and the sum in Eq. (42) runs over all roots. Eq. (42) expresses the Heaviside partial fraction rule. Thus we find

$$c_1(z,t)/c_1^0=e^{2A(z-L)}\{(e^{AL}G(0)/F(0))-1\}+e^{Az}\sum_k\{G(p_k)/p_kF'(p_k)\}$$
$$\times\{\gamma_k^{-1}\sinh\gamma_kA(z-L)+\cosh\gamma_k(z-L)\}\exp[p_kt], \quad (44)$$

in which γ_k is obtained by substituting p_k for p in the expression for γ (Eq. (31)). The first term on the right-hand side gives the equilibrium state,

$$c_1^{(e)}/c_1^0=Ke^{2Az}, \quad (45)$$

with

$$K=2A(M+\rho\mathfrak{A}L)/(2MA+\rho\mathfrak{A}(e^{2AL}-1)). \quad (46)$$

The series in Eq. (44) gives the transient terms. To evaluate them we must find the roots of $F(p)=0$, which equation may be expressed in the form:

$$\tanh\gamma_kAL=\gamma_k/\{1-(\rho\mathfrak{A}/MA)-\tfrac{1}{2}R(\gamma_k^2-1)\}. \quad (47)$$

Depending on the value of R, there may or may not be a real value of γ_k which satisfies this equation. There are always an infinite number of pure imaginary roots. If γ_k is a root of this equation then, from Eq. (31) we find

$$p_k=-(AH/2\rho\mathfrak{A})(1-\gamma_k^2).$$

The value of p_k is always real and negative.

Differentiating the expression for $F(p)$ given by Eq. (38) and making use of Eq. (47), we find

$$p_kF'(p_k)=(2\gamma_k)^{-1}(1-\gamma_k^2)\{R\sinh\gamma_kAL+\gamma_k^{-1}\cosh\gamma_kAL-AL\operatorname{csch}\gamma_kAL\}. \quad (48)$$

With these substitutions, we finally obtain:

$$c_1/c_1^0=Ke^{2Az}+\sum_k\frac{2(R+(H/Mp_k))(e^{AL}-\gamma_k\sinh\gamma_kAL-\cosh\gamma_kAL)-4\cosh\gamma_kAL}{(1-\gamma_k^2)(\gamma_k^{-1}\sinh\gamma_kAL+\gamma_k^{-2}\cosh\gamma_kAL-AL\gamma_k^{-1}\operatorname{csch}\gamma_kAL)}$$
$$\times[\gamma_k^{-1}\sinh\gamma_kA(z-L)+\cosh\gamma_kA(z-L)]\exp[Az+p_kt]. \quad (49)$$

[12] See any book on operational calculus, e.g., J. R. Carson, *Electric Circuit Theory and Operational Calculus* (McGraw-Hill, 1926), p. 33.

This expression may appear rather formidable, but it is not difficult to use because the series converges so rapidly that at most only two or three terms are necessary.

Case (2) (infinite reservoir at the top, so that $c_1(=c_1^0)$ is constant in time at $z=0$) is obtained in the limit $M\to\infty$, $R\to 0$. Case (3) (no connecting tube, so that the concentration in the reservoir is the same as that in the top of the tube) is obtained in the limit $R\to 0$.

Nier[4] made one run when a reservoir of 20 liters capacity was attached to the top of the column. The equivalent length/area of the connecting tube was rather large, 27.7 cm^{-1}. As we shall see, this materially lowered the rate of approach to equilibrium. The pressure (0.6 atmos.) was that which should give the largest possible separation factor ($\exp[2AL]=6.62$). The total mass of gas in the reservoir (which was at room temperature) was about 7.8 grams as compared with about 1.89 grams in the column. The expected equilibrium concentration in the bottom of the column is (from (45) and (46)) $4.84c_1^0$.

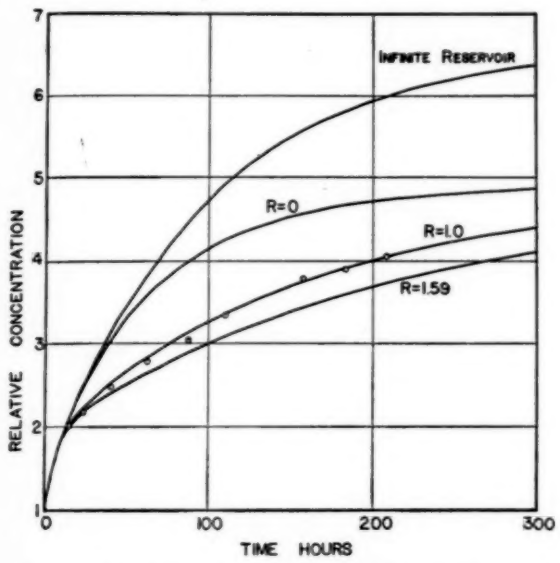

FIG. 3. Plot of the relative concentration of $C^{13}H_4$ at the bottom of a thermal diffusion column as a function of time. In all cases, the bottom of the column is closed. The upper curve represents the case of an infinite reservoir directly connected to the top of the column. The other three cases are for a reservoir of finite size connected to the top of the column by means of a tube along which a concentration gradient may exist. The parameter R is a measure of the resistance of this tube to flow by diffusion or convection. The experimental points are from a run made by Nier. The calculated value of R for the connecting tube used by Nier is 1.59 if it is assumed that flow is by diffusion alone; actually R may be smaller because of convection. Methane pressure = 46 cm (0.6 atmos.).

To evaluate the transient terms in Eq. (49) we need the following further data:

$$H=0.6^2\times 2.52\times 10^{-5}$$
$$=0.91\times 10^{-5}\ \text{gram/sec.}$$
$$AL=0.945$$
$$2\rho\mathfrak{A}/AH=4.2\times 10^5\ \text{sec.}=117\ \text{hours.}$$
$$R=27.7H/(1.4\times 1.12\times 10^{-4})=1.59.$$

Using the first three terms of the series, we find that at $z=L$ (bottom of the column)

$$c_1/c_1^0=4.84-2.9\exp(-t/213)-0.84\times\exp(-t/8.2)+0.14\exp(-t/2.7).$$

The time is measured in hours. This gives a rapid rise to a multiplication of about 2 and a slower rise thereafter. A plot of the curve is shown in Fig. 3. The experimental values of c_1/c_1^0 rise more rapidly than the theoretical with $R=1.59$. This may be due to the fact that there may be some convection in the vertical portion of the connecting tube, so that R is not as large as predicted from diffusion alone.

An excellent agreement between the experimental and theoretical values is obtained if we take arbitrarily $R=1.0$ instead of 1.59. The calculation then gives

$$c_1/c_1^0=4.84-3.0\exp(-t/155)-0.74\times\exp(-t/7.6)-0.03\exp(-t/2.4).$$

Also shown in the figure are the curves for $R=0$ (equilibrium is assumed at all times between the reservoir and the top of the column) and the curve for an infinite reservoir. In the latter case the equilibrium value of c_1/c_1^0 at the bottom of the column is 6.62 instead of 4.84.

In order to obtain the maximum possible speed, it is necessary to use a large connecting tube, so that R is made small in comparison with unity.

The author wishes to thank Professor A. O. Nier for frequent illuminating discussions, and for use of the experimental data in advance of publication.

Conductivity and Mobility of Thin Lead Films[1]

M. G. FOSTER
Cryogenic Laboratory, California Institute of Technology, Pasadena, California
(Received November 7, 1939)

From measurements of electric conductivity made on thin films of Pb obtained by condensing the metal on cooled glass surfaces at rates from 5×10^{12} to 100×10^{12} atoms sec.$^{-1}$ cm^{-2} under high vacuum conditions designed to eliminate contamination, the following results are obtained: The critical film thickness (d_c) at which the (specific) conductivity (σ) begins changing rapidly from its low value ($\approx10^{-6}$ mho·cm^{-1}) in the thinnest films to that of the bulk metal (σ_0, $\approx10^{6}$ mho·cm^{-1}) is in the neighborhood of 60A for room temperature films, and of 30A for films cooled with liquid air. The mutual configuration of the condensed Pb atoms is unstable and changes with time, shown by a decrease observed in the conductivity when the film is isolated from external influences, and in the eventual appearance of a granular structure visible under the ultramicroscope. In some cases a reproducible dependence of the conductivity on the applied potential difference was observed. These effects are in harmony with the mechanism expected from considerations of the thermodynamic stability of such films, i.e., with a tendency toward aggregation resulting in the removal of mobile atoms into crystallization centers, and thus in formation of gaps which obstruct the conduction electrons. Certain deficiencies in quantitative reproducibility are ascribed to variations in the physical surface conditions on the plate where the film is condensed, presumably affecting the mobility of the layers condensed first.

INTRODUCTION

MANY experiments have been made in the past to measure the electrical properties of thin metal films, but agreement among the results of different workers has been at best largely qualitative, and in some cases definite contradictions exist. A fairly representative bibliography is given by Mitchell,[2] and, of the numerous results published, the films deposited by Kramer,[3] Anderson,[4] Mitchell,[2] Lovell,[5] and Was[6] exhibit typical comparability.

It is found that the (specific) conductivity,[7] σ, of metals in thin-film form is much lower than that of the same metal when in bulk, σ_0, although Lovell observes only a factor of 10 between a 40A Rb film and the bulk metal, and Anderson notes factors of 10^{12} and more up to several hundred atomic layers of Ag.

Nearly all experimenters observe that there is a certain critical average thickness (d_c) of the film at which this low value of conductivity begins to grow rapidly toward the bulk value with increasing thickness: Lovell finds his sharpest changes at about 6A, Anderson at about 1000A, and Was between 50A and 100A. Distinct lack of agreement is also obtained for the variation of conductivity with time which is almost universally observed when a newly deposited film is left to itself while the atoms settle into equilibrium positions. Anderson and Lovell give extensive data showing that the conductivity decreases with time under these conditions, Mitchell finds an increase with time, and the conductivity of Was' gold films first increases, then decreases.

Kramer reports that, as the average thickness is held constant and the temperature (kept low with liquid air during deposit) is allowed to rise, at a certain transformation temperature ("*Umwandlungstemperatur*")—characteristic of the metal used—the conductivity abruptly and irreversibly increases. Mitchell is unable to find this sudden change, but observes a gradual irreversible increase in conductivity instead. He asserts further that this increase will occur at constant temperature as well, if the film be given many hours time to age. It is also found that the condition of the surface on which the deposit

[1] M. G. Foster, Thesis, 1939, California Institute of Technology.
[2] A. C. G. Mitchell, Phys. Rev. **53**, 250 (1938).
[3] L. Kramer, Ann. d. Physik **19**, 37 (1934).
[4] A. B. C. Anderson, Thesis, California Institute of Technology, 1933; Anderson and Goetz, Phys. Rev. **45**, 293 (1934).
[5] A. C. B. Lovell, Proc. Roy. Soc. **157**, 311 (1936).
[6] D. A. Was, Physica **4**, 382 (1939).
[7] By σ is meant the quantity l/Rwd, where R is the measured resistance of the film, l is the distance between end electrodes, w is the width, and d is the average thickness of the film, determined by the method discussed below. It is clear that this quantity gives the conductivity in mhos per centimeter cube for a thick film but it is quite certain that this concept loses its meaning for a film of a few atomic layers.

occurs has great influence on the observed properties of the deposited film of metal. To deal with this effect, Lovell outgasses his Pyrex backing plate many hours at high temperatures, and finds his thinner films more stable as a result of this treatment. Was finds that his critical thickness (d_c) changes from about 50A to about 100A when a similar outgassing technique is employed.

In the following sections, experimental methods and results will be presented which are employed to gain a deeper insight into the nature of the instability of freshly deposited films, with the resulting variations in σ with time. These data will be discussed particularly with regard to the variations of the phenomenon with temperature, and their implications as to atomic behavior in thin metal films in general.

Apparatus and Experimental Methods

The evaporation chamber previously used in the work of Anderson was employed in this work also, after a number of improving changes were made. Fig. 1 shows the apparatus.

A resistance-heated MgO crucible described previously by Goetz,[8] the construction of which assures uniform temperature throughout, produces the molecular beam. A thermocouple is mounted in the center of the metal filling of the crucible; the wall of the latter is protected against chemical reactions with the metal by a lining of pure Fe (insoluble in Pb). The vacuum was measured with an ionization gauge, the lead to which opens in the close neighborhood of the crucible, i.e., the region of the least perfect vacuum.

The beam passes a number of collimating slits and a magnetically operated shutter before reaching the surface upon which condensation takes place.

In order to establish a good thermal contact between this surface (thin cover glass) and the cooling vessel (quartz) special precautions (g.v.) were taken.

All glass parts were thoroughly scrubbed in dilute nitric acid and rinsed in distilled water before each run. Metal parts received the same treatment, and were thoroughly outgassed with a 5-kw induction furnace after the apparatus was assembled. Particular attention was given to the cleaning of the plate where condensation occurred. This thin glass plate (a microscope coverglass 0.25 mm thick) was rubbed with cotton under concentrated nitric acid, as recommended by the National Bureau of Standards,[9] rinsed in distilled water, dried in air, and promptly inserted in the apparatus. Contamination from the sealing wax (Apiezon W) was reduced to a minimum by keeping the wax only on the outer portion of the otherwise clean ground joints. These precautions to avoid contamination were necessary, since even a trace of grease vapor gave rise to films of uneven thickness and nonmetallic appearance. All the films used for the data presented were even in thickness and mirror-like in aspect; others were discarded.

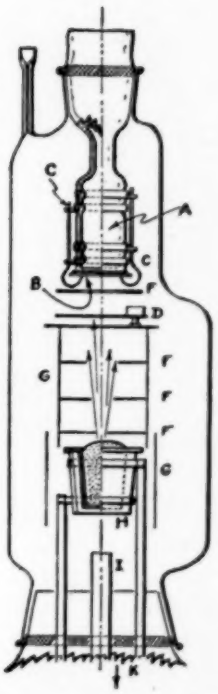

Fig. 1. Vacuum chamber, Pyrex. (A: quartz chamber for cooling fluid; B: film backing plate; C: contact and support hooks; D: shutter; F: stops; G: shields; H: crucible; I: tube to ionization gauge; K: to liquid-air traps and pumps.)

Thermal contact with the cooling fluid was obtained by melting solder between the glass backing and the quartz bottom of the chamber for cooling liquids. This was done in vacuum with the induction furnace during the process of outgassing. Electrical contact with the film was obtained by platinizing two areas on the face of the backing plate, so that the deposited film would bridge the gap, and soldering the insulated supporting hooks to these areas at the

[8] A. Goetz, Zeits. f. Physik **42**, 328 (1927).

[9] Letter Circular 32, National Bureau of Standards.

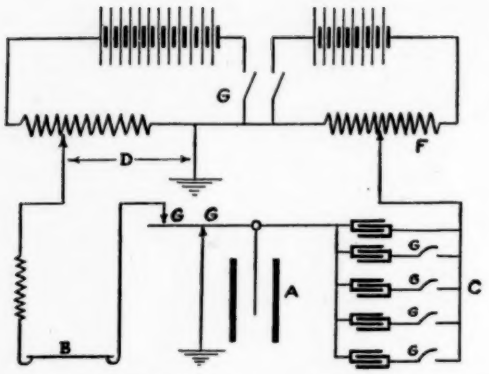

FIG. 2. Diagram of measuring circuit. (A: electrometer; B: film; C: condenser; D: potential across film; F: potentiometer, manually adjusted to keep A reading zero; G: switches.)

same time as the solder was melted for thermal contact.

Pure lead was chosen as material for these experiments, partly because of its low vapor pressure at room temperature, the possibility of evaporating adequate quantities at practicable temperatures (500°-600°C) and partly on account of its large density, which permits more accurate determination of the weight of thin films.

The thickness (d_c) of deposits was determined from the rates of deposit, measured in calibration runs performed over long time intervals with known constant temperatures of the crucible. Such deposits were weighed on a microbalance (sensitivity 7×10^{-6} g/div.). If the density of the metal deposited is assumed to be identical with the density in bulk, the time rate of increase of thickness for each temperature can be determined from the time required to deposit a known weight of lead. Rates between 5 and 100 $\times10^{12}$ atoms cm^{-2} $sec.^{-1}$ were employed, which are equivalent to an increase of from 6×10^{-2} to 1 atomic layers of the deposit per minute.

The conductivity of the deposit was measured by the rate at which one of the calibrated condensers (see circuit diagram Fig. 2) must be charged in order to keep the insulated side of the deposit at ground potential. A sensitive string electrometer was used. In order to measure with commensurable accuracy over sufficiently large variation of σ, five different capacities (Fig. 2) were employed.

Measurements were taken at room temperature (quartz cell cooled with water) and at temperatures below -100°C obtained by cooling the backing with liquid air.[10] In the condensing process the shutter was open for a certain length of time, then the beam was shut off for at least half an hour, until the film approached equilibrium, as evidenced by the approach of σ toward constant value. The process was then repeated several times. The conductivity measurements were made at short intervals throughout the deposit times and the aging periods; the total time required for a complete set of measurements varied from two to six hours.

RESULTS

The data obtained in four typical runs (taken from a total of twenty) are plotted in the graphs (Figs. 3, 4 and 5). The subtitles under each graph explain the conditions under which the data shown were obtained.

It will be seen that in every case the conductivity of a film *decreases with time* when the lead beam is shut off. The general appearance of the curves is that changes in conductivity observed seem to occur more sharply and over greater ranges for liquid-air-cooled films than for room temperature deposits. The critical thickness, d_c, is seen to be somewhat larger for room temperature films (about 60A) than for low temperature films (about 30A) when these films are obtained by continuous deposit.

Figure 6 is an ultramicroscopic view of the central part of a typical film after it has been given time to come to equilibrium, as indicated

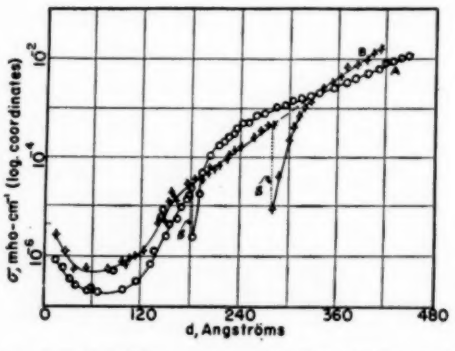

FIG. 3. Conductivity *vs.* average film thickness for two typical films deposited at room temperature. Film (A) deposited at 1A per minute, film (B) at 2.5A/min. At points marked S the shutter was closed for a short time.

[10] A thermocouple attached at various points showed that considerable temperature differences could exist between the cooling fluid and the film, but these did not raise the temperature of the surface above 40°C and -100°C during water and liquid-air cooling, respectively.

by the invariance of σ with time. A statistical granular structure is apparent, whose representative parameter is estimated to lie between 0.1 and 0.5μ.

A voltage dependence of conductivity is observed in Fig. 4b, where for thin films it is seen that the observed conductivity is smaller when a smaller potential is used to measure it. Since measurements were so taken that the film was alternately measured at 40 volts and at 20 volts, with consistent results in this respect, the effect cannot be ascribed to any permanent deformation of the film when voltage is applied.

Discussion

Attempts at theoretical treatment of the concept that thin metal films consist of patches rather than uniform structure have been made by

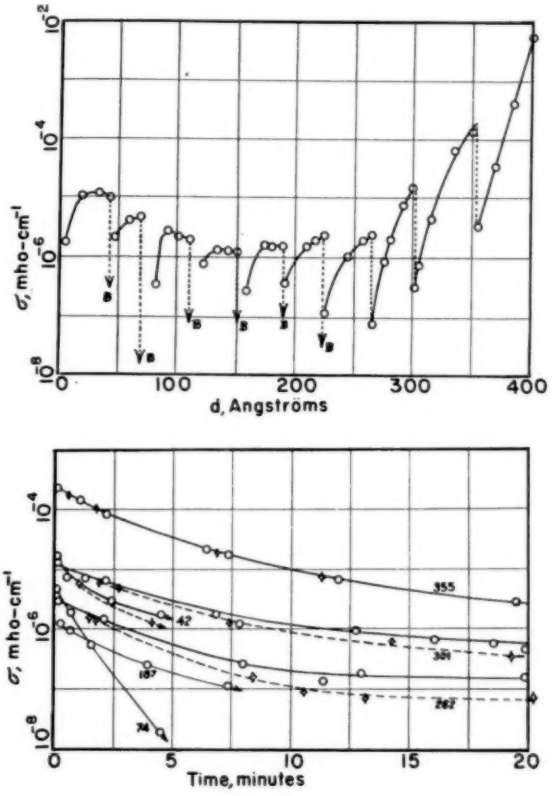

Fig. 4a. (Upper) Conductivity *vs.* average film thickness for condensation at room temperature, rate 7.5A/min. The vertical dotted lines show where the beam was cut off; *B* indicates the point where conduction becomes too small to measure. 4b. (Lower) Aging curves for 4a, showing the approach of conductivity towards constant values during intervals when no deposit was taking place. The numbers attached to each curve give the average film thickness in angstroms, the dotted lines are the curves for 20 volts applied potential, the solid lines for 40 volts.

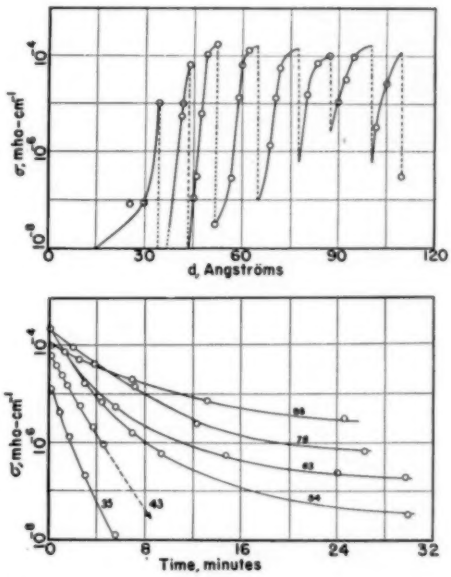

Fig. 5a. (Upper Conductivity *vs.* average film thickness for condensation on liquid-air-cooled plate, rate 2A/min. 5b. (Lower) Aging curves for 5a.

Swann[11] and others. The data which have been in part presented lead to the following considerations of the temperature dependence of atomic mobility in condensed metal films:

The freshly deposited film will consist of atoms condensed from the vapor, distributed at random on the cooled solid backing surface. In view of the possibilities for a large decrease in thermodynamic potential in case the atoms are either adsorbed on the backing plate or drawn together into groups, a purely statistical configuration cannot be expected to be stable and permanent. This is even more pronounced if the disturbing influence of the surface forces at the plate permit the growth of groups of crystalline character. It is known, however, that very few atomic layers are sufficient to neutralize the adsorptive forces of the van der Waals type, particularly if other atoms (e.g., material not removed in the outgassing process) have been adsorbed first. Since the first few layers are not accessible to accurate observation with this method, the effects actually observed should be due to atoms arriving later and are not influenced directly by these forces.

The observed tendency for the deposited material to lose its conductive qualities, whenever the supply of newly arriving atoms ceases, by a process producing gaps due to withdrawal of

[11] W. F. G. Swann, Phil. Mag. **28**, 467 (1914).

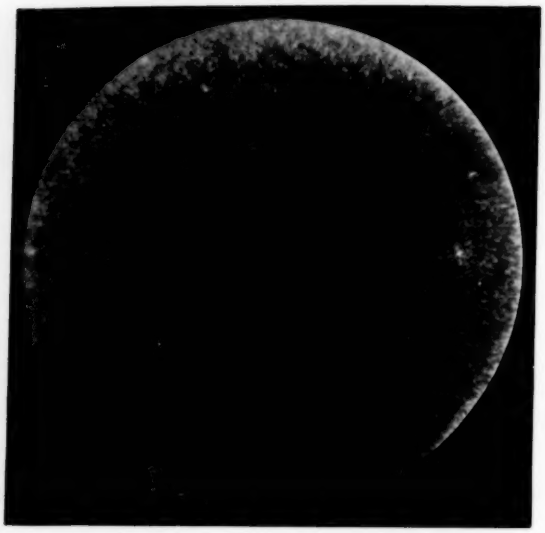

FIG. 6. Photomicrograph of center of film, cardioid condenser, glycerin immersion objective (Zeiss), photo-eyepiece, 850 diameters magnification.

material into configurations of lesser surface aggregation is thus to be expected from thermodynamic criteria of equilibrium.

The mobility of the atoms is expected to be larger at higher temperatures, and with it the rate with which the conductivity changes with time. This relation is not evident from the experiments (Figs. 4b and 5b) very probably because of the large absolute value of the mobility at room temperature, causing a considerable approach of the equilibrium configuration to take place while the deposit is made. The measured values will thus indicate only the relative rates of deposit[12] and aggregation. The observed relations support this assumption.

It is seen above that theoretical considerations require that the observed conductivity decrease with the approach to equilibrium configuration within the film. This result should be independent of the conduction process—i.e., whether ionic or electronic conduction occurs. A conduction electron is able to leap small gaps but when the film draws apart into closely packed groups the (fewer) gaps grow larger, and thus the path of an electron is interrupted, inhibiting conduction. On the other hand, any electrolytic conduction which occurs must be due to atoms which are still able to migrate, that is have not yet been captured, since the temperature is so low that any atom which joins a group is unlikely to escape from the strong forces binding it there. Hence as aggregation grows more nearly complete the number of such carriers becomes very small. The appreciable conductivity observed for the film itself (over and above that of the background) for many cases where equilibrium has been practically reached shows, however, that a substantial part of the conduction is electronic in the films observed.

That room temperature films do not become as conducting at the start as do those deposited at the lower temperature, although both types fall rapidly back to the conduction of the background during aging, indicates that the aggregation has been more extensive during the deposit at high than at low temperature of the background. The smaller critical thickness for cold films can be ascribed to the same effect.

When the patches of metal on the backing become large enough so that appreciable attraction is exerted between the edges of separate groups, the surface forces will tend to close the gaps. Thus the appearance of large-scale surface tension phenomena should be accompanied by the appearance of much greater conductivity for the equilibrium state.

Also as the gaps grow wider with time in the thinner films, it will be expected that some gaps become nonconducting for 20 volts applied potential before this happens for 40 volts, since the ease with which electrons jump these gaps should depend on the energy available to them. For example, because of the discontinuous nature of the film, large potential gradients can exist between the groups; hence electrons could conceivably be pulled across the film by a process approaching cold emission from successive patches.

ACKNOWLEDGMENT

The writer wishes to record his especial obligation to Professor A. Goetz, under whose stimulating direction the work was carried out, and also to Dr. A. B. C. Anderson whose apparatus and methods furnished the starting point of the experiments.

[12] The rate of deposit can be controlled with satisfying accuracy by the apparatus described, but adequate standardization of the deposit surface to give really reproducible values of the aggregation rate may not have been always assured by the methods used here. It may be that success in this direction lies along the line of outgassing the deposit surface for times as long as those used by Lovell, although it is uncertain how much such drastic treatment will injure the structure of the surface itself while driving off adsorbed atoms.

Examination of Colored Alkali Halides for Photoelectric Hall Effect

JULIAN EVANS
The Rice Institute, Houston, Texas
(Received November 8, 1939)

Five additively colored alkali halides have been examined for photoelectric Hall effect by means of two different arrangements, a single cross-electrode set-up and Tartakowsky's divided electrode method. The consistently null results obtained were checked by using zincblende, a substance of known photoelectric galvanomagnetic properties, in both arrangements. From the upper limit assigned to the Hall effect, it was computed that the mean free path of photoelectrons in rocksalt is not much greater than the dimensions of a lattice cell—in agreement with Von Hippel's result for the electronic mean free path on the basis of electrical breakdown experiments. This interpretation of the null result was supported by the fact that the large initial surge of electron current in KCl and KBr at the outset of illumination also showed no Hall effect. The magnetic deflection of photoelectric current reported in rocksalt by Tartakowsky was not found, either for additively or photochemically colored specimens.

POHL[1] and his collaborators have made exhaustive studies upon the photoelectric properties of additively colored alkali halide crystals, but so far have not reached a definite decision as to the nature of the color centers or of the complete conduction mechanism of the photoelectric current. Lukirsky[2] has reported a Hall effect in photochemically colored rocksalt such that the mean free path of the photoelectrons was calculated (according to Joffé[3]) to be "of the order of 10^{-5} or 10^{-6} cm." Tartakowsky[4] has described an apparatus by means of which he demonstrated an "electron polarization" set up in photochemically colored rocksalt by the magnetic deflection of the lines of current flow to a divided collecting electrode. Von Hippel,[5] however, on the basis of experiments upon electrical breakdown in rocksalt, has concluded that the mean free path of electrons therein is of the order of the dimensions of one lattice cell. His conclusion was supported by a theoretical calculation of the "relaxation time" of electrons in rocksalt made by Fröhlich.[6] In view of the discrepancy between Lukirsky's and Von Hippel's results when applied to the determination of electron mean free paths in rocksalt, and also because of the sparseness of available data on photoelectric Hall effects in general, it was considered desirable to examine several colored alkali halides in detail for the photoelectric Hall effect.

[1] R. W. Pohl, Proc. Phys. Soc. **49**, supplement, 3 (1937).
[2] P. Lukirsky, J. Russ. Phys. Chem. Soc. 1916 (in Russian).
[3] A. F. Joffé, *The Physics of Crystals* (McGraw-Hill), p. 129.
[4] P. Tartakowsky, Zeits. f. Physik **66**, 830 (1930).
[5] A. von Hippel, J. App. Phys. **8**, 815 (1937).
[6] H. Fröhlich, Proc. Roy. Soc. **A160**, 230 (1937).

APPARATUS

First measurements on NaCl, KCl and KBr were by means of a single cross-electrode arrangement, shown schematically in Fig. 1. The cross electrode was connected directly to the grid *A* of a sensitive direct-current amplifier, with circuit as given by Harnwell and Van Voorhis.[7] A current sensitivity of 4×10^{-15} amp. = 1 scale division was used. B-batteries connected in series to the amount of about 500 volts were applied to the ends of the crystals. These batteries were

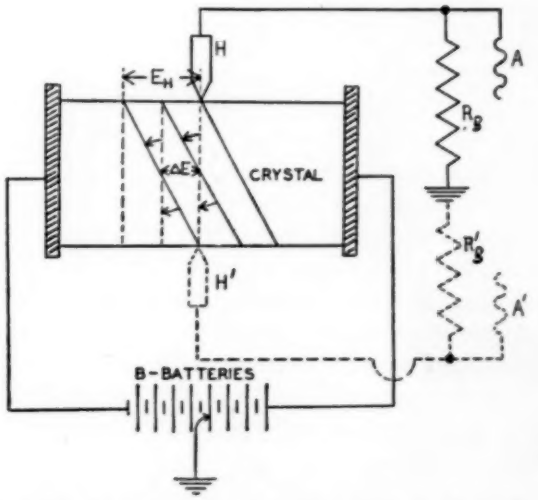

FIG. 1. Schematic showing single cross-electrode method for testing Hall effect in crystal. The rotation of equipotential lines by the Hall field is also shown.

[7] G. P. Harnwell and S. N. Van Voorhis, Rev. Sci. Inst. **5**, 244 (1934).

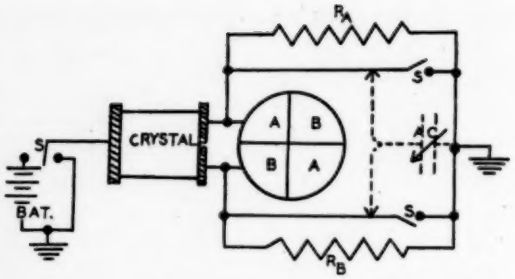

FIG. 2. Differential electrometer method of Tartakowsky. The high resistors R_A and R_B were not part of Tartakowsky's circuit, which included instead the equalizing variable air condenser AC (shown in dashed lines).

grounded near their center, the grounded point G being varied by steps of 1½ volts until no current flowed into H when the crystal was steadily illuminated. Batteries and leads were electrostatically shielded.

Measurements on NaCl, KCl and KBr were repeated by means of Tartakowsky's divided electrode arrangement (Fig. 2). KI and NaBr were also measured with this latter apparatus.

Single crystals of the substances studied were manufactured from chemically-pure, fused salts with an apparatus similar to that described by Walther.[8] Photoelectric contacts with the crystals were made by sputtering mirror-like, platinum coats on to freshly cleaved faces. The small side electrodes were made by scraping away all of the sputtered coat on one side of a specimen except that covered by a clamped safety razor blade (thickness 0.24 mm). Crystals were additively colored by electron impregnation at high temperature (500 to 700°C) and then "quenched" in an air stream to secure atomic dispersion of color centers.

The crystals were gripped between brass electrodes by the steady pressure of spiral brass springs, the electrodes being mounted in a hard rubber block frame. The frame, with glass plates, also served as a low vacuum chamber. The Hall electrode was protected fron leakage currents by a guard ring. Crystals were illuminated over their complete length by the full light from the tungsten filament of a 6–8-volt, 50-cp automobile headlight bulb, the focused light beam being sent through a long hole in one pole piece of the Weiss electromagnet which produced the magnetic field.

[8] H. Walther, Rev. Sci. Inst. **8**, 406 (1937).

PROCEDURE AND RESULTS

The procedure was to adjust the position of the grounded point of the applied batteries until with the light shining on the specimen, no photoelectric current flowed into the cross-electrode. Then a magnetic field was applied normal to the principal plane of the specimen, and any resulting effect upon the current into the Hall electrode observed.

The arrangement was empirically tested for its sensitivity to small e.m.f.'s by shifting the grounded point of the batteries by a small amount and noting the corresponding effect on the *steady* deflection of the indicating instrument. Such a shift had the effect of increasing the potential difference between the Hall electrode and the respective ends of the crystal by an amount $\pm\Delta E$.

It was assumed, from considerations of symmetry, that a transverse Hall e.m.f. E_H across the crystal would rotate the equipotential lines of the electric field about their points of intersection with the longitudinal center of the crystal, i.e. (Fig. 1), that the potential difference between the Hall electrode and the ends of the crystal would be changed by $\pm\frac{1}{2}E_H$, respectively. This assumption was made plausible by an experiment upon zincblende, which from Lenz'[9] work is known to have an easily detectable photoelectric Hall effect. With zincblende in the apparatus it was found that the direction of the Hall current into the single cross-electrode could be reversed by reversing the direction of the applied electric field, indicating that *if* a second cross-electrode H' (Fig. 1) had been connected to a second amplifier A', the latter, during application of a magnetic field, would have recorded a Hall current equal and opposite to that recorded by A. Hence it was assumed that the Hall e.m.f. E_H across the width of a given alkali halide crystal could not be greater than the smallest voltage shift ΔE of the grounded point which would produce a positive effect.

No positive indication of a Hall e.m.f. or associated Hall current was found for the steady photoelectric current in additively colored NaCl, KBr or KCl. In one set of readings upon rocksalt it was found that the *steady* change in the

[9] H. Lenz, Ann. d. Physik **77**, 449 (1925); **82**, 775 (1927).

reading of the indicating instrument for small shifts of the grounded point was 7.5 cm/volt, whereas turning on the magnetic field (of 12,200 gauss) produced random shifts of about 1.5 cm. The variations apparently caused by application of the magnetic field were found to be present with or without the light shining on the crystal. The average of 8 readings taken with the magnetic field in one direction differed by less than 0.3 cm from the average of 8 readings with the magnetic field reversed. Therefore, assuming that for the very small currents involved any Hall e.m.f. present would be proportional to the transverse photoelectric current produced by it, it was concluded that the effect of *reversing* the magnetic field was less than that produced by shifting the grounded point of the batteries by 0.1 volt. With the calibrating factor of $\frac{1}{2}$, the Hall e.m.f. was less than 0.2 volt across the crystal (dimensions 7.5×4.0×1.2 mm), or, the Hall field Y was less than 0.5 volt/cm.

The steady photoelectric current under the applied voltage, 520, was found to build up a photoelectric "back e.m.f." of 90 volts, as determined by the applied potential which would just prevent the built-up back photoelectric e.m.f. from sending a current in the opposite direction. Then the total "effective" potential difference over the length of the crystal was 430 volts, and the average resultant field 570 volts/cm. Therefore the ratio Y/X of the Hall field to the electric field near the center of the crystal was less than 1/1150.

The measurements just described were taken with a very lightly colored specimen, color density estimated at about 5×10^{16} centers/cm^3. According to Glaser and Lehfeldt[10] the so-called "thrust paths" of the photoelectrons in rocksalt are inversely proportional to the color center density. A thrust-path, however, presumably consists of many free paths.

The measurements were checked and confirmed by using the amplifier in a slightly different manner, namely, by allowing the grid to "float" (R_g=insulation leak resistance=about 10^{13} ohms) and noting its rate of increase of potential, if any, caused by application of a magnetic field to the illuminated crystal.

Lenz[9] found the photoelectric Hall effect in zincblende to depend in sign and magnitude upon the orientation of the specimen, while Von Hippel[5] found preferred directions of electron movement in rocksalt. It therefore appeared likely that the Hall effect in rocksalt might be a function of the orientation of the specimen. A plate was cut and sputtered so that the electric field could be applied in a 110-direction, and the possible Hall field measured in another 110-direction. No effect was found, the upper limit to the ratio Y/X for a magnetic field of 12,200 gauss being set at 1/200.

It seemed possible that the small value of the Hall effect indicated for the *steady* photoelectric current was due to opposite and canceling contributions by the equal components of electron and "hole conduction" current, since, according to an application of quantum mechanics by Fowler,[11] the Hall coefficient for an electronic semi-conductor is

$$R=\frac{kY}{HX}=-\frac{3}{8}\frac{\sigma_1-\sigma_2}{e(n_1+n_2)},$$

where k=constant, H=magnetic field, e=charge on a carrier, n_1 and n_2 are the numerical concentrations of the negative and positive carriers, respectively, and σ_1 and σ_2 are the corresponding conductivities. Now the colored potassium salts are characterized by a comparatively large initial surge of photoelectric current[1, 10] at the outset of illumination, followed by a rapid decrease to a final "steady" (but still decreasing) value about 100 times smaller than the initial current. The rapid decrease of current is attributed to the formation of space charge, resulting from the failure of the positive component of photoelectric current to remove positive charge as rapidly as the negative charge is drawn out. The initial photoelectric surge therefore consists mostly of electrons, and consequently in it the canceling contribution of the positive carriers to the Hall effect should be small. Therefore measurements were taken of the effect of an applied magnetic field upon the photoelectric current flowing during a 1/10 second flash of light in KCl and KBr, with the amplifier, still connected to the cross-electrode, as a ballistic instrument.

[10] G. Glaser and W. Lehfeldt, Gott. Nachr. **2**, 7 (1936).

[11] R. H. Fowler, Proc. Roy. Soc. **A140**, 504 (1933).

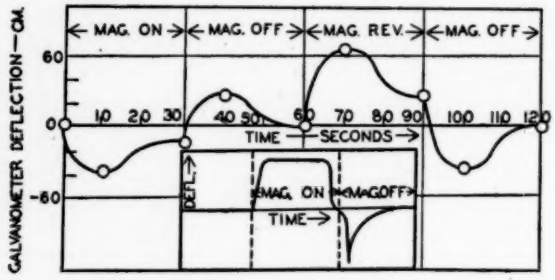

FIG. 3. Upper curve, "photoelectric Hall back e.m.f." effect in ZnS by single cross-electrode set-up. The initial large throw of the indicating instrument upon application of a magnetic field was ascribed to a lack of photoelectric back e.m.f. initially opposing the Hall current; the decrease to a nearly steady value within 30 seconds was ascribed to the formation of a photoelectric back "Hall" e.m.f., whose presence then caused the reverse throw upon release of the magnetic field. Inset lower curve, Tartakowsky's curve for rocksalt, showing a similar "polarization" by means of the divided electrode arrangement.

With the KCl specimen (7.0×3.5×1.0 mm) and intense illumination, the smallest obtainable unidirectional throw of the indicating galvanometer (for 0.1-second flashes) was about 25 cm. (Space charge built up rapidly during the flash, changing the potential distribution along the length of the crystal, so that for some positions of the grounded battery point the direction of the photoelectric current into the Hall electrode reversed during the flash.) Changing the grounded point by 3 volts changed the ballistic throw, on the average, 6 cm, or 2 cm/volt, whereas, for 12 pairs of readings, the average for the magnetic field in one direction did not differ by more than 0.1 cm from the average with the magnetic field reversed. Random fluctuations between consecutive readings were of the order of 1 cm but a persistent effect of $\frac{1}{2}$ cm would have been easily detected. The assumed maximum unobserved effect of $\frac{1}{2}$ cm was due to reversing the magnetic field, so that the effect of applying the magnetic field in one direction must have been less than $\frac{1}{4}$ cm, the effect which according to the calibration would have been produced by a Hall e.m.f. of $\frac{1}{4}$ volt, or a Hall field of 0.7 volt/cm. The upper limit to the ratio Y/X then came out to be 1/850 for $H=12{,}200$ gauss.

However, the photoelectric back e.m.f. developed during the flash was about one-half of the total applied e.m.f., or the resultant time average of the longitudinal electric field near the Hall electrode during the flash was about three-fourths of the initial applied field; likewise with the time average of a possible accompanying Hall field. Making this correction, the limit for ratio Y/X for the initial electron surge of current was taken as $4/3\times1/850=1/640$.

The crystal was grounded and illuminated for $3\frac{1}{2}$ minutes between consecutive flashes, or long enough to remove at least 99 percent of the developed photoelectric back e.m.f. and to restore the crystal to approximately the same condition for each reading.

In similar measurements upon KBr, in which the photoelectric polarization built up by successive flashes was not completely discharged between consecutive trials, the upper limit to Y/X was 1/225.

To test whether the experimental arrangement was capable of detecting the presence of a small Hall current or e.m.f., a specimen of clear yellow zincblende (sphalerite), 7.27×4.8×2.0 mm, cut with its length parallel to a direction symmetrical with respect to the crystal axes (following a suggestion by Lenz[9]), was substituted in the apparatus. A Hall current, whose direction reversed both with reversal of the electric and the magnetic fields, was found to flow upon application of the magnetic field. Data (averages of 20 trials for both directions of the magnetic field) are shown in Fig. 3 for one direction of the electric field.

The change in steady deflection per unit shift of grounded point was 5.7 cm/volt, while the change produced by reversing the magnetic field was 40 cm. From these data, and using the calibration factor of 2, it was found that the Hall field was 14.5 volts/cm, the *average* applied electric field being 890 volts/cm. According to Lenz the electric field near the middle of a photoelectrically polarized zincblende plate is equal, approximately, to the average applied field. Therefore the value, 1/60, found for the ratio Y/X in zincblende subjected to 12,200 gauss, agreed well, at least in order of magnitude, with Lenz' value for the same ratio, 1/44, extrapolated to the same value of magnetic field. (Lenz showed that the Hall field in zincblende is linearly proportional to the strength of the magnetic field.) The difference could be due to structural differences between the specimens of the zincblende, to the assumption made

here that the Hall e.m.f. was proportional to the Hall current, or to the fact that Lenz' current densities were about 40 times greater than those used here. In any event it appeared that the single-electrode method was capable of detecting a photoelectric Hall effect.

An effect ascribed to "photoelectric Hall back e.m.f." is shown in the graphical display of the data on zincblende. Upon turning on the magnetic field the galvanometer deflection was about $2\frac{1}{2}$ times greater than its steady deflection. If the magnetic field was then removed, an opposite initial deflection occurred, of the same order of magnitude as the original initial deflection. The original large initial deflection was ascribed to a lack of photoelectric back e.m.f. at the Hall electrode initially opposing the Hall current. The decrease of Hall current was ascribed to the building up of a photoelectric back "Hall" e.m.f., and the reverse current to the action of this built-up e.m.f. after removal of the original Hall field.

A similar effect, obtained by using a divided electrode and a differential electrometer, has been described for x-rayed rocksalt by Tartakowsky.[4] His curve is reproduced as an insert in Fig. 3 for the purpose of comparison. An attempt to duplicate Tartakowsky's curve for rocksalt by means of his set-up was unsuccessful.

The photoelectric back e.m.f. developed by a steady current in KCl was found to be about 90 percent of the total applied e.m.f., and about 99 percent in KBr. Potential measurements made with a movable side electrode showed that the developed back e.m.f. was mostly due to charges collected near the ends of a crystal. The potential distribution along a photoelectrically "excited" KBr crystal is shown in Fig. 4. The irregularity of individual points is a result of the procedure of taking the crystal-holder out of the apparatus between readings in order to move the probe.

The potential distribution resembles closely that found in a gaseous discharge tube. The electric field intensity is greatest close to the electrodes and comparatively small near the middle of the specimen. It might therefore be expected that the Hall field generated by a magnetic field would also be greater near the ends of such a crystal, so that a method for detecting such a possible concentration of Hall field near the electrodes was needed.

According to Lenz the potential distribution along a photoelectrically polarized zincblende crystal is such as to indicate a resultant positive space charge throughout. The electric field intensity, in accordance with Poisson's equation, is increased near the cathode and diminished near the anode. In the present investigation, zincblende was placed in the divided electrode arrangement of Tartakowsky. It was then found that the magnetic deflection of current from one part of the divided electrode to the other was approximately 12 percent greater when the divided electrode was used as cathode than when used as anode. The difference was about ten times greater than the average random fluctuation between consecutive readings. It therefore appeared that the Tartakowsky arrangement (first set up for the purpose of checking Tartakowsky's experiment with colored rocksalt) should be suitable for the detection of small Hall fields concentrated near the ends of a specimen. (It was ascertained that the zincblende specimen as a whole had no rectifying effect upon the photoelectric current.)

Check measurements upon NaCl, KCl and KBr were made with the divided electrode arrangement, as well as measurements upon NaBr and KI. No *conclusive* evidence of a Hall deflection of current was found in any of these substances. Upper limits to the possible Hall fields in the various substances were assigned by direct comparison with the behavior

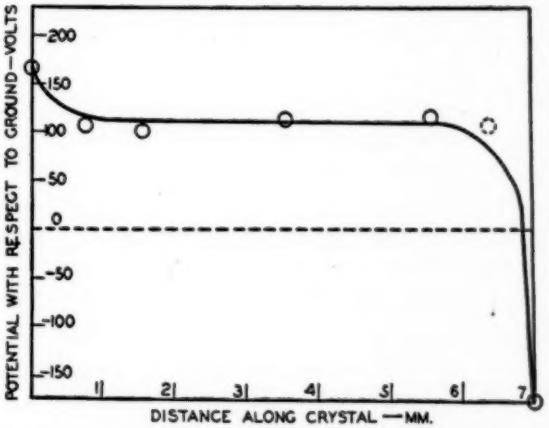

FIG. 4. Potential distribution along photoelectrically polarized KBr crystals, as determined by a movable probe.

of zincblende in the same apparatus. In Table I, i is the total (average) current to one segment of the divided electrode, $\Delta_h i$ is the change of current to that segment (average of 10 readings) caused by the magnetic field, and $\Delta_f i$ is the average fluctuation in the current for a single observation from its average value i. In the last column, R is the effect of the magnetic field upon the current flow in a given alkali halide as compared to its effect upon zincblende. This ratio has been assigned the positive sign if the apparent (very small) current deflection indicated by the average of 10 readings was in the same direction as for zincblende.

There is probably no significance to the fact that the very small magnetic deflection (if any) in KCl, KBr, and NaBr had the correct sign for a normal Hall deflection of current, because for these the average fractional change of current to one part of the divided electrode after application of the magnetic field was several times smaller than the average fractional fluctuation of current between consecutive readings. In rocksalt, however, a small "anomaly," slightly larger than the average fluctuations, and of the correct sign for a normal Hall current, was found. The anomaly was not recognized as an indication of a bona fide Hall effect for the following reasons:

1. In 6 specimens tested, the anomaly had the "wrong" sign in one, and did not exist in another (which happened to be a plate with non-uniform coloring).

2. Most of the effect was found to be produced by application of the magnetic field in *one* direction; the other direction of field had no effect, or even a small effect in the "wrong" direction.

3. Similar effects, but several times smaller, were sometimes observed with the crystal unilluminated.

A possibility remains, however, that this anomaly was an indication of a small Hall effect on the borderline of observational limit, superimposed upon a small, spurious, unidirectional effect of the magnet or magnetizing circuit. The effect was too small to be observed with the original "balanced-rate-of-charge" method of Tartakowsky; it was only observed with the steady deflection method, using high resistors to impress potential differences upon the differential electrometer (Fig. 2).

TABLE I.

Substance	Specimen Size (mm)	$\Delta_h i/i$	$\Delta_f i/i$	R
NaCl	6.7×4.6	1/880	±1/1000	1/22
NaBr	4.4×3.6	1/4000	±1/1500	1/20
KCl	5.8×4.5	1/1700	±1/600	1/50
KBr	7.5×4.5	1/2300	±1/1000	1/50
KI	3.7×3.5	±1/5000	±1/2000	±1/40

The differential electrometer could also be used to measure the difference in charge collected by the two parts of the divided electrode as a function of the applied magnetic field during a short flash of light. It was found that the charge collected by one electrode-part was changed by less than 1 part in 800 for KCl, 1 in 225 for KBr, and 1 in 600 for KI, by application of a magnetic field of 12,200 gauss, lending further confirmation to the previous null results.

Null results thus far described were obtained with *additively* colored specimens, having a stoichiometric excess of alkali atoms. Lukirsky's and Tartakowsky's reported positive results had been with *photochemically* colored rocksalt. It seemed possible that the discrepancy was due to the difference in the method of preparation of the specimens. Rocksalt colored by exposure to 50-kv tungsten x-rays was therefore tested in the Tartakowsky set up, using the balanced rate-of-change method.

An unsuspected difficulty was immediately encountered—namely, that the x-rayed crystals faded so fast under the fairly bright illumination needed to give "steady" currents of sufficient magnitude that it was hard to make the adjustment of the equalizing condenser before all the photo-sensitivity had disappeared; also it was impossible to obtain a steady state of photoelectric polarization. A fairly dense coloring would last only about five minutes. However by resensitizing the crystal several times, and by making small adjustments between consecutive pairs of readings (one reading for each direction of the magnetic field) so that little photoelectric sensitivity of a specimen was "wasted" and the adjustment constantly improved, sufficient data was finally accumulated. The conclusion was that no persistent effect

greater than 1/10 of the corresponding effect observed in zincblende under the same conditions existed in rocksalt colored by x-rays.

The electrometer used had almost exactly the same sensitivity as that of Tartakowsky's instrument. The working of the arrangement was tested with zincblende. The discrepancy is hard to explain. Tartakowsky, however, used a magnetic field of 30,000 gauss, compared to 12,200 gauss used here.

Besides being tested for possible photoelectric Hall effect, NaCl, KBr, and KCl, and also zincblende were examined for possible changes in photoelectric resistance caused by a magnetic field. Fluctuations in the longitudinal photoelectric current itself were found to limit the sensitivity to the extent that the null result uniformly found indicated only that large magneto-resistance anomalies do not exist in the photo-conductors studied. Upper limits to the magneto-resistance change caused by a field of 12,200 gauss were set as follows: NaCl, 0.15 percent; KCl, 0.3 percent; KBr, 0.25 percent; ZnS, 0.14 percent. The maximum expected effect in ZnS, according to calculations based upon the photoelectron mean free path as deduced from Lenz' Hall effect measurements, was only 0.05 percent.

The fluctuations of photoelectric current were five to ten times greater than those which would be expected from shot and Johnson effects[12, 13]. The fluctuations apparently were due to some phenomenon in the crystals. They were observed, not only with the direct-current amplifier, but also with the differential electrometer, which, when electrically shielded, is less sensitive to random ionization of the air about it than the amplifier. The ratio of the fluctuations in current to the entire current increased with increasing applied voltage. In KBr, for example, the fluctuations were about 50 percent of the total current when 600 volts were applied to a crystal 7.2 mm long.

Conclusion and Discussion

It has been established, by means of two different experimental arrangements, both checked with a substance of known properties, that the photoelectric Hall field in additively colored rocksalt, if it exists at all, is less than 1/1000 of the applied electric field (for $H=12{,}200$). Similar upper limits have been obtained for four other colored alkali halides. If, to take the particularly important case of rocksalt, the null result is interpreted as meaning that the free paths of the photoelectrons in the crystal lattice are comparatively short, the equation of Gans,[14]

$$\frac{Y}{X}=\frac{1}{4}\left(\frac{3\pi m}{kT}\right)^{\frac{1}{2}}\frac{e}{m}\lambda H,$$

for the *isothermal* Hall effect in an electronic conductor could be used to determine the order of magnitude of the maximum mean free path (λ) consistent with the experimentally determined upper limit of the ratio Y/X. Putting $Y/X=1/1000$ and $H=12{,}000$ gauss in the foregoing equation, it is found that

$$\lambda=4.5\times10^{-8}\text{cm}.$$

Such a length is not much greater than the dimensions of a lattice cell. Von Hippel, from his experiments on electrical breakdown in rocksalt, concluded that the electronic mean free path was of the order 2×10^{-8} cm. Such a mean free path, by Gans' formula, would give a Hall field, for 12,000 gauss, of

$$Y/X=1/2250.$$

Detection of a Hall effect of such a magnitude was slightly beyond the sensitivity of the measurements which have been described.

An alternative interpretation, that the contribution of the photoelectrons to the Hall field in colored alkali halides is nearly or entirely canceled by the contribution of the positively-charged carriers, might be made, but appears unnecessary in the view of the fact that no Hall effect was found even in the comparatively large initial surge of photoelectric current in KCl, KBr, and KI, this initial surge being, in all probability, almost entirely composed of electrons.

The writer wishes to acknowledge his indebtedness to Professor C. W. Heaps for suggestion of the problem, as well as for many helpful discussions concerning it; and to Professor H. A. Wilson for his continued interest in the investigation and valuable advice in the design of apparatus.

[12] Barnes and Silverman, Rev. Mod. Phys. **6**, 162 (1934).
[13] L. R. Hafstad, Phys. Rev. **44**, 201 (1933).
[14] R. Gans, Ann. d. Physik **20**, 293 (1906).

The Elastic, Dielectric and Piezoelectric Constants of Heavy-Water Rochelle Salt[1]

A. N. HOLDEN AND W. P. MASON
Bell Telephone Laboratories, New York, New York

(Received October 30, 1939)

Crystallization of Rochelle salt from heavy water raises the upper Curie point of the material by 11°C and lowers the lower point by 5°C, but leaves the other properties substantially unchanged.

THE unusual behavior of Rochelle salt in exhibiting an extraordinarily high dielectric susceptibility for fields along the *a* axis between two critical temperatures (Curie points) has been the subject of numerous investigations.[2] This paper presents the results of dynamic measurements of the elastic, electric and piezoelectric constants of Rochelle salt crystallized from heavy water (deuterium oxide).

I. Preparation of Crystals and Measurement of Low Frequency Dielectric Constant

To prepare the samples for measurement, 65 grams of dehydrated Rochelle salt, which had been kept at 100°C for eight hours in vacuum and then at room temperature over dehydrite until the residue reached constant weight, were dissolved in 100 grams of 99.5 percent heavy water. The resulting solution is somewhat supersaturated at ordinary temperatures. Crystal plates were then grown one at a time from this solution at room temperature in a square cell fitted with horizontal glass plates spaced about 100 mils by glass spacers, seeded with ordinary Rochelle salt seeds of the desired orientation.

Two such plates perpendicular to the *a* axis, about 2 square centimeters in area, were used for measurements of dielectric constant at 1000 cycles per second. From these plates the surface irregularities were polished with carborundum and machine oil, the resulting powdery surface was dissolved off in the growing solution, warmed to unsaturation, and a fresh surface was crystallized on for about five minutes. Electrodes of tin foil were affixed with petrolatum and the plates were freely suspended in the temperature-controlled glass tubes. Measurements were made with an oscillator and impedance bridge, at a peak voltage gradient of approximately 35 volts per centimeter. The resulting measurements are shown in Fig. 1, where similar measurements on a similarly prepared plate of ordinary Rochelle salt are shown for comparison. The substitution of heavy water for ordinary water in the crystal has raised the upper Curie point by about 11°C and has lowered the lower point by about 5°C.

The upper Curie points of crystals grown from solution in 50 percent and 20 percent heavy water were found to lie at 26.6°C and about 24°C, respectively.

II. Measurements of the Dynamic Properties of Heavy-Water Rochelle Salt at High Frequencies

In order to measure dynamically the dielectric and piezoelectric properties of an *a* or X-cut heavy-water Rochelle salt crystal, a bar was cut with its length at 45° from the *Y* and *Z* axes and having the dimensions, length = 20.62 mm, width = 4.24 mm, thickness = 2.01 mm. These dimensions were chosen so that no secondary resonances appeared near the main one. The crystal was gold-plated by a modified evaporation process, and its resonance and antiresonance frequencies were measured as a function of temperature. These frequencies plotted

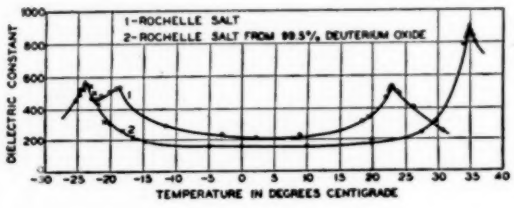

FIG. 1.

[1] A preliminary description of this work is published in a Letter to the Editor in the August 15, 1939 issue of the *Physical Review*.

[2] H. Mueller, Phys. Rev. **47**, 175 (1935).

for a crystal one centimeter long are shown on Fig. 2 by the curves A and B. Curve C shows a measurement of the resonant frequency of the same crystal (with the plating removed) placed in an air-gap holder with a large air-gap.

The relation between the resonant and anti-resonant frequencies and the electromechanical coupling factor k has been discussed at length in a former paper.[3] It is there shown that the electromechanical coupling factor k defined by the equation

$$k=\frac{d_{14}}{2}\left(\frac{4\pi}{Ks_{22}'}\right)^{\frac{1}{2}} \tag{1}$$

determines the ratios of the resonant and anti-resonant frequencies to the natural mechanical resonant frequency (measured as usual without plating on the crystal) according to the curves shown on Fig. 3. In Eq. (1), d_{14}, K and s_{22}' are the open circuit constants, i.e., d_{14} is the piezoelectric constant measured with a high impedance electrical instrument, K is the dielectric constant of the crystal clamped, while s_{22}' is the inverse of Young's modulus measured without plating on the crystal.[4]

Comparing the curves of Figs. 2 and 3, the electromechanical coupling k is easily evaluated and is shown on Fig. 4. To determine the piezoelectric constant d_{14}, we need to know the elastic constant s_{22}' and the dielectric constant K of the clamped crystal. The elastic constant of the

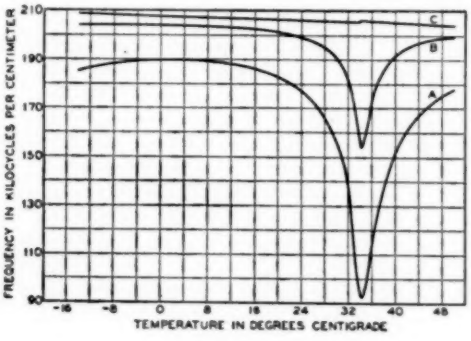

FIG. 2.

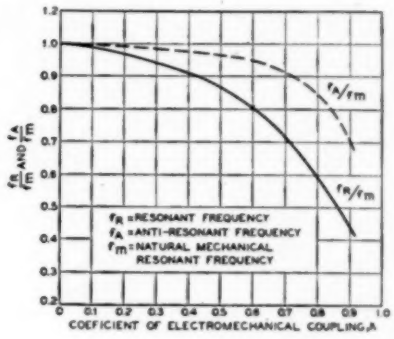

FIG. 3.

crystal free from plating can be determined from the measured frequency of the crystal in an air-gap holder (curve C of Fig. 2) by using the equation

$$f_m=\frac{1}{2l}\left(\frac{1}{\rho s_{22}'}\right)^{\frac{1}{2}}, \tag{2}$$

where l is the length of the crystal and ρ the density. By pycnometer methods Mr. W. L. Bond finds the density of heavy-water Rochelle salt to be

$$\rho=1.830\pm0.003. \tag{3}$$

Hence, the value of s_{22}' as a function of temperature can be calculated from Eq. (2) and is shown as curve s_{22}' of Fig. 4. To determine the dielectric constant K, crystals were cut so small that they had no resonances in the frequency range of interest and their capacitances were measured as a function of the temperature. The dielectric constant K_F of the crystal free to move is shown on Fig. 5. These measurements are at a considerably higher frequency than those of Fig. 1 and show a lower value. The clamped dielectric constant K has been shown[5] to be

$$K=K_F/(1-k^2). \tag{4}$$

Hence, from Fig. 5 and curve k, Fig. 4, the dielectric constant K can be evaluated and it is shown as curve K of Fig. 4. Since we have evaluated k, s_{22}' and K, the value of d_{14}, the piezoelectric constant, can be evaluated and is shown as curve d_{14} of Fig. 6. In general between the Curie points, d_{14} has a lower value for dynamic measurements than ordinary Rochelle salt, but above the upper Curie point it has a higher value.

[3] W. P. Mason, Phys. Rev. **55**, 775 (1939).

[4] It should be pointed out that to agree with the definition given by Voigt, the constant d_{14} should be measured with a low impedance electrical instrument while the elastic constant s_{22}' should be measured with plating on the crystal and this short-circuited. Both quantities as defined by Voigt can be obtained from those shown on Figs. 4 and 6 by dividing d_{14} and s_{22}', respectively, by $(1-k^2)$.

[5] See reference 3, Eq. (55).

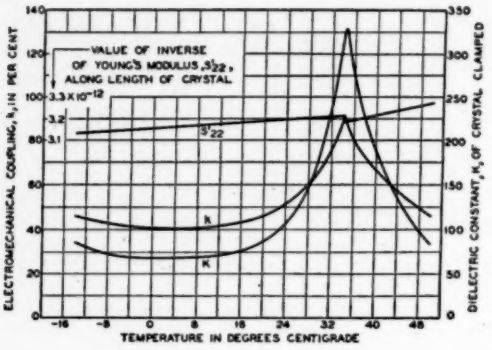

FIG. 4.

Another piezoelectric constant, e_{14}, is often used, which is related to d_{14} by the equation

$$e_{14}=d_{14}/s_{44}, \qquad (5)$$

where s_{44} is the shear elastic constant. This was measured for a heavy-water crystal and found to be nearly the same as for ordinary Rochelle salt, namely

$$s_{44}=7.98\times10^{-12}. \qquad (6)$$

The value of e_{14} can then be determined and is shown on Fig. 6 by curve e_{14}. It was shown in the paper referred to above that another piezoelectric constant, f_{14}, relating the piezoelectric stress and the applied charge density, was more closely related to the usually measured constants than either d_{14} or e_{14} and furthermore, was nearly a constant for all temperature and frequency conditions. The value of f_{14} is

$$f_{14}=4\pi e_{14}/K \qquad (7)$$

and is plotted as curve f_{14} of Fig. 6. The value 7.8×10^4 is nearly the same as for ordinary Rochelle salt. This indicates that the piezoelectric stress caused by the attraction between the bound charges in the material and the applied charge is the same for both Rochelle salts and that their difference in behavior is caused by the difference in the clamped dielectric constants of the two materials.

The difference in the clamped dielectric constant, in particular the lower value between the two Curie points, is accounted for by the wider separation of the Curie points.

Some measurements were also made on Y-cut and Z-cut crystal plates (perpendicular to the b and c axes, respectively) in order to determine the other two piezoelectric constants. By cutting crystals at 45° from the other crystallographic axes and repeating the process described above, the following constants were measured:

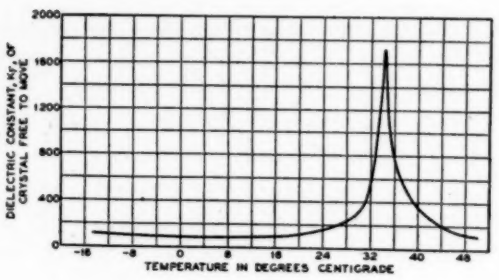

FIG. 5.

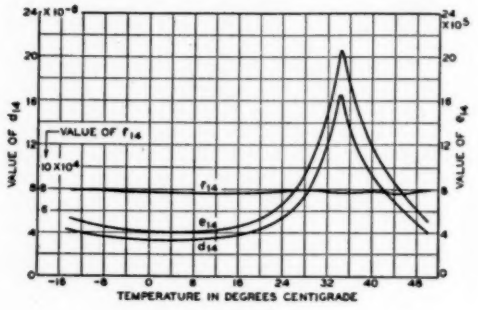

FIG. 6.

Y-Cut Crystals at 30°C

k	K_F	K	s_{11}'	d_{25}	e_{25}	f_{25}
0.305	18.0	16.3	9.93×10^{-12}	220×10^{-8}	6.67×10^4	5.14×10^4

This crystal has a somewhat larger piezoelectric effect than the corresponding ordinary Rochelle salt crystal. Over a temperature range the piezoelectric constant d_{25} increases slightly with temperature.

The measurements for the Z-cut crystal are:

Z-Cut Crystal at 30°C

k	K	s_{11}'	d_{36}	e_{36}	f_{36}
0.107	10.4	4.2×10^{-12}	40.1×10^{-8}	3.97×10^4	4.80×10^4

The constants are very similar to those for an ordinary Z-cut Rochelle salt crystal.

The authors are indebted to Drs. S. O. Morgan and G. K. Teal for suggesting this work, to Dr. G. T. Kohman for the low frequency dielectric constant measurements, and to Mr. W. L. Bond for his measurements of density.

On After-Effects in Solid Dielectrics

B. GROSS
Instituto Nacional de Tecnologia, Rio de Janeiro, Brazil
(Received July 24, 1939)

The discharge- and residual charge-curves observed in anomalous dielectrics are discussed and two general relations between them are established.

IT is generally known that the capacity of a condenser which shows the phenomenon of residual charges, depends on the charging time. For instance a Leyden jar, which can give successive sparks, discharges slowly if a potential difference has been applied for some minutes, before but will discharge very rapidly if the potential difference has been applied only for a few seconds. This behavior seems often very irregular. We should like to point out some very simple, but general relations existing there, which result from the principle of superposition, always used successfully for the explanation of phenomena of this kind.

Let us consider the three following experiments characteristic of the behavior of anomalous dielectrics: (Fig. 1).

(I) A charging potential U_0 is applied to the condenser during an interval T, which is so long that at its end the after-effects produced by the application of the potential U_0 have dispersed completely. Then U_0 is withdrawn and one of the plates of the condenser remains insulated while the other one is connected to earth. The discharge is then very slow and does not depend on T.

(II) The potential U_0 is applied during an interval t_0 much smaller than T. The discharge now depends on t_0 and is much faster than in the foregoing case.

(III) Finally U_0 is applied during the interval T, then it is removed and the condenser is short-circuited during t_0, and then one of the plates is again insulated. A potential difference will appear again between the plates and we have a residual-charge effect.

These three effects are related to the fundamental property of the anomalous dielectrics, i.e., the anomalous- or after-current and can be described mathematically, if we assume the validity of the principle of superposition introduced into the theory of after-effects by Hopkinson,[1] and subsequently used by many authors, such as v. Schweidler,[2] Whitehead,[3] Neufeld,[4] and Yager.[5]

Let $\Delta U\varphi(t-\tau)$ be the after-current produced by the discontinuous variation ΔU of the applied potential difference at an instant τ. Then the principle of superposition enables us to express the after-current i flowing in the instant t and produced by any continuous variation of the potential, as follows,

$$i=\int_{-\infty}^{t}\frac{dU(\tau)}{d\tau}\varphi(t-\tau)d\tau. \qquad (1)$$

If we assume that a continuous variation of the potential difference between the plates begins at $t=0$ and take into account the leakage current U/R and the displacement current CdU/dt, the

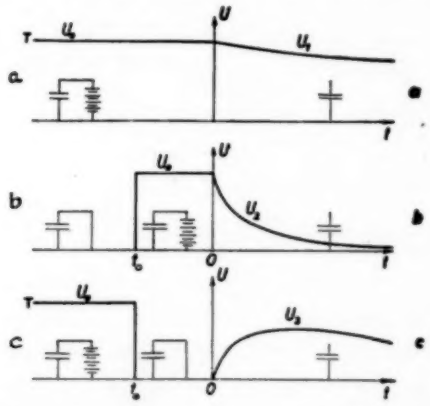

FIG. 1. *a*, Discharge after complete charge. *b*, Discharge after instantaneous charge. *c*, The residual charge.

[1] L. Hopkinson, Phil. Trans. **166**, 489 (1876); **167**, 599 (1878).
[2] E. v. Schweidler, Ann. d. Physik **24**, 711 (1907).
[3] J. B. Whitehead, *Lectures on Dielectric Theory and Insulation* (McGraw-Hill, New York, 1927).
[4] J. Neufeld, J. Frank. Inst. **222**, 327 (1936).
[5] W. A. Yager, Physics **7**, 434 (1936).

total current-flow across the dielectric is given by

$$J=C\frac{dU}{dt}+\frac{U}{R}+\int_0^t \frac{dU(\tau)}{d\tau}\varphi(t-\tau)d\tau+i(t), \quad (2)$$

where $i(t)$ is the after-current produced by all the potential difference variations which eventually had occurred before $t=0$.

If the plates are insulated the total current J must become 0.

$$J=0. \quad (3)$$

We thus obtain $U(t)$ as the solution of an integro-differential equation

$$C\frac{dU}{dt}+\frac{U}{R}+\int_0^t \frac{dU(\tau)}{d\tau}\varphi(t-\tau)d\tau+i(t)=0. \quad (4)$$

With regard to the mathematical description the three cases referred to above differ only in the form of the right member $i(t)$. In (I) it has become 0; in (II) it is given by $U_0\varphi(t+t_0)$, and in (III) it has the same absolute value, but the opposite sign. Hence we may write more generally

$$i(t)=\begin{cases}0 & \text{for case (I)}\\ +i_0(t) & \text{for case (II)}\\ -i_0(t) & \text{for case (III).}\end{cases} \quad (5)$$

The rigorous evaluation of the functions $U(t)$ is rather complicated,[6] but we can deduce some simple relations among the curves $U(t)$ in all three cases, reducing them to a unique one.

For this purpose we write at first Eq. (4) in the form

$$F[U(t)]=-i(t), \quad (6)$$

observing the linearity of the operator F:

$$F[U_1(t)]+F[U_2(t)]=F[U_1(t)+U_2(t)]. \quad (7)$$

If $U_1(t)$, $U_2(t)$ and $U_3(t)$ are, respectively, the potential difference curves in the three cases concerned here, they satisfy the equations

$$F[U_1(t)]=0 \quad \text{with } U_1(0)=U_0, \quad (8)$$

$$F[U_2(t)]=-i_0(t) \quad \text{with } U_2(0)=U_0, \quad (9)$$

$$F[U_3(t)]=i_0(t) \quad \text{with } U_3(0)=0. \quad (10)$$

Summing up (9) and (10) and using relation (7) we find

$$F[U_2(t)+U_3(t)]=0 \quad \text{with } U_2(0)+U_3(0)=U_0. \quad (11)$$

Comparing this with (8) we have

$$U_2(t)+U_3(t)=U_1(t). \quad (12)$$

The three curves are therefore correlated in a very simple manner and it is always possible to deduce one of them from the two other ones. But even between these we find a direct relation.

By the substitution

$$dU/dt=\psi(t), \quad (13)$$

introduced by F. M. de Oliveira Castro[7] into the theory of Eq. (4) and using the new kernel

$$\rho(t)=\varphi(t)/C+1/RC, \quad (14)$$

we write (4) in the form

$$\psi_1(t)+\int_0^t \psi_1(\tau)\rho(t-\tau)d\tau=-U_0/RC \quad \text{for case (I),} \quad (15)$$

$$\psi_2(t)+\int_0^t \psi_2(\tau)\rho(t-\tau)d\tau=-\frac{U_0}{RC}-\frac{1}{C}\int_0^t \frac{di_0(\tau)}{d\tau}d\tau-\frac{i_0(0)}{C} \quad \text{for case (II).} \quad (16)$$

Eq. (15) is an integral equation of the Volterra-type with constant right member and (16) the same equation with variable right member. The equations being linear it seems logical to apply a principle of superposition, for we may consider $i(t)$ as an external "force" acting on a system of which we know the "movement" produced by the constant "force." So we try the solution in the form

$$\psi_2(t)=f(t)+\int_0^t \frac{di_0(\tau)}{d\tau}g(t-\tau)d\tau, \quad (17)$$

where $g(t)$ and $f(t)$ are two arbitrary functions.

Introducing (17) into (16) and noting the identity

$$\int_0^t \rho(t-\tau)d\tau\int_0^\tau \frac{di_0(\sigma)}{d\sigma}g(t-\sigma)d\sigma = \int_0^t \frac{di_0(\tau)}{d\tau}d\tau\int_0^{t-\tau} g(\sigma)\rho(t-\tau-\sigma)d\sigma, \quad (18)$$

[6] For an approximative solution see B. Gross, Zeits. f. Physik **107**, 217 (1937); a more rigorous treatment is given by F. M. de Oliveira Castro, Zeits. f. Physik **114**, 116 (1939).

[7] F. M. de Oliveira Castro, Ann. Acad. Bras. Sc. **11**, 150 (1939).

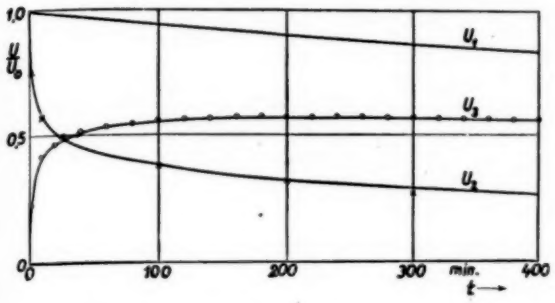

FIG. 2. Measurements with carnauba-wax. U_1, Discharge after 24-hour charge. U_2, Discharge after 10-sec. charge. U_3, Residual charge after 24-hour charge and subsequent 10-sec. short circuit. The circles of curve U_3 are calculated by aid of relation (12). The crosses of curve U_2 are calculated by aid of relation (23).

which follows from the well-known Dirichlet-formula, we obtain

$$\int_0^t \frac{di_0(\tau)}{d\tau}\left[g(t-\tau)+\int_0^{t-\tau} g(\sigma)\rho(t-\tau-\sigma)d\sigma+\frac{1}{C}\right]d\tau$$

$$+\left[f(t)+\int_0^t f(\tau)\rho(t-\tau)d\tau+\frac{U_0}{RC}+\frac{i_0(0)}{C}\right]=0. \quad (19)$$

This equation will be satisfied, if $f(t)$ and $g(t)$ satisfy equations of the type (15), because then each of the two members of (19) will disappear separately. Thus it follows that

$$f(t)=[1+(R/U_0)i_0(0)]\psi_1(t) \quad (20)$$

and $$g(t)=(R/U_0)\psi_1(t). \quad (21)$$

By introducing (20) and (21) into (17) we obtain, after a further integration, $U_2(t)$ in function of $U_1(t)$. Noting the identity

$$\int_0^t \frac{di_0(\tau)}{d\tau}g(t-\tau)d\tau=\frac{d}{dt}\int_0^t i_0(t-\tau)g(\tau)d\tau$$

$$-i_0(0)g(t), \quad (22)$$

there results finally

$$U_2(t)=U_1(t)+\frac{R}{U_0}\int_0^t \frac{dU_1(\tau)}{d\tau}i_0(t-\tau)d\tau. \quad (23)$$

We are now able to calculate the discharge-curve for every possible charging-time t_0, if we know the discharge-curve for complete charge and the expression of the after-current.

We have tested these results experimentally. Some measurements were made with carnauba-wax, a substance which was found to show dielectric absorption in a high degree. The full lines of Fig. 2 give the functions U_1, U_2, U_3 obtained by measurement; the circles give the values calculated for U_3 by subtracting U_2 from U_1; the crosses give the values calculated for U_2 by using relation (23). The constant RC was determined in such a way as to obtain a good agreement for $t=100$ minutes; for $\varphi(t)$ we put $\beta t^{-0.75}$. We see that the calculated values fit well the measured ones.

I am greatly indebted to Professor E. L. da Fonseca Costa who made this study possible. My grateful acknowledgment is made to Dr. F. M. de Oliveira Castro for his helpful advice.

LETTERS TO THE EDITOR

Prompt publication of brief reports of important discoveries in physics may be secured by addressing them to this department. Closing dates for this department are, for the first issue of the month, the eighteenth of the preceding month, for the second issue, the third of the month. Because of the late closing dates for the section no proof can be shown to authors. The Board of Editors does not hold itself responsible for the opinions expressed by the correspondents.

Communications should not in general exceed 600 words in length.

Contributions to the Shear Constants of Hexagonal Crystals

The shear constants for copper and some of the alkali metals have been calculated by Fuchs[1] on theoretical grounds. In this work account was taken of the increase of electrostatic energy, and also of the energy of ionic core repulsion, with distortion. Since these metals in general appear to vary but little from the free electron picture, it was estimated that the Fermi energy, exchange energy and correlation term would change little with a deformation which did not alter the volume. In the case of sodium the results showed good agreement with the measurements of Goens[2] at low temperature, as might be expected since the free electron model fits particularly well for this metal. For the hexagonal crystals no such model is possible, yet it is of interest to see to what extent the elastic constants can be estimated on the basis of such a simple theory.

For such crystals there are three independent deformations which leave the volume unchanged. To continue the notation of Fuchs we may chose a distortion, ϵ, so that the unit on the hexagonal axis is multiplied by $(1+\epsilon)$, and the units in the hexagonal planes by $(1+\epsilon)^{-\frac{1}{2}}$, respectively. A second deformation, γ_1, alters the angles between the axes in the planes, and a third deformation, γ_2, alters the angle of the hexagonal axis. (There are in addition two independent, volume-changing deformations.) The following relations hold between the elastic constants and the second derivatives of the energy with respect to these distortions:

$$\tfrac{1}{2}\partial^2 E/\partial\epsilon^2 = \tfrac{1}{2}(c_{11}+c_{12}+2c_{33}-4c_{13})\Omega$$
$$\tfrac{1}{2}\partial E/\partial\gamma_1 = \tfrac{1}{2}(c_{11}-c_{12})\Omega$$
$$\tfrac{1}{2}\partial E/\partial\gamma_2 = c_{44}\Omega$$

where Ω is the atomic volume.

The Ewald method[3] was used to obtain the potential contributions arising from the two simple hexagonal lattices which make up the crystal. Evaluation of this sum at a site of the close-packed lattice gave directly twice the average energy per atom. (The choice of the ideal value for the c/a ratio for this calculation was both a convenient and a natural specialization.) The second derivatives of this energy were then found in a manner exactly analogous to Fuchs' treatment for the face-centered and body-centered lattices. The result gave

$$E(\epsilon,\gamma_1,\gamma_2) = E(0)+(ne)^2(2.04\epsilon^2+0.47_5\gamma_1^2+0.26_7\gamma_2^2)/a$$

where n was the number of charges on an ion and a the distance between nearest neighbors.

TABLE I. *Elastic constants in 10^{11} dynes cm^{-2}.*

	Elastic Constants	Electrostatic Term	Ion Core Term	Sum	Observed
Mg[4]	$c_{11}+c_{12}+2c_{33}-4c_{13}$	12.32	0.468	12.79	12.51
	$c_{11}-c_{12}$	2.86	0.113	2.97	3.35
	c_{44}	0.80_8	0.033	0.84	1.68
Ca[5]	$c_{11}+c_{12}+2c_{33}-4c_{13}$	5.24	0.172	5.41	9.49
	$c_{11}-c_{12}$	1.22	0.043	1.26	7.29
	c_{44}	0.34	0.015	0.36	1.85
Zn[4]	$c_{11}+c_{12}+2c_{33}-4c_{13}$	19.35	3.28	22.63	10.57
	$c_{11}-c_{12}$	4.49	0.74	5.23	13.65
	c_{44}	1.26	0.20	1.46	3.79

Full elastic data are available for the nearly close-packed hexagonal crystals of Mg, Ca and Zn, and the combinations studied here are listed in the fourth column of Table I. The calculated electrostatic contributions ($n=2$ in all cases) are in column one, and comparison shows that this is only a portion of the elastic energy involved. A very rough estimate of what might be expected from the repulsion of ion cores can be gained from the values listed in the third column. These were computed from the Born-Mayer formula with modified Goldschmidt's ionic radii.[3] They are comparatively much smaller, and their inclusion in the third column does little to improve the agreement.

It is not surprising that these calculated values should in general fall so far short of the observed elastic constants, since the free electron model is no longer applicable. Certainly the higher electron states will have their energies widely altered with distortion, and the Fermi energy can no longer be considered a function of volume only. Unfortunately there is at present no apparent way to attack the very complex problem.

I wish to thank Dr. Conyers Herring for having suggested this problem to me, and Dr. Frederick Seitz for his valuable suggestions and criticism.

H. B. Huntington

Department of Physics,
University of Pennsylvania,
Philadelphia, Pennsylvania,
November 20, 1939.

[1] K. Fuchs, Proc. Roy. Soc. **A153**, 622 (1936); **157**, 444 (1936).
[2] P. P. Ewald, Ann. d. Physik **64**, 253 (1921); K. Fuchs, Proc. Roy. Soc. **151**, 585 (1935).
[3] V. M. Goldschmidt, *Skrifter det Norske Videnskaps*, 1926–27.
[4] See Landolt-Börnstein, Erg. III a, 75.
[5] E. Grüneisen and E. Goens, Zeits. f. Physik **26**, 240 (1922).

Simultaneous Penetrating Particles in the Cosmic Radiation

Some experiments were made to examine whether showers with two or more penetrating particles could be found in cosmic radiation.

The apparatus used has been described in a previous paper.[1] It consisted of a fourfold coincidence set provided with a Neher-Harper circuit; its coincidence time was of 7×10^{-7} min. The counters used were of 100 cm² area and were filled with hydrogen and argon at a total pressure of 15 mm of mercury. Their efficiency, measured according to the method of Street and Woodward, was 100 percent.

The arrangement of the counters consisted of two sets of telescopes in coincidence (Fig. 1), each counting only rays which produce coincidences through a layer of lead 16 cm thick.

The results of the measurements (made at an altitude of 800 m above sea level), are given in Table I. The observed average frequency of the showers was 15 times greater than the random fourfold coincidences. (The greatest contribution to the "zero-effect," which was very carefully studied, comes from the random coincidences between the two telescopes.) Such showers cannot be produced by a "knock-on" process in the lead, as follows from the arrangement I. The above results show therefore the existence of showers of two or more simultaneous penetrating particles.

Further studies on the number of penetrating particles in a shower and on the extension of those showers are in course, and results already obtained lead us to think that the observed particles are associated with the penetrating cores of the extensive showers discovered by Auger and his co-workers.

The existence of simultaneous penetrating particles is of remarkable interest chiefly if such particles are mesotrons. A quantum theory of such showers has been recently proposed by one of us.[2] Drs. M. Schoenberg[3] and M. D. de Souza Santos have indepently discussed the absorption processes of the mesotron producing radiation in the high atmosphere and have pointed out that in order to explain the high absorption of this radiation in the upper region of the atmosphere and the penetrating power of the mesons, it is necessary to assume that at least two mesotrons are simultaneously created (which makes improbable the inverse process.)

A further report of these measurements will be published elsewhere.

G. Wataghin
M. D. de Souza Santos
P. A. Pompeia

Department of Physics,
São Paulo University,
São Paulo, Brazil,
December 8, 1939.

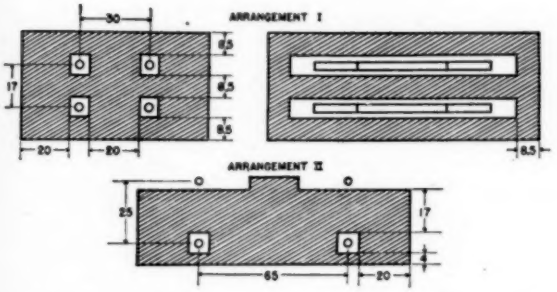

FIG. 1. Arrangement of counters. Linear dimensions are in centimeters.

TABLE I.* *Number of coincidences per minute for arrangements I and II at an altitude of 800 meters.*

ARRANGEMENT	NUMBER OF COINCIDENCES	TIME IN MINUTES	COINCIDENCES PER MINUTE $\times10^4$	ERROR $\times10^4$
I	54	17,400	31	3
II	46	18,700	25	3

* Frequency of random fourfold coincidences: $2\cdot10^{-4}$ min.$^{-1}$.

[1] Annaes da Academia Brasileira de Sciencias. T. XI, p. 1.
[2] La Ricerca Scient., in the press.
[3] Annaes da Academia Brasileira de Sciencias, in the press.

A New Proof of the Instability of the Mesotron

Clay[1] has recently published a series of measurements concerning the Pb absorption of cosmic rays coming at an angle of 60° to the zenith. These measurements are striking in that for the first 30 cm a lack of absorption is found, while beyond 30 cm the absorption coefficient is less than for the vertical radiation. We have repeated this measurement with a coincidence system between four pairs of 3-×-30-cm² counters arranged at such a distance as to permit the insertion of 86 cm of Pb between them. The results are just the same as those of Clay, and they are given in Fig. 1, curve (a). The measurements with zero cm

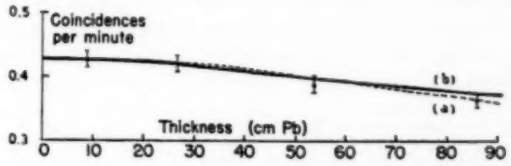

FIG. 1. Absorption in lead of cosmic rays which make an angle of 60° with the zenith.

of Pb have not been taken because the electronic component which appears in them does not interest us in this case. We think that this peculiarity can be explained by the instability of the mesotron.

With the usual hypotheses in regard to the production of mesotrons in the high atmosphere, the conclusion[2] is easily arrived at that the probability for a mesotron to reach the pressure H (expressed in g/cm²) with the vertical direction without being disintegrated in the air, is:

$$P_0(H,W)=\left[\frac{(W_0-aH)100}{(W_0-100a)H}\right]^{A/W_0},$$

where W is the energy of the mesotron, a the loss of energy per g/cm² of air, $W_0=W+aH$ the initial energy of the mesotron, and $A=(mc/\tau\delta)10^3$ (τ=mean life of the mesotron, δ=the specific gravity of the air, m=mass of the mesotron).

For a mesotron having a direction of 60° with respect

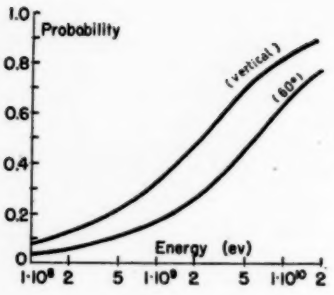

FIG. 2.

to the zenith, the foregoing formula is changed as follows:

$$P_{60}(H,W)=\left[\frac{(W_0-2aH)100}{(W_0-100a)2H}\right]^{2A/W_0}.$$

Figure 2 shows the course of the two equations with a change of the energy W of the mesotron for $H=1000$ g/cm², $\tau=2\times10^{-6}$ sec. and $mc^2=0.8\times10^8$ ev.

Qualitatively it is seen at once that the lesser energy mesotrons are eliminated more in the slanting direction of 60° than in the vertical direction, and this may be the origin of the lack of particles in the first 30 cm of Pb. Quantitatively the absorption curve of Ehmert (of which the change of the exponent with the depth can be explained with this same process)[2] has been taken into consideration, the correction applied to it for the slant of 60°, and the curve (b) of Fig. 1 had been obtained.

The satisfactory agreement between the curve observed and the calculated curve, leads one to think that the phenomenon can be explained in conformity with the foregoing; in this case an increase of the zone not showing absorption, is to be expected for still larger inclinations to the zenith. Experiments are being carried out to check this particular.

GIUSEPPE COCCONI

Physical Institute of the Royal University,
Milan, Italy,
November 20, 1939.

[1] J. Clay and A. van Gemert, Physica **6**, 649 (1939).
[2] G. Cocconi, Ricerca Scient. **10**, 958 (1939).
[3] A. Ehmert, Zeits. f. Physik **106**, 757 (1937).

Multiple Scattering of Charged Particles

1. This subject has recently been discussed by E. J. Williams and by Goudsmit and Saunderson.[1] The latter authors considered the scattering of electrons by nuclei whose Coulomb fields are cut off at a radius ρ. Williams uses a single scattering curve due to Bullard and Massey and based on the Thomas-Fermi atom model. Multiple scattering at small angles is not very sensitive to screening by the atomic electrons, but clearly it is desirable to make the best assumptions we can as to the effect of screening. A convenient method is the use of a simple approximation to Hartree's values of the potential V at distance r from the nucleus. An approximation good enough for scattering calculations is

$$V=(Ze/r)[c_1e^{-x/a_1}+c_2e^{-x/a_2}+\cdots]. \qquad (1)$$

The a's and c's are adjustable; x is the variable occurring in the Thomas-Fermi theory, $1.13Z^{\frac{1}{3}}r/a_0$, where a_0 is the hydrogen radius. Curves showing rV/Ze as a function of x were drawn for argon and for mercury. They agree closely over a considerable range of x, and interpolation for intermediate values of Z appears to be a reasonable procedure. For scattering problems, two terms in Eq. (1) will often suffice, e.g., for argon the bracket is roughly $0.34e^{-2.77x}+0.66e^{-0.55x}$.

From (1), the Born cross section for scattering into $d\theta$ is

$$dq=\tfrac{1}{2}\gamma\sin\theta\,d\theta\left(\frac{c_1}{\sin^2\frac{1}{2}\theta+L_1^2}+\text{similar terms}\right)^2; \qquad (2)$$

where $L_i=l/2a_i$; $l=$(de Broglie wave-length)$/2\pi$;

$$\gamma=\pi Z^2r_0^2(1-\beta^2)/\beta^4; \quad r_0=e^2/m_0c^2.$$

2. For rough computations we may use one term of Eq. (1). Then we have the Wentzel formula

$$dq=\frac{2\gamma\sin\theta\,d\theta}{(m-\cos\theta)^2}; \quad m=1+2L^2; \qquad (3)$$

and the total cross section is $\gamma(2a/l)^2/(1+L^2)$. Here a is of the order of magnitude $a_0/Z^{\frac{1}{3}}$. Using (3), I have evaluated the cross section $f(\theta_1,\theta_2)d\theta_2$ for scattering of an electron from direction θ_1 to the range $d\theta_2$. This enters prominently in Wentzel's[2] treatment of multiple scattering, but calculations by his method are laborious. Goudsmit and Saunderson use a method due to Ornstein, which gives the average of $\cos\theta$, $P_2(\cos\theta)$, etc., for electrons scattered by a foil with N atoms/cm². They obtained

$$\langle\cos\theta\rangle_{Av}=[1+(\rho/k)^2]^{-2\pi k^2N}; \quad k=\gamma/\pi. \qquad (4)$$

This formula contains a large number raised to a small power, so the result is insensitive to changes of the cut-off radius ρ. Of course, the cosine is an insensitive function when θ is small, but this insensitivity persists to large values of θ, as Goudsmit and Saunderson showed. This condition is not accidental, for I find the same behavior when (2) or (3) is employed. From (2), the result is

$$\langle\cos\theta\rangle_{Av}=\exp\left(\frac{2\pi k^2N}{1+L^2}\right)[1+(2a/l)^2]^{-2\pi k^2N}. \qquad (4^1)$$

3. For *small angles and not-too-great thicknesses* the angular distribution of scattered particles is often treated as a Gaussian one, $C\exp(-\theta^2/\Lambda^2)$. Using (3) I get approximately

$$\Lambda^2=4N\gamma\{\log[(m-\cos\theta_1)^{\frac{1}{2}}2^{\frac{1}{2}}a_0/Z^{\frac{1}{3}}]-1\}, \qquad (5)$$

where θ_1 arises from neglecting large angle deflections in a way originally explained by Bothe.[3] With θ_1 properly chosen, this is essentially Williams' formula (30b), and we see how it can be improved by using (2) instead of (3).

ARTHUR E. RUARK

University of North Carolina,
Chapel Hill, North Carolina,
December 11, 1939.

[1] E. J. Williams, Proc. Roy. Soc. **169**, 531 (1939); S. Goudsmit and J. L. Saunderson, Phys. Rev. **56**, 122 (1939); **57**, 73(A) (1940).
[2] G. Wentzel, Ann. d. Physik **69**, 335 (1922).
[3] W. Bothe, *Geiger-Scheel Handbuch*, 2nd ed., Vol. 22, p. 15.

A Laboratory Study of Spark Discharge Between Conducting Clouds

It is usually assumed that the lightning flash and the laboratory spark are essentially the same phenomenon when account is taken of the greater magnitude of the voltage, current, and path length of the lightning flash. There are, however, important differences since the lightning discharge takes place between two charged clouds, or between a charged cloud and the ground, while the laboratory spark is between metal electrodes. Little is known of the manner in which the initial leader stroke is started from the cloud or what happens in the cloud during the flash.

It seemed to us that an investigation of these obscure points necessitated the production of discharges on a small scale between conducting, charged clouds. The preliminary work reported here does not reproduce lightning cloud conditions exactly but is sufficiently similar to be of interest.

It is well known that steam passing through a properly designed nozzle becomes charged. This is the basis of the generator designed by Armstrong.[1] This generator was copied and attempts made to obtain a discharge between the steam cloud and a grounded metal point electrode. A field at the point sufficient to start an intermittent corona discharge visible in a slightly darkened room was easily obtained. The current to this point, observed by means of an oscillograph, had the usual characteristics of a discharge of this type, starting suddenly and then decreasing comparatively slowly (maximum 10–20 μamp.). This is evidently the type of discharge known popularly as St. Elmo's fire. We were not able to produce a distinct spark by this method. This is probably to be expected, since there is no appreciable ionizing process in the cloud after it

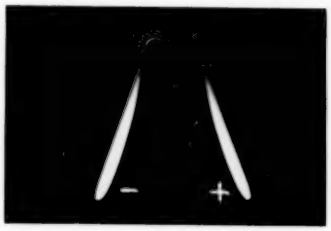

FIG. 1. Snapshot of a spark discharge between the tips of two oxygen gas flames.

leaves the nozzle. As a consequence its conductivity rapidly decreases because of the formation of large ions, so that a long spark discharging a considerable region of the cloud is unlikely to occur.

A more promising approach to the problem involving the use of long flames at various temperatures arose in a discussion with Dr. F. T. Holmes, of this laboratory. An impulsive voltage (80 kv) was applied between two adjacent oxygen gas flames about 30 cm long. With the flames inclined toward each other so that the tips are

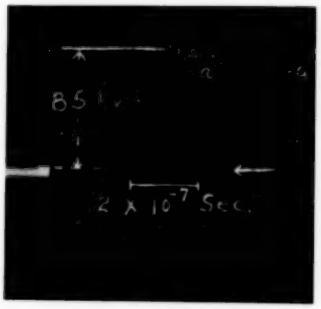

FIG. 2. Two oscillograms of the potential difference between two gas flames during the period of spark formation, the breakdown in each case starting at the point (a).

about 10 cm apart, sparks will pass from tip to tip. A snapshot of this discharge is shown in Fig. 1. The flames are overexposed but it will be noted that the bright part of the spark channel starts and ends rather abruptly in the highly conducting core of the flame. Consequently this is effectively the same as a discharge between a negative cloud and an adjacent positive cloud. In nearly every picture several short faint channels in addition to the main channel can be seen. Unfortunately they are so faint on the original film that they are lost in the reproduction. Branching of the main channel is also observed. This would indicate that at least over part of the path the initial ionizing process proceeds similarly to that of the lightning flash. We do not as yet know whether or not the leader stroke is "stepped."

An oscillogram of the potential difference between two gas flames during the period of spark formation is shown in Fig. 2. The discharge is characterized by a long and erratic time lag and by the slow breakdown taking place in stages as shown. Since the gas flames were relatively cool with low conductivity, compared to the oxygen gas flames, the discharge channel does not end abruptly but extends through the flame to the metal nozzles. Consequently the last part of the oscillogram probably represents the formation of an arc. These results would seem to indicate that a lightning flash should penetrate some distance into a poorly conducting cloud but scarcely at all into a cloud in which the air is highly ionized.

L. B. SNODDY
J. W. BEAMS

Rouss Physical Laboratory,
University of Virginia,
Charlottesville, Virginia,
December 12, 1939.

[1] Armstrong, Ann. d. Chim. et Phys. **10**, 105 (1844).

Proceedings of the New England Section of the American Physical Society

MINUTES OF THE DARTMOUTH COLLEGE MEETING, OCTOBER 14, 1939

THE fourteenth regular meeting of the New England Section of the American Physical Society was held at Dartmouth College, Hanover, New Hampshire, on October 14, 1939. Eighty-five persons attended the meeting. On the previous evening members were guests of Dartmouth College at a social gathering. Four invited papers made up the program:

Short Electrical Wave Phenomena and Contrasts with Optical Analogs.—G. F. HULL, *Dartmouth College.*
Applied Geophysics.—D. A. KEYS, *McGill University.*
Fluorescence.—S. DUSHMAN, *General Electric Company.*
The Microphone and Research.—F. S. GOUCHER, *Bell Telephone Laboratories, Inc.*

At the business meeting the following officers were elected for the ensuing year:

Chairman, K. S. Van Dyke Vice Chairman, F. H. Crawford Secretary-Treasurer, J. C. Boyce
Members of Program Committee, G. A. Anslow and J. J. Livingood

Article IV of the Constitution of the Section was amended to read: "Membership—Any member or fellow of the American Physical Society, *or of any of the other founder societies of the American Institute of Physics*, residing in New England may become a member of the Section by payment of the annual dues of the Section." (The italicized portion is new.)

A vote of thanks was extended to Professor Hull, his colleagues, and to Dartmouth College for their hospitality.

The winter meeting of the Section will be held at the Massachusetts Institute of Technology on January 27, 1940.

J. C. BOYCE, *Secretary-Treasurer, New England Section*

Proceedings of the New York State Section of the American Physical Society

MINUTES OF THE FALL MEETING AT RENSSELAER POLYTECHNIC INSTITUTE, OCTOBER 21, 1939

ONE hundred members and guests of the New York State Section of the American Physical Society met at the Sage Laboratory of Rensselaer Polytechnic Institute on Saturday, October 21. The program for the meeting as well as the local arrangements were planned by a committee of which Professor R. A. Patterson was Chairman. Announcement was made of the spring meeting and election of officers to be held at the University of Buffalo.

In addition to an inspection of the Metallurgical and Physics Laboratories including an exhibition of undergraduate projects in physics, the following program of invited papers was enjoyed.

Address of Welcome. DR. W. O. HOTCHKISS, *President, R. P. I.*
Electrostatic Deposition of Fine Particles (with demonstrations). J. O. AMSTUZ, *Behr-Manning Corporation*
The Teacher and Industrial Physics. W. L. EGY, JR., *W. & L. E. Gurley*
Quantum Ideas in Undergraduate Physics. DR. V. ROJANSKY, *Union College*
Recent Developments in Nuclear Physics (with demonstrations). DR. J. R. DUNNING, *Columbia University*
Recent Developments in Million-Volt X-Rays. DR. W. F. WESTENDORP, *General Electric Company*

PAUL R. GLEASON, *Secretary*

Proceedings of the American Physical Society

Minutes of the Chicago, Illinois, Meeting, December 1–2, 1939

THE 230th regular meeting of the American Physical Society was held at Chicago, Illinois, on Friday and Saturday, December 1 and 2, 1939, at the University of Chicago. The presiding officers were Professors Arthur H. Compton, Carl H. Eckart, W. D. Harkins and Ralph A. Sawyer. The attendance at the meeting was about three hundred.

On Friday evening the Society held a joint dinner with the Chicago Physics Club at the Windermere Hotel. Dean George B. Pegram presided at the dinner. After the dinner a demonstration lecture was given in the Lecture Room of the Museum of Science and Industry by Dr. Frederick S. Goucher of the Bell Telephone Laboratories on "Microphonic Action and Contact Phenomena."

Meeting of the Council. At the meeting of the Council held on Friday, December 1, 1939 the deaths of four fellows (Arthur E. Kennelly, Charles F. Lorenz, J. B. Nathanson and F. K. Richtmyer) and of six members (Arthur F. Dittmer, A. A. Dixon, Hampton D. Ewing, E. E. Free, Samuel V. Hoffman and Harold Mestre) were reported. Two candidates were transferred from membership to fellowship and one hundred and one candidates were elected to membership. *Transferred from membership to fellowship:* Stanley N. Van Voorhis and Viktor F. Weisskopf. *Elected to membership:* Ernest J. Abbott, Royal P. Allaire, Charles L. Andrews, Robert M. Ashby, James F. Bacon, George J. Baldwin, William Band, A. E. Benfield, Edward P. Bentley, Phillip R. Beutel, Herman R. Branson, Charles J. Burton, D. M. Chapin, Frances L. Christison, George C. Claridge, Robert K. Clark, Eric T. Clarke, Francis L. Code, Kenneth S. Cook, Herbert C. Corben, Gilbert H. Curl, Louis J. Cutrona, Max Dresden, Beulah P. Field, A. Theodore Finkelstein, Verne Frese, Max Garbuny, Eugene Gardner, Paul F. Gast, Sanford C. Gladden, Harold C. Glahe, Moses A. Greenfield, Richard O. Grisdale, Bruce L. Hicks, Mary W. Hodge, J. Vance Holdam, Haig Iskenderian, Donald H. Jacobs, James A. Jacobs, George Jaffé, George A. Jarvis, Robert C. Jones, J. A. Jukes, Brother Gabriel Kane, G. A. Kelsall, Arthur E. Kenney, Harold J. Kersten, George S. Klaiber, Alexander Kolin, Masao Kotani, Gustav Kuerti, James A. LeConte, Jr., Sidney Lees, Franklin A. Long, A. C. B. Lovell, Johann F. Ludloff, Malcolm R. MacPhail, Henry P. Manning, Jr., F. Albert Matsen, H. N. Maxwell, Nicholas Metropolis, Max Morand, Edward B. Nelson, Itaru Nonaka, Kiichiro Ochiai, Russell D. O'Neal, Floyd W. Parker, S. L. Parsons, William T. Payne, Alexander A. Petrauskas, Robert D. Rawcliffe, Nelson F. Riordan, Bruno Rossi, W. Rowles, Sister M. Roswitha Schauls, William T. Scott, William C. Sears, Frederick G. P. Seidl, Thomas M. Shaw, Hsi-yin Sheng, John N. Shive, G. J. Sizoo, Harold L. Stout, Eiiti Takeda, Mitsuo Taketani, Hidehiko Tamaki, Hubert M. Thaxton, George J. Thiessen, E. Ward Tillotson, Fred M. Uber, M. P. Vore, Eric A. Walker, Paul Weisz, H. L. Welsh, Robert W. Woods, John E. White, Wilfred C. White, J. O. Wilhelm, Evan J. Williams, John D. Williams, and Garnet A. Woonton.

The regular scientific program of the Society consisted of thirty-eight contributed papers of which one, number 7, was read by title. The abstracts of these papers are given in the following pages. An *Author Index* will be found at the end.

HAROLD W. WEBB
Acting Secretary

Abstracts of Contributed Papers

1. A New General Effect in the Diffraction of X-Rays by Crystals. W. H. Zachariasen, *University of Chicago.*—The writer has made a simplified derivation of the intensity expression for the coherent scattering of x-rays by a small crystal. The usual intensity formula for the "diffuse" scattering is to be replaced by a more complicated expression which predicts diffraction maxima in the directions u given by: $(1+\tau_0)u=u_0+\lambda B_H$, where u_0 is the direction of the incident beam and B_H a vector of the reciprocal lattice. The intensity for a direction near such a maximum is:

$$I_{(\epsilon)}=Sf^2e^{-2M}4\sin^2\theta\frac{kT}{Vmc^2}\frac{2\pi L^3}{\lambda^2+2\pi L^2(\tau_0^2+\epsilon^2)}\delta V.$$

S is the Thomson scattering for a single electron, fe^{-M} is the atomic scattering power, k the Boltzmann constant, T the temperature, V the volume of the unit cell, m the atomic mass, $\overline{c^2}$ the average square of the elastic wave velocities, L and δV the average linear dimension and the volume of the crystal. The half-width of the diffraction maximum is in radians $(\lambda^2+2\pi L^2\tau_0^2)^{\frac{1}{2}}/(2\pi)^{\frac{1}{2}}L$, thus giving very sharp peaks when τ_0 is small. The average value of the intensity over a large solid angle leads to the Debye expression for the "diffuse" scattering. Earlier work by Faxén[1] and by Waller[2] will be discussed, and it will be shown that the theory explains quantitatively some puzzling observations including the radial streaks of Laue photographs.

[1] Faxén, Zeits. f. Physik 17, 266 (1923).
[2] Waller, Dissertation, Uppsala (1925).

2. Preliminary Experimental Studies of the New Diffraction Maxima in X-Ray Photographs. S. S. Siegel and W. H. Zachariasen, *University of Chicago.*—An x-ray beam from a copper target tube falls on the cleavage face of a stationary crystal of rocksalt or calcite under a glancing angle of incidence $\theta_B+\Delta$, where θ_B is the Bragg angle for Cu $K\alpha$. Δ is varied by steps of a few minutes of arc over a range of several degrees. Some wave-lengths of the continuous spectrum produce an ordinary Bragg reflection with a scattering angle of $2(\theta_B+\Delta)$. In addition we find a diffraction line with a scattering angle slightly different from $2\theta_B$. This is a diffraction maximum due to Cu $K\alpha$ predicted by the theory presented in the preceding abstract. The position, the peak intensity, the integrated intensity and the width of this spurious line have been studied as functions of Δ. The results agree with the theory.

3. Relations Between Elastic Properties of Solids. H. Ludloff, *Cornell University.* (*Introduced by H. A. Bethe.*)—From the quantum theory of solids one can derive for $T\lesssim\theta$ the approximate equation of state:

$$p\sim f_1(v)+f_2(T). \qquad (1)$$

f_1 corresponds to the lattice forces and f_2 to the radiation pressure of thermal waves. From (1) we obtain the compressibility:

$$\kappa=-\frac{1}{v}\left(\frac{\partial v}{\partial p}\right)_T\sim\kappa(v), \quad \text{so that} \quad \left(\frac{\partial\kappa}{\partial T}\right)_v=0. \qquad (2)$$

For a solid whose isotropic contraction ϵ may be produced by either isothermal compression (hydrostatic pressure) or isobaric cooling, we have the relation:

$$\left(\frac{\partial\kappa}{\partial\epsilon}\right)_p=\left\{\left(\frac{\partial\kappa}{\partial\epsilon}\right)_T+\left(\frac{\partial\kappa}{\partial T}\right)_\epsilon\Big/\left(\frac{\partial\epsilon}{\partial T}\right)_p\right\}, \qquad (3)$$

which by the introduction of (1) yields:

$$(\partial\kappa/\partial\epsilon)_p\sim(\partial\kappa/\partial\epsilon)_T. \qquad (4)$$

Therefore we can put:

$$(\partial\kappa/\partial T)_p\sim(\partial\kappa/\partial\epsilon)_T\cdot(\partial\epsilon/\partial T)_p. \qquad (5)$$

Few examples are known, in which all 3 functions have been measured; the best example, Na, shows deviations less than $\frac{1}{2}$ percent between 80°K and 250°K. If $(\partial\kappa/\partial\epsilon)_T$ has not been measured, it can be replaced by a theoretical expression. One can recognize that $(\partial\kappa/\partial\epsilon)_T$ can be derived exclusively from elastic considerations. The theory of finite strain yields:

$$(\partial\kappa/\partial\epsilon)_T=5\kappa+27(l+m+n), \qquad (6)$$

l, m, n being the elastic constants of the 3 order. If $\partial\kappa/\partial T$ and $\partial\epsilon/\partial T$ are measured, relation (5) determines the 3rd-order constants, whose magnitude is i.g. more than 10 percent of that of the normal constants of 2nd order.

4. The Initial Stage of Plastic Deformation in Lead. W. James Lyons, *Loyola University of the South.*—Long-time tensile and compressive tests on metals indicate that in the steady-creep stage, the hyperbolic sine function relates the velocity of deformation to the stress. In the case of lead and tin at constant temperature it has been shown that this law reduces to a simple exponential relation. These laws, however, fail completely to describe the initial stage of plastic deformation in lead. The present series of tests is an investigation of this initial stage in compression. An optical lever system and high speed kymograph are employed. On the photographic time records obtained, the resolution is 0.0042 sec./cm, while the magnification of the deformation is about 56. Tests under pressures of 121 and 142 kg/cm² indicate that the initial stage lasts about 0.09 sec. The deformation *vs.* time relation is essentially linear.

5. Transformations of Radiation-Material Gas Mixtures. R. M. Whitmer, *Purdue University.*—Emden, in his *Gaskugeln*,[1] has found that for a perfect material gas the transformations along the isochor, adiabat, isotherm and isobar are particular forms of the general polytropic transformation $dQ/dT=$const. An alternative expression for a polytrope is $pv^\Gamma=$const., or in differential form $\Gamma=-(dp/p)/(dv/v)$, where Γ is also a constant. In the present investigation it has been found that when radiation energy and pressure are considered, Γ is not a constant for any of

the above-mentioned transformations, and dQ/dT is constant only for the adiabat. The relation of these results to the polytropes discussed by Eddington[2] and Milne[3] are indicated.

[1] Emden, *Gaskugeln* (Leipzig, 1907).
[2] Eddington, *The Internal Constitution of the Stars* (Cambridge, 1926).
[3] Milne, *Handbuch der Astrophysik*, III/1, p. 215.

6. The Phenomenological Theory of Superconductors. EMORY COOK, *University of Chicago.* (*Introduced by Carl Eckart.*)—The usual derivation of the London equations for a superconducting medium starts from the Maxwell field equations and the idea that the conduction electrons are free classical particles under the influence solely of the electrostatic field. The additional assumption must then be made that an arbitrary function of integration vanishes identically. When the same ideas are put into a variation principle, the need for this assumption disappears. The nonpenetrating fields demanded by experiment are obtained directly. In the very precise linear approximation, the Eulerian equations are equivalent to the London system. Uniqueness theorems developed show that the persistent currents of the London theory do not partake of the rotation of the medium. The second-order terms seem much too small to cause this effect. The second-order terms, however, may possibly effect a coupling between the various characteristic solutions of the linear system, amounting to a small resistance.

7. Derivation of Boltzmann's Law by Means of Bohr's Frequency Condition. ARTHUR E. HAAS, *University of Notre Dame.*—Boltzmann's law according to which (1) $P_1/P_2=e^{-E_1/kT}/e^{-E_2/kT}$ (where two atomic states are considered with the energy values E_1 and E_2 and P_1 and P_2 are the probabilities of these states) may be derived from Bohr's frequency condition by using Wien's displacement law and the postulate of equilibrium between spontaneous and induced transitions in the radiation field. If we put the number of atoms in a state of energy E equal to $p\phi(E)$, where p is the *a priori* probability, the calculation leads to the functional equation (2) $[p_1\phi(E_1)/p_2\phi(E_2)][B_{12}/B_{21}]=f[(E_2-E_1)/T]$ where B_{12} and B_{21} are the coefficients of positive and negative absorption of radiation. The solution is found to be (3) $p\phi(E)=(n_0/E)e^{-\gamma E/T}$ where n_0 is the number of atoms in the state of zero energy with an *a priori* probability one. By applying this result to the distribution of the kinetic energy in a monatomic gas, γ is finally found to be equal to $1/k$ so that Eq. (1) results.

8. On the Mechanics of Protoplasmic Streaming. GALE YOUNG, *University of Chicago.* (*Introduced by N. Rashevsky.*)—Living cells frequently show a steady circulation or streaming of their protoplasm. The motion is slow, being of the order of twenty centimeters per hour. The energy equation for the steady motion of a viscous compressible fluid within a fixed boundary under the action of an applied force field shows that a *necessary* condition for the existence of such streaming is that either (1) the applied forces do not have a potential per unit mass of fluid, or (2) the density of the fluid is not determined solely by its pressure. A dissolved substance affects the mechanics of the solvent in two ways: (a) it exerts drag forces on the latter whenever there is relative motion between them (diffusion), and (b) it introduces another argument into the equation of state of the solvent, since the solvent density is, in general, affected by that of the solute. The diffusion drag (*a*) may produce nonpotential forces on the solvent as in (1), while the expansion effect (*b*) gives rise to condition (2). There is thus the possibility of streaming being caused by the diffusion of a dissolved substance, and several cases have been worked out actually to exhibit such motion.

9. Circuit for Anticoincidences with G-M Counters. G. HERZOG, *University of Chicago.*—Anticoincidences can be used to suppress the recording of the discharges in a coincidence circuit when one additional G-M counter is fired simultaneously. This is achieved by taking off an impulse from the anticounter which is opposite in sign to the usual impulses. With vapor-filled counters the sign can be changed by shifting the quenching resistance together with the coupling capacity from one side of the h.v. supply to the other. When using the Neher-Harper circuit for quenching, a reversed pulse is achieved by coupling to the grid of the first tube instead of to the anode. The coincidence pulses are mixed with the anticounter pulse in a Rossi circuit, where the tube amplifying the antipulses has a negative bias. Simultaneous discharges in all counters thus give only small pulses on the mixing resistance, whereas coincidence pulses which are not accompanied by an antipulse are not reduced in size. Both kinds can be separated by adjustment of the grid bias on the output-Thyratron. A set for threefold coincidences balanced by one anticoincidence stage was tested and showed an efficiency of 98.6 percent. The 1.4 percent of anticoincidences which are missing can easily be explained by disturbing effects.

10. The Variation of the Hard Component of Cosmic Rays with Height and the Disintegration of Mesotrons. BRUNO ROSSI, *University of Chicago*, H. VAN NORMAN HILBERRY, *New York University*, AND J. BARTON HOAG, *University of Chicago.*—The vertical intensity of the hard component of cosmic rays was measured at different altitudes with a threefold coincidence counter tube arrangement. Measurements were taken with and without a graphite layer above the counters in order to compare the absorption of the hard component in air and carbon. The counting rate observed under a given mass of air-plus-carbon was found to be considerably larger than the rate observed under the same mass of air alone. We interpret the difference as due to the spontaneous decay of the mesotrons which form the hard component of cosmic rays. Three independent values of the average range before decay (L) can be deduced from our measurements. They are listed below, together with the atmospheric depths between which they were measured.

Depth intervals in g/cm²	616–700	700–787	856–943
L in 10^4 cm	9 ± 0.5	10 ± 1.0	9 ± 1.3

A lifetime of the order of 2×10^{-6} second follows from the above values of L.

11. East-West Asymmetry of Cosmic Rays at 40° N Latitude. P. S. GILL, *University of Chicago.*—A study of the east-west asymmetry in cosmic radiation using two triple coincidence counter sets (A and B) was made in Beverly Hills, California, geomagnetic latitude 40° N. In the counter set A, 12 cm of lead was placed between the tubes, while no lead was used in set B. The east-west difference in the countrate in percent at three different zenith angles has the following values, given with probable errors:

ZENITH ANGLE	15°	30°	45°
A	5.4±2.0	3.7±1.2	2.4±1.2
B	0.0±1.6	1.6±1.0	0.9±1.0

At the knee of the ionization-latitude curve the average of these data thus shows a west-east difference of about 2.2 percent. Comparison of data A and B strongly suggests that this difference is greater for the penetrating than for the nonpenetrating component.

12. Fine Structure in the Zenith Angle Distribution of Cosmic-Ray Intensity. DENSIL M. COOPER, *University of Missouri.* (*Introduced by N. S. Gingrich.*)—Studies of "fine structure" in the directional intensity of cosmic rays have been made with a triple coincidence circuit of Geiger counters. Three counters, each of diameter 8.8 cm, active length 36 cm, and with a separation of 50 cm between adjacent counters, were used in a modified circuit of the Neher-Harper type. Readings were taken in a cyclic fashion to minimize errors due to possible instrumental sensitivity drifts, changes in barometric pressure, and changes in the magnetic field of the earth. Five-degree intervals were investigated in the range from 0° to 45°, inclusive, in the directions studied. The survey of intensities in the east, west, north, south, south-east, and south-west directions exhibits intensity patterns with small oscillations. The prominences measured in terms of the largest positive deviations from the $\cos^2$ curve are of the order of two or three percent of the intensity, and they occur at approximately 7°, 20°, and 37°. These "fine structure" prominences are roughly the same for all the above directions; that is, these patterns show symmetry about the zenith. These results tend to confirm the predictions of Schremp[1] relative to the possible existence of this "fine structure" due to a line or banded nature of the energy spectrum for cosmic rays at infinity.

[1] E. J. Schremp, Rev. Mod. Phys. July & Oct. (1939).

13. Mesotron Intensity and Rate of Production in the Stratosphere. MARCEL SCHEIN, W. P. JESSE AND E. O. WOLLAN, *University of Chicago.*—Two high altitude flights have been made with a coincidence counter arrangement which records the vertical intensity of mesotrons and also the number of mesotrons which are produced in a 2-cm lead block.[1] At a pressure of 8 cm the mesotron intensity was 11 times as great as at sea level. This is about 12 percent of the total intensity of the cosmic rays at this altitude. From the second flight, which reached a barometric pressure of 3.6 cm, it was determined that the mesotron intensity attains a maximum at a pressure of about 6.6 cm Hg and then falls off rapidly reaching, at a pressure of 3.6 cm Hg, a value which is approximately half that at the maximum. The production of mesotrons in the 2-cm lead block sets in noticeably at about 35 cm pressure and increases with altitude at about the same rate as the soft component. From our measurements we obtain a value for the resulting cross section for the creation process equal to 1.7×10^{-27} cm² per proton of lead which agrees with that calculated by Nordheim.

[1] Cf. Phys. Rev. **56**, 613 (1939) for counter arrangement.

14. The Effect of the Slowing Down in the Source on the High Energy Portions of Beta-Spectra. EMIL J. KONOPINSKI, *Indiana University.*—Because forward scattering predominates for high energy electrons and back scattering cannot occur without large fractional energy losses, it is to be expected that the backing used for beta-ray sources should contribute very little to the distortion of the high energy portion of beta-spectra. If such distortion occurs it must be due to losses incurred during passage out of the source. This effect can be calculated if use is made of the linearity of the range-energy relation for electrons of more than 200 kv. It was done for the Fermi distribution and more completely for the simplified distribution $\sim E(E_0-E)$. Essential to the results is the value given to the maximum angle of emission accepted by the detecting device. If the usual values of the angle subtended by spectrograph slits are taken, it is found that a significant alteration of the spectrum shape (sufficient to distort a Fermi distribution into an apparent K-U type) takes place only for source thicknesses corresponding to an energy loss comparable with the mean spectrum energy. It can be argued, however, that due to the large angle straggling of even high energy betas, a much larger "effective" angle should be taken. This results in an effective thickening of the source so that a significant distortion of the spectrum may occur for even some of the thinnest sources which have been used.

15. The Scattering of Fast Electrons by Thin Foils of Metal. JASON L. SAUNDERSON* AND O. S. DUFFENDACK, *University of Michigan.*—Beta-rays from radium E of energy between 0.2 and 1.1 Mev were scattered by thin foils of Al, Cu, Ag, and Au under conditions which made possible a comparison with the single scattering theory of Mott. The scattered electrons were observed at various angles of scattering between 0° and 45° by means of a Geiger-Müller counter placed inside the evacuated scattering chamber. Metal foils of equal scattering power, Z^2nt constant, were made by the evaporation of the metals from a tungsten filament on to an organic film. A beta-ray spectrograph was used to determine the energy spectrum of the radium E source, using the same counter as was used in the scattering experiments, and an integration over this energy spectrum was carried out in order to compare the experimental results with the theory. Near the Wentzel angle the number of scattered electrons is greater than the number predicted by the theory for the elements of small atomic number, indicating that the Wentzel criterion for single scattering is too lenient for the lighter elements. The Wentzel criterion improves with increasing Z.

* Now with Dow Chemical Company.

16. Electrical Fields Produced in Interstellar Space by Cosmic Rays. FOSTER EVANS, *University of Chicago. (Introduced by Carl Eckart.)*—Swann[1] has shown that if cosmic rays passed through empty space as charged particles predominantly of one sign, the resultant space charge would produce enormous potential differences between points not very widely separated. Further, that a star emitting such cosmic rays would acquire a very large potential in a short time. Later, Alfvèn[2] showed that space charge might be neutralized by displacement of interstellar ions, but that large magnetic fields would be produced by the cosmic-ray current. In the present work it is shown that if interstellar ions neutralize the space charge, they will also neutralize the current flow, and, therefore, the magnetic field. For a single star the electric field E is given by $A=r^2kE$, where k is the conductivity of interstellar space at a distance r from the center of the star, and $4\pi A$ is the quantity of charge emitted, or intercepted, by the star per second. Ohm's law enters into the derivation of this equation; the justification for its application to interstellar space is discussed. For a star that only intercepts cosmic rays, the resulting potential turns out to be exceedingly small—approximately 10^{-12} volt—and the average potential produced on the galaxy is even smaller. For the case of emission, an upper limit for the potential is of the order of 1000 volts.

[1] W. F. G. Swann, Phys. Rev. **44**, 124 (1933).
[2] A. Alfvèn, Phys. Rev. **55**, 425 (1939).

17. Interpretation of the Proton-Proton Range. R. D. PRESENT, *Purdue University.*—The "charge independent" formulations[1] of the vector meson theory give a second-order proton-proton ^1S potential with the simple spatial dependence $e^{-\kappa r}/r$ where $\kappa=\mu c/\hbar$ and μ is the meson mass. Analysis of the proton-proton scattering data in terms of this potential[2] leads to a range $1/\kappa=0.42e^2/mc^2$ within an accuracy of 5 percent and the corresponding value of μ is 326 ± 16 m. Since recent[3] measurements of meson tracks give $\mu\sim170\pm20$ m, the range is about half the predicted value. A general argument shows that the $2n$th-order interaction of meson perturbation theory has a leading term of range $\sim\hbar/n\mu c$. The observed proton-proton range corresponds to a force that either (1) enters in fourth order or (2) enters in second order but is large in fourth and higher orders, this conclusion being independent of the exact form of the fourth-order potential (which unfortunately does not converge). Alternative (1) avoids introducing the unobserved[4] neutral meson but implies that the neutron-proton force has a larger range than the proton-proton force. Alternative (2) implies that the lowest order of perturbation theory does not give even approximately correct results. A third possibility is that the cosmic and nuclear mesons are not identical particles.

[1] Kemmer, Proc. Camb. Phil. Soc. **34**, 354 (1938); Bethe, Phys. Rev. **55**, 1261 (1939).
[2] Breit, Hoisington, Share and Thaxton, Phys. Rev. **55**, 1103 (1939); Share, Hoisington and Breit, Phys. Rev. **55**, 1130 (1939).
[3] Nishina, Takeuchi and Ichimiya, Phys. Rev. **55**, 585 (1939); J. G. Wilson, Proc. Roy. Soc. **172**, 517 (1939).
[4] A. C. B. Lovell, Proc. Roy. Soc. **172**, 568 (1939).

18. The Theory of β-Decay and the Radius Discrepancy for Sirius B. R. E. MARSHAK, *University of Rochester*, AND H. A. BETHE, *Cornell University.*—Recently several papers have appeared[1,2] which lend theoretical support to the Gamow-Teller selection rules for the β-decay of light nuclei. We wish to call attention to the astrophysical implication of these selection rules which has emerged from our investigations into the energy sources of the white dwarf stars. Using accurate expressions for the radiative and conductive opacities and the free electron density, the extension of the nondegenerate envelope and the internal temperature have been calculated for Sirius B. This calculation has been performed under several widely different assumptions regarding the chemical composition of the star as well as possible errors in the observed luminosity and radius. Even under the most extreme assumptions (pure helium star, etc.) the envelope constitutes only a very small fraction (about one percent) of the radius of the star and the central temperature must be at least five million degrees. At this temperature and at the high densities (up to 3.10^7 g/cm^3) which prevail in the degenerate core, the proton-proton reaction (on the Gamow-Teller theory) sets an upper bound to the hydrogen content of 10^{-3}. The theoretical value of the radius of Sirius B is then only $5.7\cdot10^8$ cm as compared with an observed radius of $13.6\cdot10^8$ cm. This large discrepancy is quite serious since the observational value seems good (in view of the agreement obtained between two distinct methods of measurement); a possible though extremely improbable solution is to return to the original Fermi version of the β-decay.

[1] B. O. Grönblom, Phys. Rev. **56**, 508 (1939).
[2] E. P. Wigner, Phys. Rev. **56**, 519 (1939).

19. Automatic Barometer Pressure Compensator for a Large Grating Spectrograph. H. BEUTLER AND MARK FRED, *University of Chicago.*—Since the refractive index of air is 1.0003, a change in barometric pressure Δp of one inch produces a wave-length shift of one part in 10^5. In the case of the laboratory's 30-foot, 150,000-line grating, having a resolving power of over 300,000, this effect shifts the maximum of a diffraction pattern to the next minimum for $\Delta p=0.3$ inch. Therefore good definition demands a smaller variation in pressure, which condition is seldom fulfilled for long exposure times (10 hr.). A compensator has been constructed for the spectrograph which has the effect of moving the position of the slit by an amount proportional to the pressure change, for variations of more than one inch. Behind the fixed slit is mounted a quartz plate (1 mm thick) which can be rotated about its vertical axis, thereby producing a lateral shift of the virtual position of the slit. This rotation is accomplished by the motion of a sealed metallic bellows acting on a lever arm fastened to the axis. Provision is made for adjusting the length of the lever arm according to the wave-length and order being studied. Ball bearings reduce the friction to a negligible amount. Details and data on the behavior will be presented.

20. Circular Dichroism in Crystalline Nickel Sulphate. L. R. INGERSOLL AND PHILIP RUDNICK, *University of Wisconsin and Vanderbilt University.*—Circular dichroism in crystalline α-$NiSO_4 \cdot 6H_2O$ has been measured for wave-lengths from 0.6μ to 2.2μ, using previously described apparatus[1] and a method of measurement which distinguishes elliptic polarization introduced by dichroism (in incident plane-polarized light) from ellipticity caused in any way by double refraction. Maximum ellipticities of 1.45° and 11.5° per mm thickness were found at respective wave-lengths 0.69μ and 1.155μ, where maxima of total absorption also occur. The dissymmetry factor,[2] $|(\mu_l - \mu_r)|/\mu$, is 0.03 at 0.69μ and 0.23 at 1.155μ. No measurable dichroism appears beyond 1.7μ. The anomalous rotatory dispersion[3] around 1.155μ is the only prominent instance of its kind reported for the infra-red region, as far as we know. The quantitative relation between circular dichroism and rotatory power can be studied in unusual detail here because the rotatory power curve is almost "purely anomalous," its maxima having about ten times the magnitude of the "normal" rotation in the region. The theoretical expectations[4] are well fulfilled. In particular, the wave-length, height, and half-width of the dichroism peak are correlated with the corresponding features of the rotatory power curve within the small experimental uncertainties.

[1] L. R. Ingersoll, J. Opt. Soc. Am. **27**, 411 (1937).
[2] T. M. Lowry, *Optical Rotatory Power*, p. 394.
[3] L. R. Ingersoll, P. Rudnick and F. G. Slack, Phys. Rev. **55**, 672 (1939).
[4] T. M. Lowry, *Optical Rotatory Power*, Chapter XXXIV.

21. Depolarization Factors of the Raman Lines of Some Derivatives of Phenylacetylene. FORREST F. CLEVELAND AND M. J. MURRAY, *Armour Institute of Technology.*—Using a method previously described,[1] depolarization factors have been measured for the main lines of twelve acetylenic compounds of the type $C_6H_5C{\equiv}CR$, where R is H, Cl, CH_3, C_2H_5, CH_2OH, CH_2Cl, CH_2Br, CH_2CH_2OH, CH_2CH_2Cl, $CHOHCH_3$, $CH_2C_6H_5$, and $CH_2CH_2CH_2Cl$. The two strong lines near 2230 cm^{-1}, when resolved, were found to have the same depolarization factors, thus indicating that they do not correspond to a symmetrical and an asymmetrical vibration, respectively, as has been suggested for dimethylacetylene. No previous data on the depolarization factors of these compounds have been reported and the Raman frequencies of $C_6H_5C{\equiv}CCH_2C_6H_5$ are listed for the first time. The single strong line at 2113 cm^{-1} in $C_6H_5C{\equiv}CH$ has the same depolarization factor as the two strong lines in the disubstituted compounds. Within experimental error, the value of this factor for the strong lines in the 2200 cm^{-1} region is 0.6 for all the compounds. The possibility that the two lines in this region may, as suggested by Badger, be due to a Fermi resonance interaction with the second overtone of a fundamental frequency near 750 cm^{-1} is discussed.

[1] F. F. Cleveland and M. J. Murray, J. Chem. Phys. **7**, 396 (1939).

22. A $^1\Sigma \rightarrow {}^1\Sigma$ Transition of the C_2 Molecule. O. G. LANDSVERK, *University of Chicago.* (*Introduced by H. Beutler.*)—The λ2300 band of the carbon arc, previously noticed by Bloomenthal and other investigators and measured by Hori, who attributed it to a C_3 molecule, has been accurately measured and analyzed, using photographs taken on the 30-foot, 30,000-line grating spectrograph. The structure consists of superposed (0,0), (1,1), (2,2), and (3,3) headless bands of a $\Sigma \rightarrow \Sigma$ transition of C_2 (or possibly C_2^+), in agreement with the earlier diagnosis of Mulliken and Dieke. Alternate lines are missing in each series, as expected for the zero spin of the carbon nucleus. Most probably the transition is $^1\Sigma_u^+ \rightarrow {}^1\Sigma_g^+$ of C_2. The molecular constants are very nearly equal for the upper and lower electronic states. They correspond rather closely to the average values of the same constants for other known states of C_2. The following values were obtained: $B_e' = 1.8334$ cm^{-1}, $B_e'' = 1.8223$ cm^{-1}, $\alpha' = 0.0204$, $\alpha'' = 0.0195$, $r_e' = 1.2382$A, $r_e'' = 1.2419$A, $\omega_e' = 1748$ cm^{-1}, $\omega_e'' = 1774$ cm^{-1}, $\nu_0^{0,0} = 43{,}227$ cm^{-1}. The ω_e values were obtained indirectly from the B and D values, since only one sequence of bands could be analyzed.

23. Hindered Rotation in Methyl Alcohol. J. S. KOEHLER AND D. M. DENNISON, *University of Michigan.*—Hindered rotation in methyl alcohol is dealt with by assuming a rigid molecule; only internal rotation and rotation of the entire molecule are considered. The entire molecule is taken to be a symmetrical top, an assumption which introduces errors of about 2 percent in the J spacing. Using as a hindering potential, $V = A \cos 3x$, the wave equation is separated into a Mathieu-like equation governing the internal motion and a symmetrical top equation describing the rotation of the entire molecule. The Mathieu-like functions, because of invariance condition, obey quasi-periodic boundary conditions. The internal energy levels, wave functions, and transition probabilities are calculated using an exact method involving continued fractions; the dependence of certain of the energy levels upon barrier height is given. The calculations predict a series of overlapping perpendicular bands each containing irregularly spaced zero branches. The extent of absorption, the irregular spacings, and the intensity distribution all agree qualitatively with the findings of Borden[1] and Lawson.[2] It is shown that hindered rotation will affect the zero branch spacings in all perpendicular bands of methyl alcohol. The barrier height in methyl alcohol is found to be 470 ± 30 cm^{-1}.

[1] Borden, J. Chem. Phys. **6**, 553 (1938).
[2] Lawson, thesis.

24. Band Spectra and Sensitized Fluorescence of Mercury-Indium Mixture. J. G. WINANS, FRANCIS J. DAVIS AND VICTOR A. LEITZKE, *University of Wisconsin.*—The sensitized fluorescence of indium in mercury vapor was excited by λ2536 light with apparatus like that previously used for tin.[1] All indium lines observed by Donat[2] and additional lines at 2860, 2775, and 2465A were obtained. A Tesla discharge through the mercury-indium mixture showed seven band systems, two resolved into bands with heads on the long wave-length side, and five either continuous or unresolved. Preliminary measurements of the wave-lengths at the intensity maxima and their estimated intensities are 4132 (3), 4449 (1), 4470 (3), 4539 (10),

4574 (2), 5227 (10), and about 5800 (3). The 5800 system extends from 6390 to 5400 with minima of intensity at 5726, 5672, 5639, and 5600. The 5227 system contained bands spaced 11–15A apart and it extended from 5270 to 4880 with a second maximum of intensity at 4998A. All of these band systems were obtained only with a relatively high concentration of both mercury and indium. A change in conditions of pressure and temperature changes the intensity of 5227 relative to 4539. The variations indicate as the emitting molecules, HgIn for 5227 and 5800, and In_2 for the remainder. Each of the band systems observed in the mercury-indium mixture corresponds to a band system previously observed in a mercury-thallium mixture.[3]

[1] J. G. Winans and R. M. Williams, Phys. Rev. **52**, 930 (1937).
[2] K. Donat, Zeits. f. Physik **29**, 345 (1924).
[3] J. G. Winans and Francis J. Davis, Phys. Rev. **53**, 930 (1938).

25. Magnetic Susceptibilities in Weak Fields. W. W. MEEKS AND N. C. JAMISON, *Northwestern University.*—Hector and Peck[1] have reported weak field measurements of the susceptibilities of benzene, carbon tetrachloride and toluene relative to water. Their measurements indicated that water was approximately 6 percent more diamagnetic in weak fields than in the intense fields usually employed. In the present investigation the relative susceptibilities of very pure samples of these same three liquids have been measured in weak fields (~50 gauss) using the modified form of Rankine balance suggested by G. Temple.[2] Six independent determinations on each of the three liquids gave for the susceptibilities of benzene, carbon tetrachloride and toluene the respective mean values (assuming 0.7200×10^{-6} for water) of 0.7036, 0.4376, 0.7172, all multiplied by 10^{-6}, with the greatest probable error, 0.0012×10^{-6}. The excellent agreement of these values with those reported by other investigators using strong fields indicates that there exists no discrepancy of the order of 6 percent between the susceptibility of water in high fields and in low fields. This work also indicates that the modified form of balance may yield absolute values of magnetic susceptibility as suggested by Temple.[2]

[1] L. G. Hector and M. F. Peck, Phys. Rev. **55**, 672 (1939).
[2] G. Temple, Proc. Phys. Soc. **48**, 39 (1936).

26. Effect of a Current Through an Iron Bar on Residual Magnetism. H. A. PERKINS AND H. D. DOOLITTLE, *Trinity College.*—A bar of Norway iron is surrounded by a solenoid composed of two windings. One of these is used to magnetize the bar; the other is connected to a galvanometer. Very small sudden changes in the flux through the iron are indicated by the throw of the galvanometer coil. A third circuit sends a current lengthwise through the bar. If the bar has been magnetized by a current whose circuit is then opened, a certain amount of residual magnetism remains. Then the galvanometer circuit is closed and the longitudinal current turned on. The galvanometer deflects in a sense which indicates a decrease of magnetism for a small residual flux, but an increase with larger values. This phenomenon has been studied with bars of various lengths and diameters and with various kinds of iron. The effect of a current flowing in a wire through the bored out axis of a bar was also examined, and finally a study was made of the effect of a succession of equal mechanical blows on the iron, in which varying amounts of residual flux had been set up.

27. The Ferromagnetic Relaxation Constant. J. BARTON HOAG, *University of Chicago.*—The domains of a ferromagnetic substance are able to adapt themselves to an external alternating field, by virtue of their restoring and damping forces, giving a comparatively high and nearly constant susceptibility χ_0 until the frequency of the alternations reaches the ultra-high radiofrequency range. Here the domains gradually fail to keep up with the applied field and the susceptibility slowly drops to the paramagnetic value. Data on the inner, initial permeability or susceptibility (χ) of iron in the high radiofrequency range have been accumulating for a number of years, to the point where a rough comparison with theory is now possible. A graph will be shown of the data in comparison with a typical dispersion equation of the form $\chi = \chi_0/(1+\omega^2/\omega_1^2)$. When the angular frequency ω is made equal to the constant ω_1, the value of χ will be just one-half of the "low frequency" value χ_0. From the data, I find $\omega_1 = 3.0 \times 10^9$ radians per second. Hence, the relaxation constant $\sigma = 1/\omega_1 = 3.3 \times 10^{-10}$ second, for iron.

28. An Ion Source of the Low Voltage Capillary Arc Type. SAMUEL K. ALLISON, *University of Chicago.*—The present status of ion source development in connection with our nuclear disintegration program will be described. The improvements introduced over a period of two years have increased the ion beam currents by a factor of 20. The present arc is made from a small rectangular copper block which can be thrust into the acceleration tube and placed some 5 cm from the first 100,000-volt focusing gap. The arc runs through a short constriction 9.5 mm long and 4.7 mm in diameter, at a current of 0.5 to 1.0 ampere. The probe is placed close to the constricted portion of the arc and consists of a solid tungsten button, 6 mm in diameter and 3 mm thick, with a probe hole 0.034 cm in diameter through it. An ingenious method of grinding this hole through the tungsten has been devised for us by Mr. F. B. Pearson. The assembly will emit 800–1000 microamperes of positive ions from the probe hole with 2000–3000 volts on the probe. Such a current is more than can be handled with the present low capacities in our Cockroft-Walton circuit, but with 250 microamperes a focal spot of magnetically analyzed protons, 6 mm in diameter and of 10 microamperes intensity, is attained.

29. Radioactive Indium Isotopes Produced by Alpha-Particles on Silver. L. D. P. KING AND W. J. HENDERSON, *Purdue University.*—The production of artificial radioactivity when silver is bombarded by 16-Mev alpha-particles has been reported previously.[1] Further work has shown that four periods are present, 20 min., 65 min., 9.4 hr., and 2–3 days. The first two periods have been chemically identified as indium. The 20-min. indium period was first reported by Lawson and Cork[2] using deuterons on cadmium and was assigned to In^{111}. Barnes[3] checked

this period using protons on cadmium. The additional information obtained by using alpha-particles assigns this period definitely to In^{112} instead of In^{111}. The 65-min. period assigned tentatively to In^{110} by Barnes[3] is checked by our results. The presence of a slight copper impurity in the silver is apparently responsible for the 9–10-hr. period. The 2–3-day period is very weak and may also be due to an impurity, or possibly be the same as the 2.7-day indium activity reported by Cork,[4] and independently by Barnes.[3] No indications of the 72-sec. period previously assigned to In^{112} was found, indicating a further revision in the indium isotope assignments.

[1] King, Henderson and Risser, Phys. Rev. **55**, 1118 (1939).
[2] J. L. Lawson and J. M. Cork, Phys. Rev. **52**, 531 (1937).
[3] S. W. Barnes, Phys. Rev. **56**, 414 (1939).
[4] J. M. Cork and J. L. Lawson, Phys. Rev. **56**, 291 (1939).

30. Excitation of the 450-Kev Level of Li^7 by Proton Bombardment. COLIN M. HUDSON, R. G. HERB AND G. J. PLAIN, *University of Wisconsin.*—The yield of gamma-rays from a thin film of lithium bombarded by protons has been investigated up to 2.08 Mev by recording both single and coincidence counts in G-M tubes. Above the 0.440-Mev resonance the gamma-ray yield of single counts is very low up to 0.850 Mev, and rises from there to a broad maximum at 1.050 Mev. From 1.150 Mev to 1.300 Mev the yield is about 0.8 as great as at 1.050 Mev. Above 1.300 Mev the yield again rises and the excitation curve up to 2.080 Mev shows a series of steps possibly indicating resonance excitation. The radiation above 0.850 Mev was predominantly soft, since very few coincidence counts were obtained at any point in the region. Lead absorption measurements of the soft lithium radiation and of annihilation radiation of positrons from N^{13} showed that the lithium radiation is softer than the positron annihilation radiation. The measurements indicate that the soft radiation is due to excitation of the 450-kev energy level of Li^7.

31. The Specific Charge of the Positron. A. H. SPEES AND C. T. ZAHN, *University of Michigan.*—The work on the specific charge of beta-rays[1] has been continued in order to include data on positive beta-rays. These were obtained from the radioactive isotope Cu^{64}, which emits both positrons and electrons with a half-life period of 12.8 hours. This branch feature made possible a good determination of the specific charge of the positron relative to that of the electron. For, in order to change from an electron to a positron source, it was unnecessary to disturb the geometry of the apparatus; only the electric and magnetic fields had to be reversed. In each case the procedure consisted of keeping the magnetic field constant and measuring the number of particles transmitted by the apparatus for various settings of the electric field. For a certain value of the electric field, corresponding to a compensated velocity, a maximum transmission occurred; i.e., a plot of the number of particles transmitted, against the values of the electric field, yielded a peak at the value for compensation. The positron peak was found to have the same position as the electron peak, indicating that the ratio e/m for positrons is the same as for electrons within an error of less than one percent.

[1] C. T. Zahn and A. H. Spees, Phys. Rev. **53**, 365 (1938).

32. Analysis of a Class C Radiofrequency Power Amplifier. S. L. SIMON, P. R. BELL, R. J. MOON AND L. SLOTIN, *The University of Chicago.*—The performance of triodes in class C operation can be calculated if characteristic data are known for many values of the space current between cut-off and saturation. This calculation is especially important for large power triodes such as are used in a cyclotron. A method has been developed for measuring complete triode characteristics which uses equipment found in most laboratories and which eliminates the difficulties in previous methods. Several sets of operating conditions have been determined from characteristic data. Application of the results gave an improvement in cyclotron performance.

33. Anode Effect as a Function of Temperature. PAUL L. COPELAND, *Armour Institute of Technology.*—Work on the anode effect previously reported[1] has been extended and refined by the use of triodes in which the surface potential of a nickel grid as a function of the electron current collected by it was investigated. The temperature of the grid was controlled and measured by the passage of a current through it. The results indicate: (1) that, with the grid at or near room temperature, its surface charge may be high enough to shift its effective contact potential by as much as two or three volts, and (2) that the magnitude of the surface charging decreases rapidly with temperature, being limited to about a tenth of a volt at 600°K, and not being detected at all above 675°K. Time studies for the drift of contact potential, like those reported by Nottingham,[2] were made. It was found that if the contact potential shift was plotted against the logarithm of the time, the resulting graphs were nearly linear. This fact suggests that the drifts involve groups of electrons with different binding forces; so that the effective time constant of the discharge of the surface varies continuously during the history of the drift.

[1] P. L. Copeland, Phys. Rev. **55**, 1145 (1939).
[2] W. B. Nottingham, Phys. Rev. **39**, 183 (1932).

34. Ionization by Positive Ions in Atmospheric Sparks. ROBERT N. VARNEY, *Washington University.*—Three problems arise in calculating the chance of ionization by positive ions in spark breakdown: First, what energy do positive ions really need to ionize by collision? Second, what chance does an ion have of gaining this energy? Third, what method of calculation is to be applied in determining this chance? In answer to these questions the following evidence is offered: (1) Recent results show that an ion must have at least three times as much energy as an electron to ionize by collision in the most favorable case. (2) Further results indicate that the mean free path of an ion of 20 electron volts energy is not very different from that of a molecule, a figure which is necessary to answer question 2.

(3) Application of these results by any reasonable method shows that the chance of ionization by positive ions is extremely small. The Townsend theory of spark breakdown based on ionization by positive ions thus becomes invalid, for that theory requires more than 10^{10} times as many ionizing collisions as can be accounted for under the most favorable circumstances.

35. Multiple Scattering of Electrons. S. GOUDSMIT AND J. L. SAUNDERSON, *University of Michigan.*—The theoretical treatment of the problem of multiple Rutherford scattering announced previously[1] has been worked out in more detail. The final scattering distribution is expressed as a series in Legendre polynomials which can be evaluated numerically. It can be shown that the results are very sensitive to deviations from the Rutherford formula caused by the screening effect of the electrons. This may probably explain the discrepancies between the experimental data and preliminary theoretical calculations. It is also shown that Williams' theory contains approximations which are not always permissible.

[1] S. Goudsmit and J. L. Saunderson, Phys. Rev. **56**, 122 (1939).

36. Time-Lag Analysis of the Townsend Discharge in Argon with Activated Caesium Electrodes. R. W. ENGSTROM,* *Northwestern University.*—The Townsend discharge was studied in the range of argon pressures 0.1 to 0.8 mm of Hg, parallel plate separations from 2 to 16 mm and gas amplification current ratios from 2 to 20. Analysis of equilibrium currents yielded ionization coefficients over the extended range from 40 to 2000 volts per cm per mm of Hg. Measurement of the instantaneous current as a function of the time after the beginning or cessation of cathode illumination was accomplished by a technique previously developed.[1] For the above range of variables, the exponential constant of the time-lag current amounts to from 0.1 to 7 milliseconds. Analysis of these data showed the source of the lag to be diffusion of metastable argon atoms and the release of about 0.4 secondary electron *per metastable atom* reaching the cathode. The coefficient of diffusion of metastable atoms in argon was determined and shown to be that expected for a metastable atom having a diameter effectively 1.74 that of the normal atom. In addition to those secondary electrons resulting from metastable atoms were those caused by impact of positive ions. The number of secondary electrons *per positive ion* varied from 0.04 to 0.41.

* Now at State Teachers College, St. Cloud, Minnesota.
[1] W. S. Huxford and R. W. Engstrom, Rev. Sci. Inst. **8**, 385 (1937).

37. Volume Rectifying Action in Cu_2O Crystals. JOSEPH M. LAMBERT, *Toledo, Ohio.*—Experiments have been made to find how far a rectifying action is connected with the crystal photoelectric effect in cuprite crystals (Dember effect). It was found that natural Cu_2O crystals, which show the Dember effect, exhibit rectifying properties when illuminated. As is proved experimentally, this new effect does not occur at the electrodes, but, like the Dember effect, is caused by action in the body of the crystal (bulk rectification). The resulting rectification in relation to the alternating voltage and illumination applied to the crystal will be shown graphically. If the spectral composition of the light is altered so as to reverse the sign of the Dember effect, the direction of the rectifying action also alters. In artificial Cu_2O crystals, which do not show the Dember effect, the rectifying effect is also absent. Some theoretical implications will be discussed.

38. Streaming of the Solvent in a Diffusion Field. GALE YOUNG, *University of Chicago.* (*Introduced by N. Rashevsky.*)—A vertical loop of solution becomes mechanically unstable and goes into circulation under the action of a dissolved substance diffusing downward when the concentration gradient of the latter exceeds a critical value. This is an instance of solvent streaming due to diffusion drag forces. If the dependence of solvent density upon solute concentration is taken into account a similar situation is realized, except that now the streaming energy originates from the solvent elements running through a cycle of expansion and contraction as they move. The situation is entirely analogous to instability of a fluid heated from below. If the small but finite viscosity of the solute is taken into account there arise streamings in the solvent quite independently of any external forces such as gravity. If a dissolved substance is diffusing along the axis of a cylinder in which the solvent is confined, it is found that the solvent circulates forward with the dissolved substance in the central part of the cylinder and returns in the opposite direction in the outer part of the cylinder. A similar result obtains for the flow between parallel flat plates.

Author Index to Abstracts of Chicago Meeting

Allison, Samuel K.—No. 28

Bell, P. R.—see Simon, S. L.
Bethe, H. A.—see Marshak, R. E.
Beutler, H. and Mark Fred—No. 19

Cleveland, Forrest F. and M. J. Murray—No. 21
Cook, Emory—No. 6
Cooper, Densil M.—No. 12
Copeland, Paul L.—No. 33

Davis, F. J.—see Winans, J. G.
Dennison, D. M.—see Koehler, J. S.
Doolittle, H. D.—see Perkins, H. A.
Duffendack, O. S.—see Saunderson, Jason L.

Engstrom, R. W.—No. 36
Evans, Foster—No. 16

Fred, Mark—see Beutler, H.

Gill, P. S.—No. 11
Goudsmit, S. and J. L. Saunderson—No. 35

Haas, Arthur E.—No. 7
Henderson, W. J.—see King, L. D. P.
Herb, R. G.—see Hudson, C. M.
Herzog, G.—No. 9
Hilberry, H. Van Norman—see Rossi, B.
Hoag, J. B.—see Rossi, B.
——No. 27
Hudson, C. M., R. G. Herb and G. J. Plain—No. 30

Ingersoll, L. R. and Philip Rudnick—No. 20

Jamison, N. C.—see Meeks, W. W.
Jesse, W. P.—see Schein, M.

King, L. D. P. and W. J. Henderson—No. 29
Koehler, J. S. and D. M. Dennison—No. 23
Konopinski, Emil J.—No. 14

Lambert, Joseph M.—No. 37
Landsverk, O. G.—No. 22
Leitzke, V. A.—see Winans, J. G.
Ludloff, H.—No. 3
Lyons, W. James—No. 4

Marshak, R. E. and H. A. Bethe—No. 18
Meeks, W. W. and N. C. Jamison—No. 25
Moon, R. J.—see Simon, S. L.
Murray, M. J.—see Cleveland, Forrest F.

Perkins, H. A. and H. D. Doolittle—No. 26
Plain, G. J.—see Hudson, C. M.
Present, R. D.—No. 17

Rossi, B., H. Van N. Hilberry and J. B. Hoag—No. 10
Rudnick, Philip—see Ingersoll, L. R.

Saunderson, J. L.—see Goudsmit, S.
—— **and O. S. Duffendack**—No. 15
Schein, M., W. P. Jesse and E. O. Wollan—No. 13
Siegel, S. S. and W. H. Zachariasen—No. 2
Simon, S. L., P. R. Bell, R. J. Moon and L. Slotin—No. 32
Slotin, L.—see Simon, S. L.
Spees, A. H. and C. T. Zahn—No. 31

Varney, Robert N.—No. 34

Whitmer, R. M.—No. 5
Winans, J. G., F. J. Davis and V. A. Leitzke—No. 24
Wollan, E. O.—see Schein, M.

Young, Gale—No. 8, 38

Zachariasen, W. H.—see Siegel, S. S.
——No. 1
Zahn, C. T.—see Spees, A. H.